Investigating Anion-Quadrupole Interactions of
Phenylalanine and Fluorinated Phenylalanine
Derivatives Using Density Functional Theory and
Infrared Multiple Photon Dissociation Spectroscopy

by

Kathleen E. Wilson

A thesis

Presented to the University of Waterloo

submitted in fulfillment of the

thesis requirement for the degree of

Master of Science

in

Chemistry

Waterloo, Ontario, Canada, 2014

Author's Declaration

I hereby declare that I am the sole author of this thesis. This is a true copy of the thesis, including any required final revisions, as accepted by my examiners.

I understand that my thesis may be made electronically available to the public.

Abstract

Electronic structure calculations have been used to provide a new model for the quadrupole moments of bare and fluorinated phenylalanine. Calculations of the quadrupole moments were performed at the B3LYP/6-311++G(d,p) level of theory with CHELPG partition scheme. Electrostatic mapping and graphical representations of the resulting quadrupole moments provides a new visual representation that accounts for the changing electrostatics of the phenyl ring. It is found that increasing fluorination increases the ability of the quadrupole moment to stabilize anions above the ring. It is also observed that position of the fluorination around the ring alters the direction of the quadrupole moment but does not affect the magnitude.

Electronic structure calculations in combination with infrared multiple photon dissociation (IRMPD) spectroscopy have been used to determine the structural conformations of phenylalanine and fluorinated phenylalanine derivatives clustered with chloride, bromide, fluoride and trifluoromethanolate ions. Anions were clustered with phenylalanine (Phe), 3-fluorophenylalanine (3FPhe), 4-fluorophenylalanine (4FPhe) and 2,5-difluorophenylalanine (25FPhe). Anions clustered with phenylalanine derivatives had optimization and frequency calculations (B3LYP/6-311++G(d,p)), single point energy calculations (MP2/aug-cc-pVTZ), and anharmonic calculations (B3LYP/6-311++G(d,p)) completed. Harmonic frequency calculations were scaled by 0.968. Presently only clusters containing chloride and the phenylalanine derivatives have been acquired. For clusters where there are IRMPD spectra available, it is observed that higher energy isomers better match the lower wavenumber vibrational modes while the most stable conformations can accurately match the higher wavenumber vibrational

modes. All calculated clusters are found to have energetically favoured structures where the anion is located in either the ring plane interacting with the ring edge and the amino carboxylic acid group or in a claw-like formation where the amino backbone hydrogens are all directing towards the anion perpendicular to the ring with CH directed towards the ring. Clusters involving chloride demonstrated that higher energy isomers better matched the IRMPD spectra suggesting carrier gas stabilization is occurring.

Systematic computational investigations of the impact that fluorination degree and location permutations around the phenylalanine ring have on anion-quadrupole stabilizations were completed with chloride, fluoride and bromide clusters. Calculations were completed at the B3LPY/6-311++G(d,p) and MP2/aug-cc-pVTZ levels of theory for optimization and single point energy calculations, respectively. It is found that three distinct classes of fluorination permutation exist which can predict the lowest energy conformations of other fluorination degrees. Class 1 structures have fluorination occurring at positions 2 and 6 of the phenyl ring. Class 1 structures have increased anion-quadrupole binding as the quadrupole moment is more strongly felt when the charge density lies near the amino backbone. Class 2 structures are where neither position 2, nor position 6 are fluorinated. Localization of the charge density furthest from the amino backbone mimics conformations for unfluorinated phenylalanine-anion interactions. Class 2 structures tend to have interactions between the anion and ring plane as opposed to the ring face. Class 3 consists of either position 2 or position 6 being fluorinated and is split up into two subclasses that depend on secondary fluorination locations, positions 3 and 5 on the phenyl ring. Class 3 conformations consist of a mixture of class 1 and class 2 isomers. Class 3A has fluorination at a secondary location directly across from the primary fluorination location (for

example positions 2 and 5 are fluorinated). Thus class 3A structures follow more closely to class 1

structures as the charge density is spread across the ring; hence the quadrupole moment has a

greater influence on anion location. Class 3B lacks the secondary fluorination location and thus

the charge density is localized on one side of the ring. This opens up ring edge interactions with

the anion, mimicking the unfluorinated phenylalanine cases more closely. It is also observed that

increasing ring fluorination increases the anion-quadrupole binding and softer anions are more

likely to interact directly with the ring face.

I would like to thank <u>Jake Fisher</u> and <u>Howard Siu</u> for helping to make graduate school fun! I always enjoy heading down to the physical chemistry lab to chat about anything and everything. Both of you have always been willing to listen to me vent and are able to help me see the humour in every situation! <u>Jake</u>, thank you for everything! You have always been available for me to bounce ideas and thoughts off of and to solidify what's going on in my head. I also want to thank <u>Jake</u> for trusting me with his CHEM 140 course while he was sick. It was an honour to teach the course for you, and one opportunity that I will never forget. I am eternally grateful for all the doors you have helped to open for me and the guidance you've given me over the last six years. Thank you, both of you!

Last but not least I would like to thank my friends and family. Special thanks to my mother, <u>Rosemary Wilson</u>, who has always been supportive and encouraging even when I doubted myself and my brother, <u>Robert Wilson</u>, who gave me a thicker skin and inadvertently taught me that if you get knocked down you get right back up and keep fighting for what you believe in, no matter what the odds against you are. To my friends (who I won't name in fear of forgetting one, but you know who you are), thank you for always being there! Whether it was getting a cup of coffee, shopping, making "jumbo meals", watching movies or having late night drinks, I will always cherish the memories we have made together. You have all, in one way or another helped me when times were tough and sleep deprivation was high. Thanks for the memories and I look forward to the many more memories yet to come! Thanks!

Dedication

I dedicate my thesis to my mother

for her continuing support and encouragement

Table of Contents

List of Figures

List of Tables

Table of Abbreviations

25FPhe	2,5-difluorophenylalanine
3FPhe	3-fluorophenylalanine
4FPhe	4-fluorophenylalanine
6-311++G(d,p)	6 primitives – valence triple zeta; heavy atoms augmented with additional one s and one p functions, diffuse s functions on hydrogens; d functions to polarize the p with p functions added to hydrogens
aug-cc-pVTZ	augmented correlation-consistent polarized valence triple zeta
B3LPY	Becke 3 parameter Lee, Yang and Parr
Br^-	Bromide ion
CF_3O^-	Trifluoromethanolate ion
Cl^-	Chloride ion
Claw formation	Amino backbone points towards the anion in a claw-like formation with all hydrogen atoms directed towards the anion with the CH group pointed towards the phenyl ring
CLIO	Centre Laser Infrarouge d'Orsay
cm^{-1}	Wavenumber
DFT	Density Functional Theory
ESI	Electrospray ionization
F^-	Fluoride ion
FEL	Free electron laser
FPhe	Fluorinated phenylalanine derivatives
FTICR	Fourier transform ion cyclotron resonance
HF	Hydrogen fluoride
IR	Infrared
IRMPD	Infrared Multiple Photon Dissociation
IVR	Intramolecular vibrational redistribution
kJ/mol	kilojoules per mole
MP2	Second-Order Møller-Plesset Perturbation Theory
MS	Mass Spectrometer
Phe	Phenylalanine
PentPhe	2,3,4,5,6-pentafluorophenylalanine
PT	Proton transfer
QIT	Quadrupole ion trap
SPE	Single point energy
Y formation	Amino backbone creates a Y where the anion is located in the bridge with the CH group directed away from the phenyl ring at the back of the molecule

Chapter 1

1.0 Introduction

Gas phase interactions are unique in that they portray chemical interactions in the absence of solvent. Prior research has shown that solution phase chemistry can provide insight into the behaviour of gas phase moieties, though this is not always the case. In many instances solution chemistry is not indicative of behaviours observed in the gas phase [1, 2]. It has been observed that solution intuition has the ability to be either the opposite of, or at least incorrect, to some degree, relative to gaseous interactions. How solvents can alter gas conformations is not yet fully understood and implicit solvation methods are being completed to characterize these differences. Due to this disconnect between solution and gas phase behaviours, both experimental and theoretical investigations must be completed to understand the chemical interactions occurring in the gas phase.

Gaseous proteins and amino acids have become an area of increasing research as their behaviours are generally unknown. Due to the increase in availability and decrease in cost of experimental and computational techniques, gaseous species can now be analyzed. Since solution behaviours of amino acids are known, delving into the gas phase is a natural progression.

It has been observed in solution that fluorination of proteins and amino acids can have a significant effect on their properties. Bovy *et al.* investigated the effect of phenylalanine ring fluorination on biological activity and conformation in solution phase angiotensin II [3]. It was found that by fluorinating the phenyl ring, activity of agonist responses were decreased thus reducing the effect of angiotensin II. This same decrease in activity upon phenyl ring fluorination

1

was seen by Geurink *et al.* who investigated how fluorination could be utilized to create antitumor agents [4]. They focused on analyzing several catalytic subunits by fluorinating phenylalanine derivatives in known inhibitors and measuring their inhibition. Fluorination of the ring not only produced increased inhibition of protein cleaving sites in proteasomes, but it also showed highly selective inhibition of the three catalytic subunits analyzed. By altering the degree of ring fluorination or changing the influence of the electron withdrawing groups though use of CF_3 instead of fluorine, they could inhibit specific subunits [4].

As trends and interactions that are observed in solution are not always indicative of gas phase behaviour, in depth analysis of amino acid phenyl rings must be completed in the gas phase. Understanding these interactions and behaviours can lead to new and novel synthesis techniques as well as intelligent drug designs and delivery systems.

1.1 Quadrupole Moment

Changes in the observed biological activity caused by ring fluorination experiments in solution phase are thought to be caused by one key ring property. It is known that phenyl rings contain a quadrupole moment and it is this quadrupole moment that permits unique binding interactions [5 - 7]. Past research describes the quadrupole moment as having negative regions above and below the ring with the ring plane being positively charged (**Figure 1a**). It has also been suggested that by adding electron withdrawing groups to the ring this quadrupole can be inverted [8 - 11]. Research describes this inverted quadrupole as having a negative ring plane and positive regions above and below the ring (**Figure 1b**) [3, 12]. These quadrupoles were initially seen by analyzing which species could be stabilized by the two quadrupoles. It was observed that cations tended to be stabilized directly above or below the ring for the normal quadrupoles while

2

anions were stabilized by the inverted quadrupole. The existence of both normal and inverted

quadrupoles are accepted by the scientific community, however the description of their

appearance is not straightforward and is highly debated [3, 4, 9 - 11, 13]. These descriptions do

not appropriately describe how ion-quadrupole interactions take place or exactly how the

electron withdrawing groups flip the quadrupole moment, just that these interactions have been

observed.
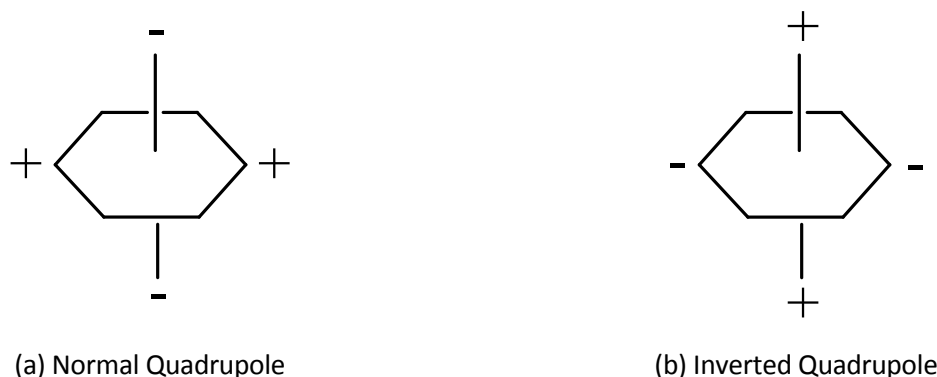
(a) Normal Quadrupole   (b) Inverted Quadrupole
Figure 1: Past quadrupole characterizations with distinct positive and negative regions **[3]**

The existence of both normal and inverted quadrupoles are concepts that are widely

recognized by researchers. However, what happens upon alteration of a quadrupole is not fully

understood. The notion that some researchers now claim is that the quadrupoles have distinct

positive and negative regions around the ring stemming from their molecular orbitals **(Figure 2)**.

However, researchers neglect to thoroughly describe this concept and rely on the classical

description of charged regions (**Figure 1**) [9, 10] . This notion has an inherent flaw in that electron

density does not behave in these inversion contexts and, as such, the answer is not that simple.

What is known is that cations can be stabilized above a species containing a normal quadrupole

while anions can be stabilized above an inverted quadrupole containing moiety. In order to fully

understand the inversion process, further experimentation of the bare phenyl containing species with and without electron withdrawing groups is required.
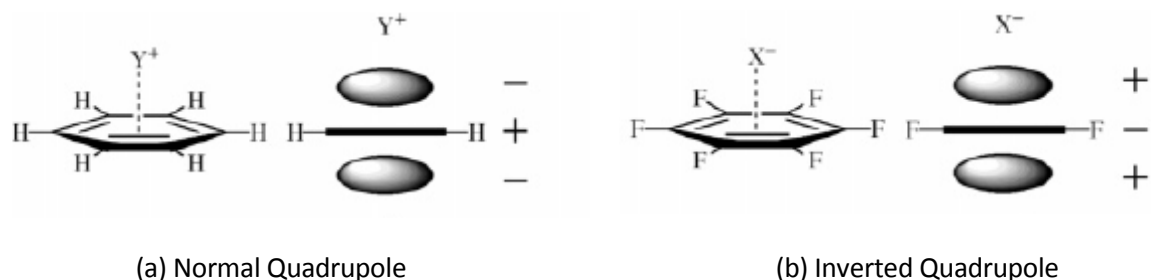
(a) Normal Quadrupole　　　　　　　　　　　　　(b) Inverted Quadrupole
Figure 2: Quadrupole descriptions stemming from molecular orbitals **[10]**

1.2 Interactions

Interactions between ions and the quadrupole moment may lead to new and novel synthesis mechanisms and unique pharmaceutical applications. Manipulation of the quadrupole may result in cage like conformations in which the ions of interest can be trapped and transported as a cluster. It is important to examine the effects of anion-quadrupole bonding in order to gain some insight into the interactions and conformations these species take. Understanding which interactions dominate in the most stable structures can aid in understanding gas phase behaviours and thus how these interactions can be manipulated.

The majority of ion-quadrupole research utilizes the simplistic quadrupole models (**Figure 1** and **Figure 2**) and therefore is based on the notion of negative and positive regions. For simplicity, past research has focused on phenyl containing benzene and benzene derivatives. It was discovered by Jackson *et al.* that two types of interactions existed for benzene, phenol and indol clustered with formate [14]. The interactions are either between the anion (formate) and the ring edge (edgewise interaction) or between the anion and the ring face. They chose to model these species as they are models for several different amino acids. Their results showed that edgewise interactions are preferred for the benzene-formate pairs as benzene contains the

4

normal quadrupole moment which is known to stabilize cations above the ring plane. They also

discovered that in addition to the magnitude of the quadrupole moment, the size and position of

the anion, both the distance from the ring and dihedral angle to the aromatic species, will dictate

the ability for binding interactions. Benzene-formate clusters had the lowest energy when 4 Å

away from the center of the ring and were in the ring plane (edgewise interactions) [14]. This is

because interactions between a point charge and a dipole moment scales as $-1/r^2$ while

interactions between a point charge and the quadrupole moment scale with $+1/r^3$ [15]. Philip *et*

al. followed up this research by using amino acids instead of benzene and formate to study the

anion-π interactions [16]. They also explored the interactions between residues in a larger

peptide. Their research showed that both anion-π and π-π stacking interactions were present

between the residues of the peptide. Since they looked at a large protein, it was difficult for

them to distinguish what the causes for the observed interactions were, only that edgewise

interactions exist [16]. Their research shows the importance of in depth analysis of these

quadrupole moments in smaller biological systems. Their research, along with the research of

others, have proven the presence of both the normal and inverted quadrupole moments in

phenyl containing species and the existence of binding interactions with appropriately charged

ions [10, 14, 16 - 18].

1.3 Phenylalanine

In order to efficiently analyze how quadrupole moments interact with anions, small

molecules containing a phenyl ring need to be analyzed. Past research has focused on

interactions of benzene and its derivatives with varying ions. The natural progression of this

research is to begin analyzing biologically relevant species. This requires analyzing amino acids

that contain phenyl rings. The smallest phenyl containing amino acid is phenylalanine (**Figure 3**) [2]. By opting for a smaller molecule, the intrinsic nature of the quadrupole moments can be examined with fewer additional interactions. Along with interaction reductions, the small size allows for high level theoretical calculations and spectroscopic determinations to be performed with relatively low cost. Phenylalanine (Phe) is an important amino acid, not just for being the smallest phenyl containing amino acid but because of its important role in many biological functions. Phenylalanine plays an important role in creating vital neurotransmitters, as it is used in the creation of tyrosine. Tyrosine then undergoes biosynthesis to create epinephrine, norepinephrine and dopamine [2, 19]. Furthermore, phenylalanine is a fairly inexpensive, easily accessible amino acid which allows spectroscopic determinations to be made with ease.
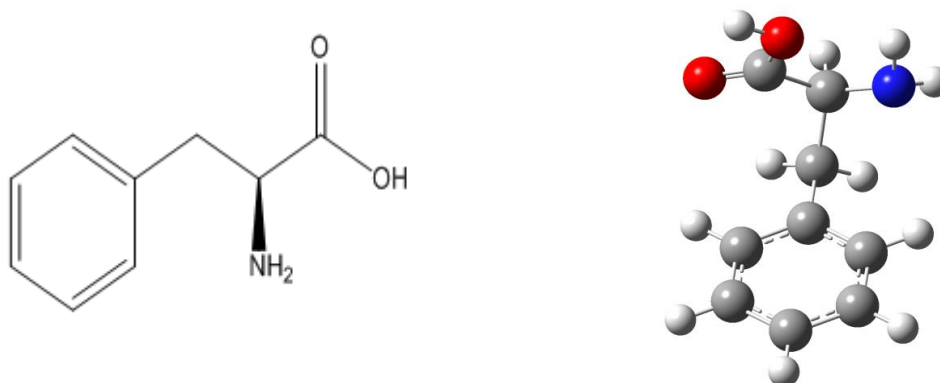
Figure 3: Visualizations of phenylalanine structure as 2D bonds and 3D ball and bond formations **[2]**

It has been observed that in solution phenylalanine is a zwitterion, however in the gas phase this phenomenon is not typically observed. Clustering of phenylalanine with either a finite amount of water molecules or specific ions/molecules has been observed to form zwitterions [19 - 22]. In addition to the potential ability to form zwitterions though quadrupole moment interactions, it has also been seen that fluorination of the phenyl ring has biologically relevant properties for antitumor agents and anesthetics [4, 6]. Extensive understanding of the

phenylalanine quadrupole moment and how fluorination affects anion-quadrupole interactions will give insight into how these observed properties are possible and why they occur.

Chapter 2

2.1 Computational Methods

In order to examine the effects of quadrupole-anion interactions and how fluorination of the phenylalanine ring alters the quadruple moment, computational chemistry must be utilized. Computational chemistry has grown exponentially along with the advances of computing power. Computational simulations and modelling allow the intrinsic properties and energetics of molecular systems to be analyzed. One of the most common software packages used to examine molecular structures and properties is the Gaussian software suite [23, 24]. The editions of the Gaussian suite used to complete the current thesis were Gaussian 09W and GaussView 5.0. To use the Gaussian software suite effectively, the computational method and basis set must be appropriately chosen. An appropriate level of theory optimizes the accuracy of the results and computational cost.

In order to probe the properties of phenylalanine quadrupole moments and anion-quadrupole interactions as well as structural conformations, density functional theory (DFT) will be utilized. DFT has become the new standard for these types of calculations as the accuracy of the results are close to *ab initio* calculations while having a reduced computational cost. DFT calculates the wave function of the system by using electron densities to calculate potentials followed by a calculation of the Hamiltonian operator to solve the Schrödinger equation [25]. A common method when probing structures of amino acids clustered with anions is B3LYP (Becke 3 parameter Lee, Yang and Parr). B3LYP is based off of Becke's previous 3 parameter exchange correlation (B3PW91) with an additional functional developed by Lee, Yang and Parr. B3LYP employs several methods to solve the Schrödinger equation. A straightforward solution is

difficult as electron-electron interactions are hard to handle. Larger systems have more electron-electron interactions, thus larger systems are increasingly difficult to compute. To circumvent this issue, Kohn and Sham postulated that the Hamiltonian for non-interacting electrons simplifies to one. This model of non-interacting electrons was used to approximate real systems. However, non-basic systems all contain, in one form or another, interacting electrons. Therefore this model is not entirely accurate. To solve this, Becke employed a theorem developed by Hellman and Feynman. This theorem allows the degree of electron-electron interactions to be incorporated into the exchange correlation energy calculation steps. It does this by using classical electrostatics to calculate the systems' forces. Using additional parameters to calculate the total correlation energy in addition to approximating that the energy found using Hartree-Fock methods is equal to the exchange for a non-interacting Hamiltonian produces a model with a high degree of accuracy. It is this combination of approximations and additional parameters that allows B3LYP to have a high level of accuracy while maintaining a lower computational cost.

Computational methods of DFT typically use a mixture of approximations and additional parameters to bypass difficult computational steps while maintaining the desired level of accuracy. This reduction in computational cost makes DFT highly desirable for optimization and frequency calculations. Although B3LYP does an excellent job of determining the thermodynamics and frequencies of phenylalanine systems, it is not the most accurate at finding the electronic energy of the system. Therefore another method must be employed to find a more accurate energy. Second order Møller-Plesset Perturbation (MP2) theory is often used for these single point energy probes of the already optimized structures. MP2 is more computationally expensive than B3LYP, but as the structure is already optimized it can be treated

as a system with fixed nuclei and therefore a higher level of theory can be used with little impact on computational resources. To use MP2 effectively, a higher level basis set is required. MP2 requires a basis set at a higher level than the original optimization in order maintain its integrity. The MP2 calculations are directly related to the basis set used, as the speed of MP2 scales as approximately N^5 where N is the number of basis functions. Therefore it is paramount that an appropriate basis set is chosen for the particular system [25 - 27].

Choosing a basis set depends on the molecular system to be analyzed. For studying the interactions between anions and phenylalanine derivatives, two basis sets are employed which have shown to produce good agreement with experiment [26 - 33]. For optimizations and frequency calculations B3LYP/6-311++G(d,p) is used. The 6-311++G(d,p) basis set allows six s-type orbitals to model the core, 3 sp-type orbitals to model the inner valence and 11 sp-type orbitals to model the outer valence. In addition to modeling the orbitals it allows diffusion of the electrons and also polarization of the orbitals. This additional flexibility of the electrons as well as the orbitals allows the interactions between the charged anion and the Phe derivatives to be modelled more accurately [25, 34]. The higher accuracy ensures that the most stable structure will be identified out of the test structures. For optimization and frequency calculations a scaling factor is needed. Although the level of theory used has been observed to show good agreement with experiment, it requires a scaling factor due to stringent limits that are used during the harmonic oscillator approximation as well as the inability of the basis set to completely map the electronic wavefunction. A scaling factor of 0.968 has been utilized throughout this thesis to correct harmonic frequencies [23 - 26, 31, 35, 36].

For single point energy (SPE) calculations using MP2, the aug-cc-pVTZ basis set is used. This basis set uses an augmented correlation consistent polarized valence triple zeta. This basis set from Dunning accounts for weakly bound electrons to be far from the location of average charge density within the cluster. This is important for the Phe systems where the anion may be far from the charge localization of the Phe species. They accomplish this feature by using diffuse s, p, d, and f functions on all heavy atoms. It is these diffusions that help to reduce the errors often seen in these types of systems where charge is distributed between anion and Phe species. By using one of Dunning's augmented basis sets, the error associated with calculations is reduced to roughly 0.05 kcal/mol for aug-cc-pVTZ so no other corrections need to be used [34, 37, 38]. Therefore the combination of MP2 with reduced error basis sets that take into account electrostatic diffusion produce highly accurate results.

Upon discovery of the most stable structures, the next step is to compare with experimental results if they are available. For structural determinations this comparison is typically between computed or simulated and experimental spectra. To create comparable spectra anharmonic calculations are performed. These calculations take into account coupling of the oscillations of vibrational modes within the molecule. For larger systems with an increase in charge density, anharmonicity may have a large impact on an infrared spectrum. Anharmonic calculations are run using the same level of theory as the original optimization steps. This is done to ensure that the harmonic calculations from the optimization and the new anharmonic calculations can be compared to discern the degree of anharmonicity in a given system. As anharmonic calculations account for coupled oscillations they are computationally expensive, therefore it is not feasible to perform anharmonic calculations for all permutations. Therefore

the number of possible isomers must be reduced. By combining the optimization and frequency calculation as well as the single point energy calculation, it can be determined which species are energetically favoured. This is done by finding the enthalpy (**Eq. 2.1.1**) and Gibbs free energy of each system (**Eq. 2.1.2**) [39].

Enthalpy (H): $$H_{total} \; = \; E(MP2) + H_{corr} \; (B3LYP)$$ **2.1.1**

Gibbs free energy (G): $$G_{total} \; = \; H_{total} \; - \; T \cdot S(B3LYP)\text{, where T = 298 K}$$ **2.1.2**

Once the enthalpy and Gibbs free energy are calculated, relative enthalpy and relative Gibbs free energies are found. This is done by setting the most stable isomer energy to zero and shifting the remaining isomers accordingly. An arbitrary cut-off of approximately 15 kJ/mol was chosen. Past research has shown no standard for these cut-off values [26, 31]. The cut-off for **Chapter 4** of this thesis was chosen to be 15 kJ/mol as past research within the McMahon group has shown this cut-off is often reliable at predicting which species are present in the gas phase [31, 26]. This is due to the assumption that populations of two species, A and B, follow a Boltzmann distribution. Assuming equilibrium conditions exist, this relationship can be described by **Eq. 2.1.3** [39]. An isomer with relative Gibbs energies of 15 kJ/mol results in a ratio of roughly 1:426 with the lowest energy isomer at 298 K. This means that the two isomers would be experimentally present in a ratio of 1:426 for a relative Gibbs free energy of 15 kJ/mol.

$$K_{eq} \; = \; e^{\frac{-\Delta G}{RT}} = \frac{[B]}{[A]}$$ **2.1.3**

However, due to unknown carrier gas effects that are only now being investigated, this cut-off ratio is not entirely accurate and therefore some higher energy isomers found using computational chemistry might be present in the gas phase [40]. Therefore, if isomers are close to the cut-off they are included for completeness as less stable structures have been seen in

some instances to have a better spectral match between computation and experiment. Thus, all isomers with relative enthalpy or Gibbs free energy less than or near the cut-off have computed anharmonic spectra generated. As B3LYP/6-311++G(d,p) was used for the optimizations, the same level of theory is used for the anharmonic calculations.

Structural identifications consist of at least two of the three steps listed in **Figure 4**. The first two steps are crucial in finding which structures are energetically favoured to be present in the gas phase. Without these steps it would be extremely difficult to hypothesize the most stable conformations. The last step is required if there is experimental data. By comparing the spectral peaks of experimental and computational results, the chosen conformations can either be confirmed or disproven as being present in the gas phase. Once the anharmonic calculations have completed, the results are fitted to a Lorentzian model with a full width half max of 15 cm^{-1}. Past research in the McMahon group has shown that a full width half max of 15 cm^{-1} shows good agreement with experimental infrared multiple photon dissociation (IRMPD) spectra [26, 28 - 31, 41].

Optimization & Frequency	B3LYP/6-311++G(d,p)
Single Point Energy	MP2/aug-cc-pVTZ
Anharmonic Spectra	B3LYP/6-311++G(d,p)
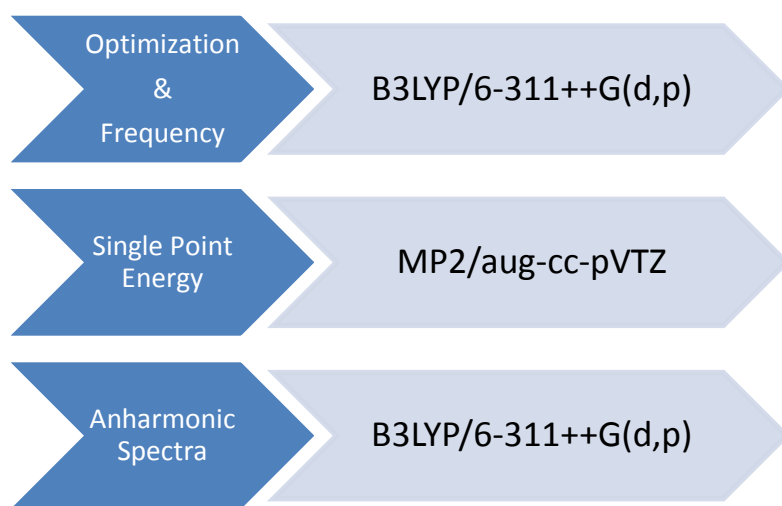
Figure 4: Structural elucidation flow chart identifying the progression of computational calculations

2.2 Experimental Methods

Identification of gaseous species requires experimental spectra. These spectra will be compared to simulated computational spectra; the simulated spectra that best matches all experimental vibrational modes will belong to the isomer that has the highest probability of being present in the gas phase. Therefore, analysis of the fingerprint region is required. The fingerprint region (~1000-2000 cm^{-1}) consists of vibrations belonging to the unique functional groups of the species being analyzed [1]. Thus, the exact structural conformation can be deduced from the experimental spectrum. In order to make structural elucidation easier, comparison with simulated spectra can show relatively quickly which isomeric conformations are likely to be present.

Prior research has shown that infrared multiple photon dissociation (IRMPD) spectroscopy is an excellent tool for generating spectra in the fingerprint region [42 - 47]. In order to use IRMPD effectively, a high powered light source along with trapping devices for concentrating and separating desired ions from the bulk solution are required. Solutions containing the desired analyte in a volatile solution matrix undergo electrospray ionization (ESI). ESI allows the desired ions to be transferred to the gas phase as the volatile solvent is easily evaporated off [48, 49].

Previous research using IRMPD spectroscopy focused mainly on the combination of a free electron laser (FEL) coupled directly to a Fourier transform ion cyclotron resonance (FT-ICR) mass spectrometer (MS) [43 - 45, 50]. This coupling provided an extremely sensitive tool for structural determinations. However, it was discovered by Mac Aleese *et al*. that this coupling was not optimal. It was determined that a trade-off between collision area and photon power was occurring. By ensuring that the light source was covering the entire ion cloud the laser power

density was reduced significantly. Thus, Mac Aleese found that by including a Paul type ion-trap which used alternating electric fields to concentrate the ions resulted in a higher efficiency of fragmentation and IRMPD resolution as the size of the collision area was greatly reduced [43, 51]. This breakthrough altered the way IRMPD is produced. Presently the standard operating procedure for IRMPD spectral generation in experiments carried out by the McMahon group uses a FEL coupled to an ion trap, typically a quadrupole ion trap [43, 44, 52, 53].

After electrospray ionization of the solution matrix, the gaseous ions are directed into the quadrupole ion trap mass spectrometer (QIT-MS). Here the ions are concentrated and mass selected. A quadrupole ion trap consists of four alternating electric fields as seen in **Figure 5**. The ions flow into this area of alternating fields; with the aid of a 1 mTorr pressure helium buffer gas, the ions are cooled and concentrated in the center of the quadrupole trap [26, 27, 54].

(a)   (b)
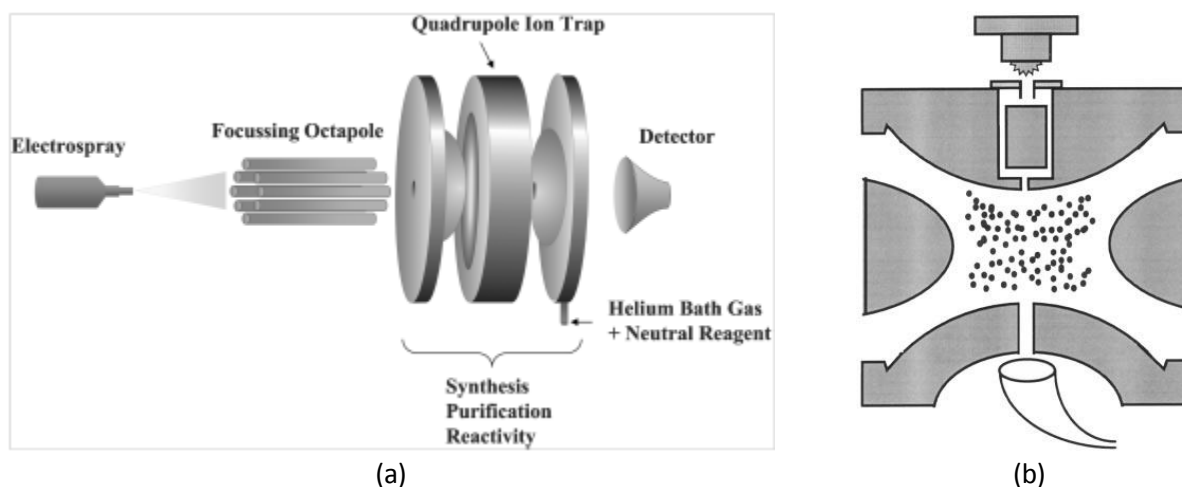
Figure 5: Quadrupole ion trap (a) schematic with ESI source demonstrating the flow of ions after ESI to the quadrupole **[50]** (b) cross section of the quadrupole ion trap illustrating ion trapping before ions are transported to a MS **[54]**

Once the ions are trapped and concentrated, they can be fragmented. Photons from the free electron laser bombard the ions. The free electron laser consists of two key regions: (**Figure**

6) (1) the accelerator portion, which generates a near light speed pulse of electrons and (2) the undulator, which is a two meter long series of magnets of alternating poles (**Figure 7**).
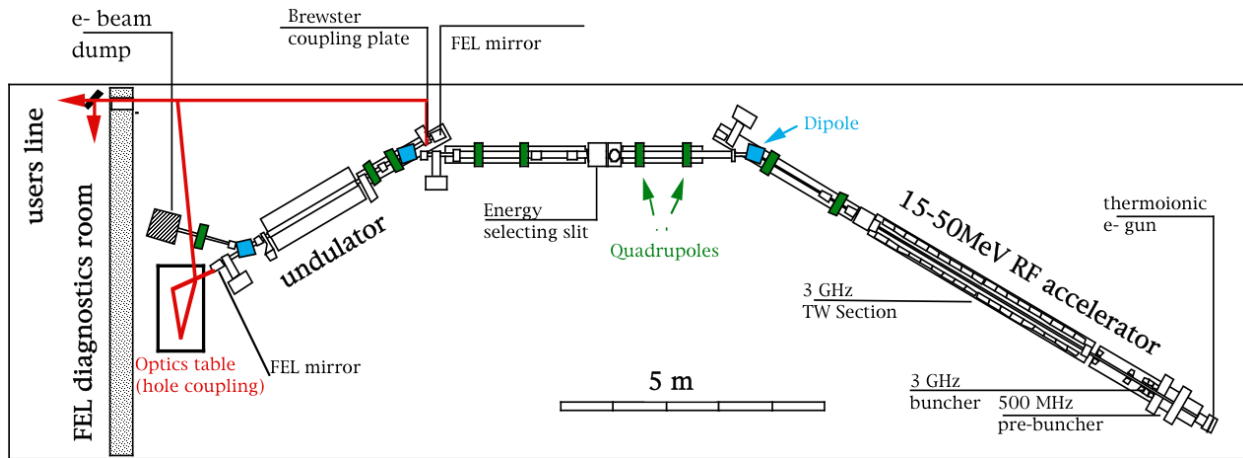
Figure 6: A FEL schematic. The accelerator creates electrons at near light speed; the undulator creates oscillations of the electrons which emits photons which are amplified by two mirrors. **[55]**

The undulator is what makes the wavelength of the FEL tunable. By altering the distance between the magnets of altering polarity the wavelength is altered. The light enters into the oscillator where the distance between the magnets changes the wavelength. The oscillations of the light through the series of magnets cause emission of photons. The mirrors on either end of the undulator serve to form a resonator, in which the radiation can be amplified by the emission photons [26, 27, 53, 55 - 57]. The tuning of the undulator allows wavelengths from the ultraviolet to the infrared region to be obtained. For this thesis, the infrared (IR) region of the FEL was used. Henceforth the light from the FEL will be referred to as IR-FEL to denote the region of interest.
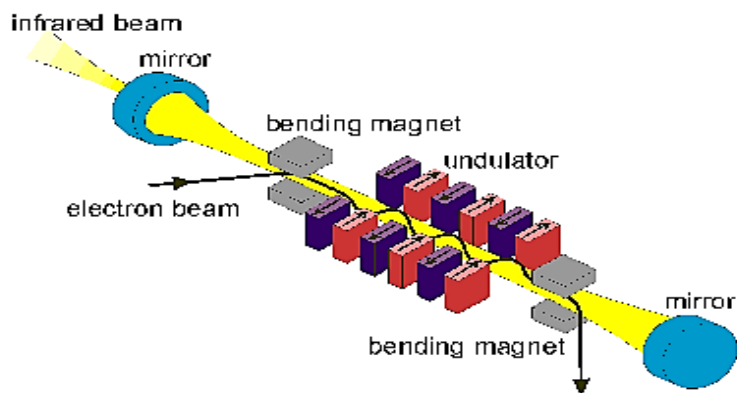
Figure 7: A schematic of the undulator region. Oscillations are created by alternating magnets which causes emission of photons, the mirrors at either end amplify the radiation from the emitted photons **[57]**

To ensure fragmentation, the light beam from the IR-FEL is expanded to be larger than the ion cloud. Just like use with an FT-ICR, by ensuring the beam is larger than the ion cloud, loss of the IR-FEL power density is observed. However, the beam needs to be larger than the ion cloud to ensure excitation. IRMPD uses discrete trains of photons to cause these excitations. The bombardment of the ions occurs one photon at a time. Upon absorption of the photon at a specific point, the molecule undergoes intramolecular vibrational redistribution (IVR). This is where the energy redistributes throughout the coupled vibrational modes of the molecule. After completion of IVR another photon is free to excite the species. Just like before, the energy redistributes throughout the coupled modes. If at any point throughout the IVR the vibrations have enough energy and are resonant with the excitation frequency, the bond will break and fragmentation will occur. Thus the efficiency of the fragmentation is directly related to the efficiency of the IVR as additional photons must wait for IVR completion [43, 44, 46, 58, 59]. If either excitation frequency or photon energy is not enough to cause bond breaking then fragmentation will not occur. Therefore, when comparing to computational spectra, all peaks present in the IRMPD spectrum must be present in the computed spectrum to be determined a

17

good fit. Thus IRMPD is known as a consequence or action spectra as the produced spectra are dependent on the FEL and IVR efficiency. Fragmentation is produced by the excitations, thus the detector is recording the fragmentation efficiency as a function of photon energy (**Eq. 2.2.1**)

$$R = -log\left(\frac{I_{parent}}{I_{parent} + \Sigma I_{fragment}}\right)$$

2.2.1

Currently the most accessible IR-FEL is located in Orsay, France at the Centre Laser Infrarouge d'Orsay (CLIO). An IR-FEL coupled to a QIT-MS was used to generate the experimental spectra shown in **Chapter 4**. Generation of future IRMPD spectra will be completed at CLIO by other group members of the McMahon lab.

Chapter 3

Systematic Quadrupole Investigation of Fluorinated Phenylalanine Derivatives

3.1 Introduction

Species containing a phenyl ring exhibit quadrupole moments that can participate in ion-quadrupole, or ion-π interactions. Unsubstituted phenyl rings can participate in cation-π interactions. By adding electron withdrawing groups to the phenyl ring, the quadrupole can be inverted thus resulting in anion-π interactions. Previously these quadrupoles have been described as having distinctive charged regions, though this notion is inherently incorrect as charges do not behave in this manner. The addition of electron withdrawing groups cannot completely invert the charge on the ring plane and the charged regions above and below the ring [3, 9, 10]. Phenylalanine is the smallest amino acid that contains a phenyl ring and therefore is an interesting case to study. However, as the amino backbone is connected to the phenyl ring this creates an interesting case in which there is already a substituent on the ring which is slightly withdrawing. This is unique since all other studies of these quadrupoles tend to analyze withdrawing substituents on a symmetric benzene ring [6, 8, 11, 12]. The addition of the amino backbone thus alters the symmetry, changing how additions of electron withdrawing substituents will alter the quadrupole. However as the amino backbone is only slightly withdrawing, Phenylalanine is considered to contain a normal quadrupole as described in **§1.1** and **§1.2**. Therefore a systematic analysis of the impact that fluorination has on the quadrupole moment has been performed.

3.2 Methods

In order to quantify the quadrupole moment, an optimization and frequency calculation with an electrostatic population is completed. For fluorinated derivatives B3LYP/6-311++G(d,p) has been used with the CHELPG (**CH**arges from **EL**ectrostatic **P**otentials with point selection algorithm) population program [60, 61]. The CHELPG program is based on the CHELP (**CH**arges from **EL**ectrostatic **P**otentials) program designed by Chirlian and Francl [60]. The CHELP program uses point charges at the center of each atom within the system to fit the electrostatic potential. By using point charges, alterations in geometry can be properly accounted for. In addition to being able to distinguish differing geometries, by utilizing point charges dipole and quadrupole moments can be more accurately calculated. CHELP calculates the full electrostatic potential by calculating the potential at a given number of points spherically placed around each atomic center, but not within the van der Waals radius of any of the other atoms. The exclusion of the points that fall within the van der Waals radius is necessary as the electrostatics of these points are distorted by the other nuclei and therefore would produce an incorrect charge for the point charge that it was intended for. Points are thus chosen so that a spherical region with a radius of three angstroms beyond the van der Waals radius of the atoms is probed [60]. Though the CHELP program revealed that there was very little dependence on molecular geometry, Breneman and Wiberg found that the CHELP program did have a dependence on molecular orientation [61]. Breneman and Wiberg developed the CHELPG program in order to remove the orientation dependence. CHELPG uses the same methods as CHELP but alters how the points are chosen in determining the point charges. CHELPG uses an array of equidistant points 0.3 Å apart, and points that are greater than 2.8 Å away from the nucleus are excluded. Thus the difference

20

between the original CHELP program and the CHELPG program is how the points are selected.

CHELP uses points that fit within concentric shells spaced 1.0 Å apart and are not within the van

der Waals radius of the nuclei, while CHELPG uses an algorithm to select points that are equally

spaced. This new point-selection method creates a cube around the molecule. This cube

contains point spaces 0.3 - 0.8 Å apart from one another and contains a buffer region of 2.8 Å on

all sides between the molecule and the cubic boundary. As with the CHELP program, points that

fall within the van der Waals radius of any nuclei are excluded. This inclusion of equally spaced

points makes the CHELPG program less sensitive to molecular orientation [61].

Phenylalanine and all of the possible permutations of fluorinated phenylalanine have

optimization and frequency calculations with the CHELPG program performed at the B3LYP/6-

311++G(d,p) level of theory. Electrostatic surface mapping relative to a positive test point charge

is then performed with the Gaussian 09 software suite with an iso value of 0.0999 and colour

scheme ranging from $-9.0 \times 10^{-6} - 8.0 \times 10^{-2}$ C (blue – red). Quadrupole moments are extracted

from the CHELPG output. Each quadrupole tensor is algebraically transformed so that all

coordinate axes are oriented along the plane of the ring as seen in **Figure 8**.
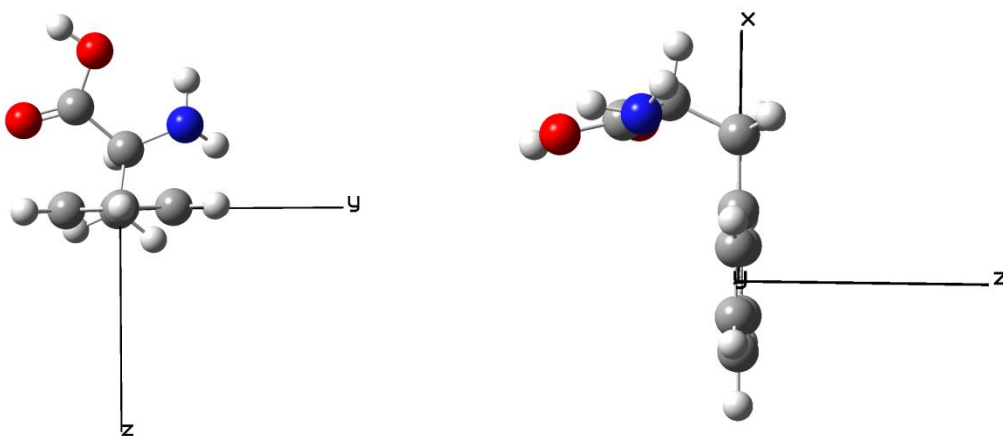
Figure 8: Coordinate system definition of the quadrupole moment axes of bare phenylalanine. The axis orientation shown is the same across all fluorination degrees and permutations allowing comparison between the quadrupole moment tensors

In order to transform the coordinate axis, four steps must be completed. The first step involves a translation of the origin to the center of the phenyl ring. This is done by finding the coordinates of the center of the ring and subtracting them from the molecular coordinate matrix. Steps 2 through 4 involve rotation matrices to align the coordinate axis to the ring plane (**Figure 9**); the subscripts denote which axis the rotation matrix rotates around. After completion of step 4, all molecules will have the coordinate axis oriented as shown in **Figure 8**.

$$R_x(\alpha) = \begin{bmatrix} 1 & 0 & 0 & 0 \\ 0 & \cos\alpha & -\sin\alpha & 0 \\ 0 & \sin\alpha & \cos\alpha & 0 \\ 0 & 0 & 0 & 1 \end{bmatrix} \qquad R_y(\beta) = \begin{bmatrix} \cos\beta & 0 & \sin\beta & 0 \\ 0 & 1 & 0 & 0 \\ -\sin\beta & 0 & \cos\beta & 0 \\ 0 & 0 & 0 & 1 \end{bmatrix}$$

$$R_z(\gamma) = \begin{bmatrix} \cos\gamma & -\sin\gamma & 0 & 0 \\ \sin\gamma & \cos\gamma & 0 & 0 \\ 0 & 0 & 1 & 0 \\ 0 & 0 & 0 & 1 \end{bmatrix}$$

Figure 9: Rotation matrices allowing the optimized coordinate axis to be rotated into the ring plane so all conformations have the same coordinate axis. The subscripts denote which axis the rotation matrix will rotate around. **[62]**

3.3 Results and Discussion

The coordinate axes for each species are the same as the transformed phenylalanine (Phe) coordinate axis in **Figure 8**. As can be seen in **Table 1**, as fluorination increases so does the magnitude of the quadrupole as seen in both the quadrupole tensors as well as the electrostatic potential surface maps. The center of the ring becomes less negative (blue) as fluorination increases; however the electrostatic mappings show low dependence on location of the fluorination. As fluorination increases, the center of the ring shows an increasing positive (red) charge which is indicative of the previously described inverted quadrupole. This should promote increased stabilization of anions. The increasing inverted quadrupole trend is most evident when comparing phenylalanine and 2,3,4,5,6-pentafluorophenylalanine (PentPhe) electrostatic maps. Phe shows a ring which appears to be slightly negative with a neutral central region, which is to

22

be expected as there is an electron withdrawing amino backbone, while PentPhe's electrostatic map is extremely different. PentPhe shows the electron withdrawing capabilities of the fluorination. The fluorines are in a region of dark blue indicating highly negative which allows alternating positive and slightly negative regions going towards the ring. The ring carbons are slightly negative just as Phe showed, however the region of the charge is quite small. There is a narrow band of negative charge with a high positive charge localized in the center of the ring. It is this central charge which allows for the stabilization of anions. Examining the change in fluorination shows a clear correlation between fluorination degree and positive charge in the center of the ring or visualization of the quadrupole moment.

An interesting phenomenon occurs when examining the location of the fluorinations. Although it is apparent the degree of fluorination increases the quadrupole, location shows little effect when analyzing the electrostatic surface maps. However, the quadrupole tensors and Cartesian representations show that although the intensity varies slightly with fluorination location, there is still importance of fluorination permutations. The fluorination location alters the direction of the quadrupole moment though the magnitudes show little variation. Though the fluorination location around the ring alters the direction of quadrupole strength there is no discernible correlation between quadrupole direction and fluorination location at this time.
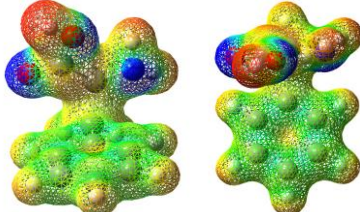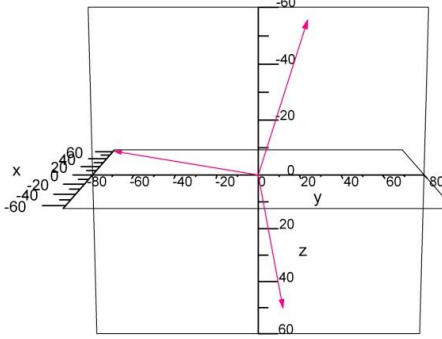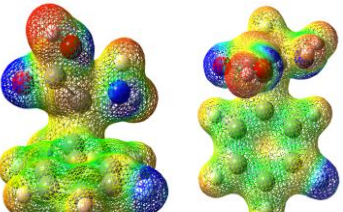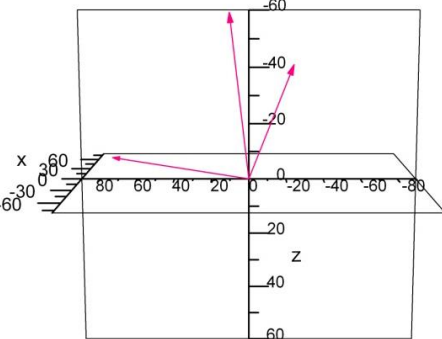
Table 1: Quadrupole Representations of Phenylalanine and Fluorinated Derivatives of Phenylalanine	
Electrostatic Surface Map and Quadrupole Moment Tensor	Cartesian Representation

	x	y	z
x	-58.01	10.49	33.62
y	-6.36	-67.92	-9.54
z	-32.62	21.33	-56.49

Phenylalanine

	x	y	z
x	-53.26	26.24	37.98
y	-19.04	-73.63	-2.29
z	-36.80	21.58	-58.33

2-fluorophenylalanine

	x	y	z
x	69.15	-27.24	-37.29
y	6.02	74.00	-7.04
z	-37.46	9.53	-59.83

3-fluorophenylalanine

Table 1: Quadrupole Representations of Phenylalanine and Fluorinated Derivatives of Phenylalanine
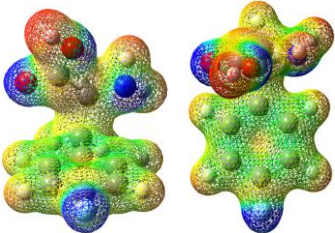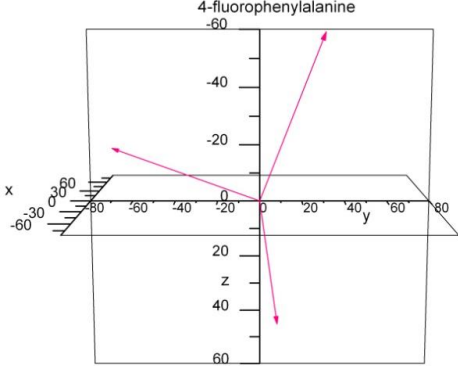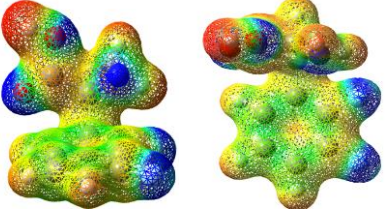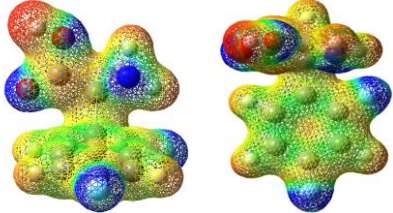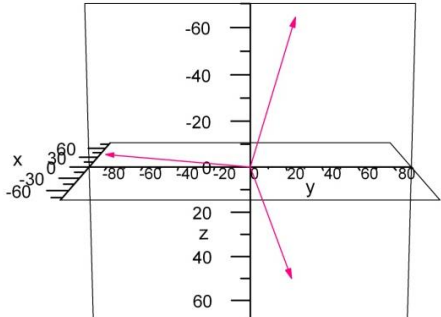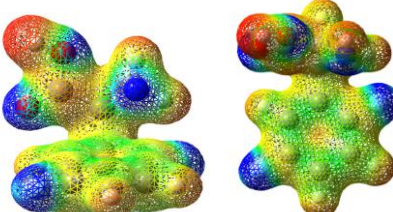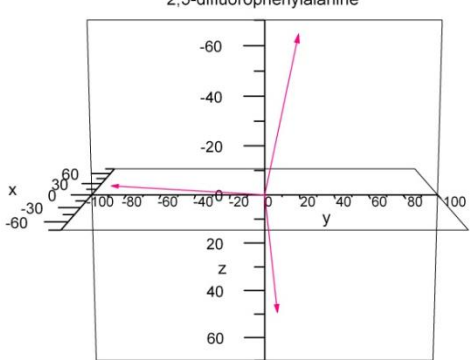
Electrostatic Surface Map and Quadrupole Moment Tensor	Cartesian Representation

	x	y	z
x	-74.63	7.16	29.65
y	-6.64	-68.42	-19.27
z	-31.94	28.90	-59.62

4-fluorophenylalanine

	x	y	z
x	65.51	-44.21	-33.84
y	22.45	76.27	-11.06
z	-37.14	12.94	-64.60

2,3-difluorophenylalanine

	x	y	z
x	-72.87	20.16	31.66
y	-17.65	-77.74	-8.12
z	-34.13	22.90	-65.27

2,4-difluorophenylalanine

	x	y	z
x	-65.02	6.55	32.00
y	-12.38	-86.39	-5.71
z	-33.17	17.85	-65.53

2,5-difluorophenylalanine
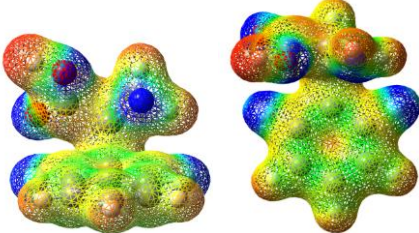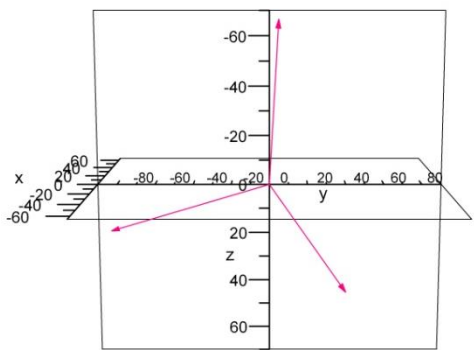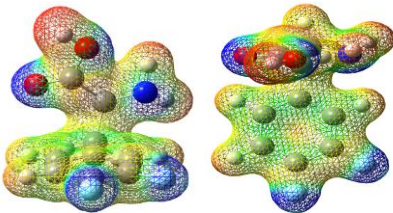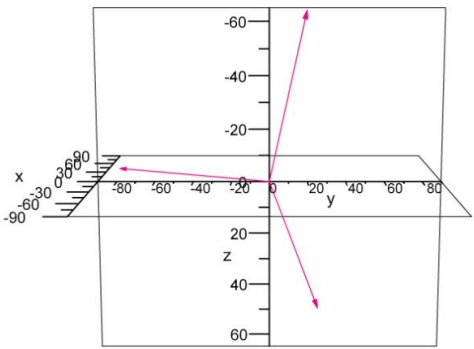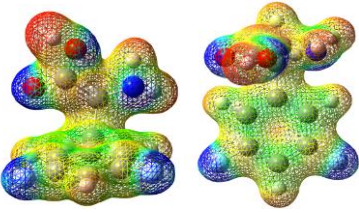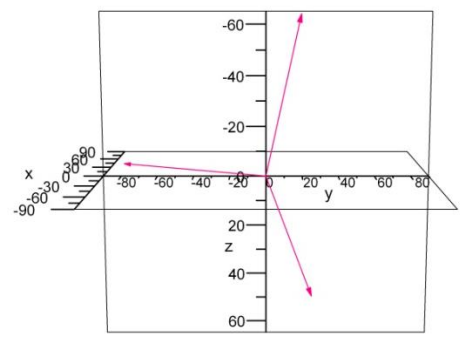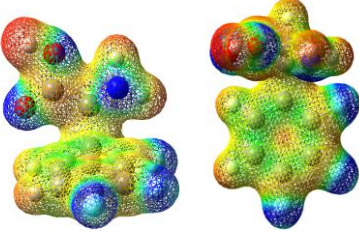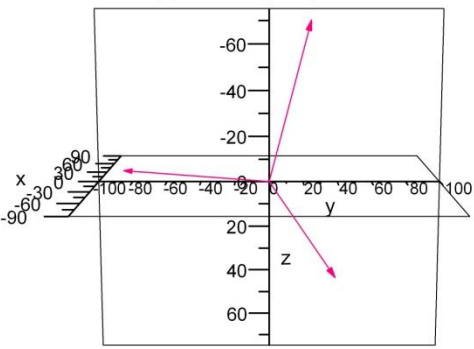
Table 1: Quadrupole Representations of Phenylalanine and Fluorinated Derivatives of Phenylalanine	
Electrostatic Surface Map and Quadrupole Moment Tensor	Cartesian Representation

	x	y	z
x	-58.56	34.88	27.90
y	-16.93	-79.91	15.48
z	-32.14	4.46	-67.52

2,6-difluorophenylalanine

	x	y	z
x	-80.16	22.17	32.50
y	-6.24	-77.45	-5.79
z	-35.92	18.09	-64.65

3,4-difluorophenylalanine

	x	y	z
x	74.08	-13.87	-34.13
y	3.75	85.43	2.80
z	-35.73	14.19	-64.48

3,5-difluorophenylalanine

	x	y	z
x	-80.56	33.94	25.67
y	-20.12	-82.19	-7.66
z	-29.42	23.16	-70.96

2,3,4-trifluorophenylalanine
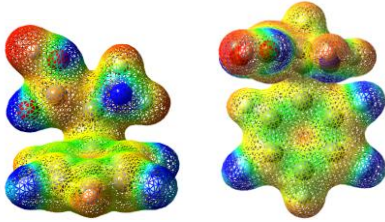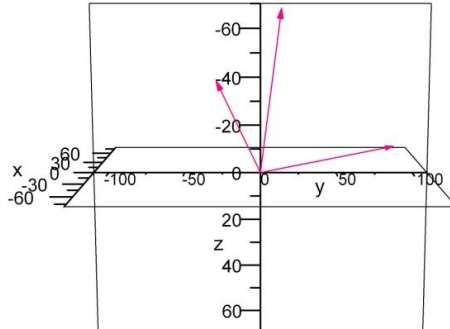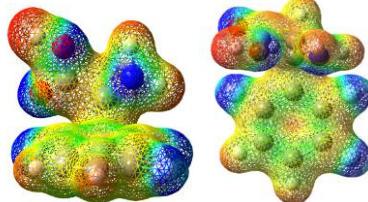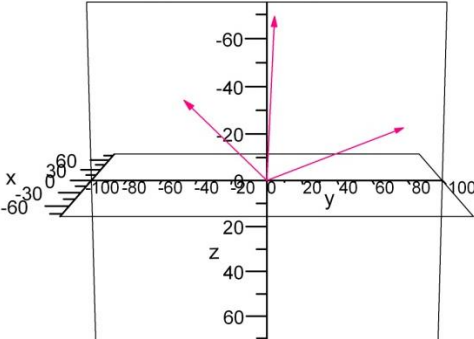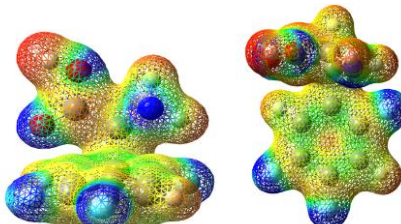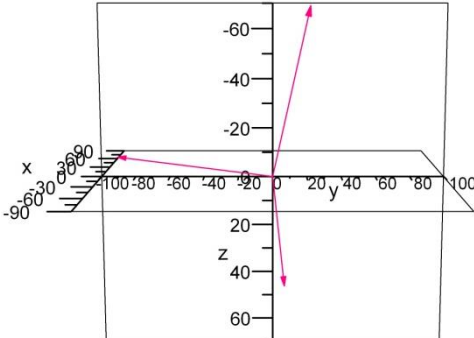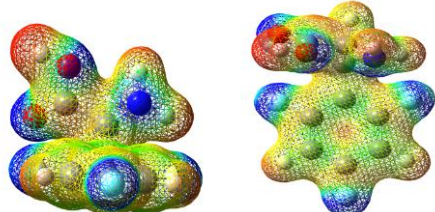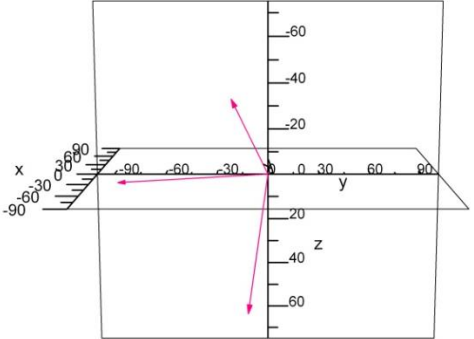
Table 1: Quadrupole Representations of Phenylalanine and Fluorinated Derivatives of Phenylalanine	
Electrostatic Surface Map and Quadrupole Moment Tensor	Cartesian Representation

	x	y	z
x	71.19	-32.85	-32.76
y	22.02	90.93	-8.25
z	-36.56	12.73	-68.87

2,3,5-trifluorophenylalanine

	x	y	z
x	69.71	-53.08	-27.46
y	23.03	80.70	-19.75
z	-34.01	4.12	-70.25

2,3,6-trifluorophenylalanine

	x	y	z
x	-80.06	6.02	28.89
y	-11.66	-88.64	-9.51
z	-33.52	20.61	-69.65

2,4,5-trifluorophenylalanine

	x	y	z
x	81.30	-24.47	-25.71
y	-13.10	-86.18	1.81
z	32.57	-12.34	72.05

2,4,6-trifluorophenylalanine
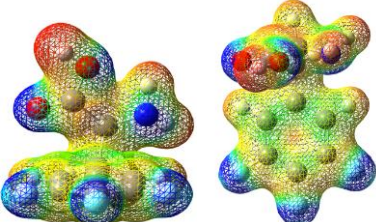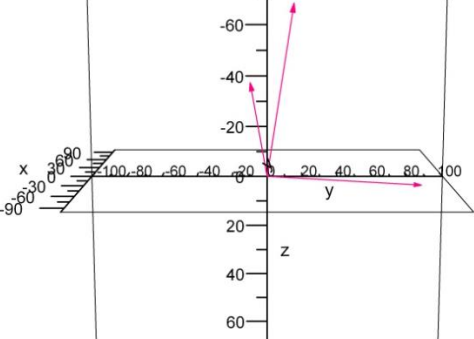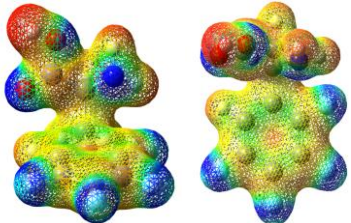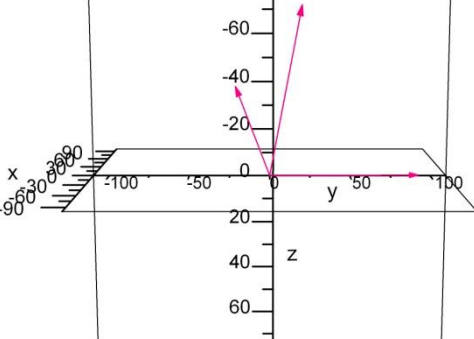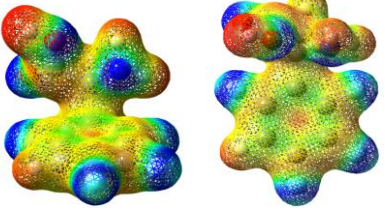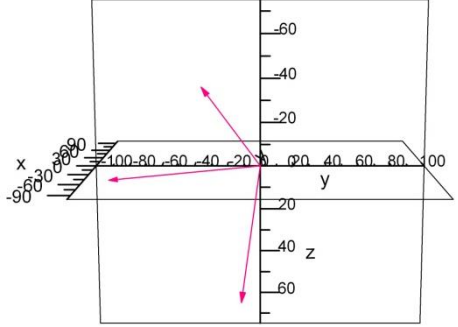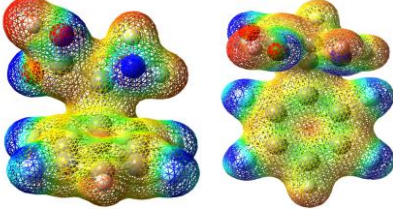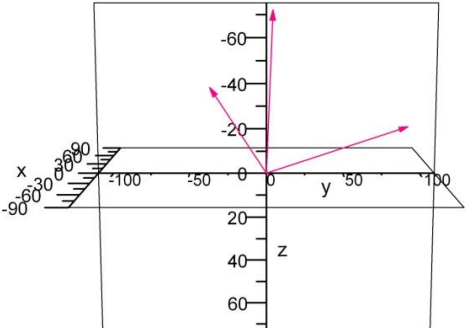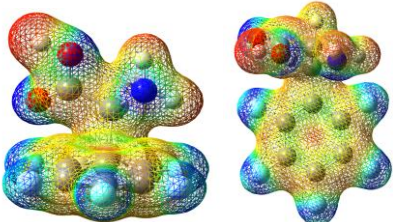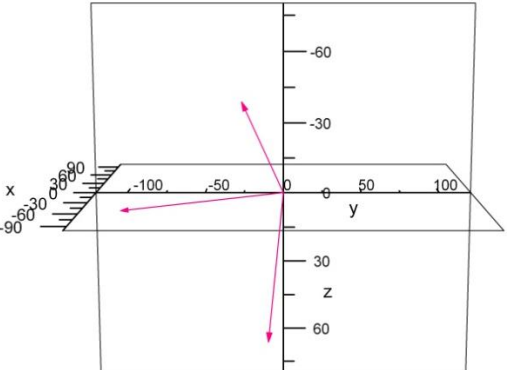
Table 1: Quadrupole Representations of Phenylalanine and Fluorinated Derivatives of Phenylalanine	
Electrostatic Surface Map and Quadrupole Moment Tensor	Cartesian Representation

	x	y	z
x	86.06	-10.86	-31.82
y	1.69	88.38	3.83
z	-36.55	14.11	-68.86

3,4,5-trifluorophenylalanine

	x	y	z
x	85.38	-23.94	-31.71
y	19.13	95.57	2.37
z	-35.96	18.78	-72.61

2,3,4,5-tetrafluorophenyalalnine

	x	y	z
x	85.78	-40.27	-29.52
y	-17.35	-89.94	4.25
z	36.55	-12.42	73.38

2,3,4,6-tetrafluorophenylalanine

	x	y	z
x	75.70	-41.38	-32.13
y	21.49	95.35	-18.46
z	-37.95	4.06	-72.82

2,3,5,6-tetrafluorophenylalanine

Table 1: Quadrupole Representations of Phenylalanine and Fluorinated Derivatives of Phenylalanine

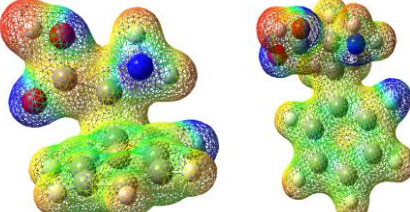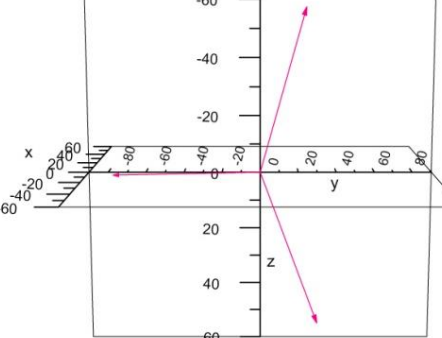| Electrostatic Surface Map and Quadrupole Moment Tensor			Cartesian Representation

	x	y	z
x	89.34	-30.17	-31.55
y	-14.82	-102.15	5.68
z	39.49	-10.37	75.96

2,3,4,5,6-pentafluorophenylalanine

3.4 Conclusions

This investigation aimed to not only quantify the quadrupole moment in phenylalanine and its fluorinated derivatives, but to also find a more accurate representation of the quadrupole moment. Past research described the quadrupole as having distinct regions of positive and negative charges due to molecular orbitals and the inclusion of electron withdrawing groups inverted these charged regions. As was seen in our investigation, the quadrupole moment can be better described as not inverting the charges but by gradually withdrawing the negative charge from the ring center creating an environment capable of accepting anion interactions. The degree of fluorination is extremely important in the strength of the quadrupole. Increasing the amount of electron withdrawing groups on the ring increases the region of positive charge in the center of the ring. However, the location of the fluorine atoms appears to alter the direction not the magnitude of the quadrupole moment. Based on the results, there is no apparent trend between location of the fluorine substituents and direction of the quadrupole tensors. This investigation completed its intended purpose of systematically characterizing and quantifying the quadrupole moments of phenylalanine and fluorinated derivatives of phenylalanine.

Chapter 4

Anion-quadrupole Interactions of Bare and Fluorinated Phenylalanine Derivatives

4.1 Introduction

It has been observed that alteration of the quadrupole moment can have important impacts on biological systems. This alteration can produce a molecule that not only has unique binding interactions, but also creates highly specific inhibitors [4]. The binding interactions of phenylalanine (Phe) and fluorinated derivatives of phenylalanine (FPhe) are of importance as they can provide insight into the specifics of these interactions. An understanding of how anions interact with the quadrupole can lead to m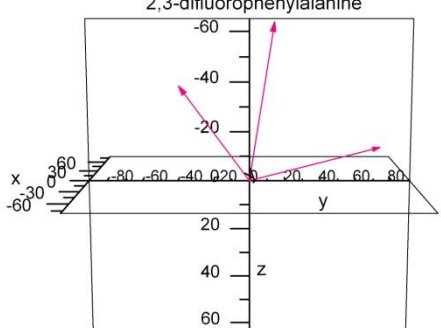echanisms for possible drug delivery systems. We have observed in **Chapter 3** that increasing fluorination of phenylalanine will strengthen the inverted quadrupole moment which should allow for increased anion-quadrupole (anion-π) binding. The interactions between the phenylalanine quadrupole moments and various anions has been analyzed to determine which conformations of the Phe-anion and FPhe-anion species are most likely to exist in the gas phase. As a preliminary investigation, four different anions are investigated along with four species of Phe and FPhe. Phenylalanine (Phe), 3-fluorophenylalanine (3FPhe), 4-fluorophenylalanine (4FPHE), and 2,5-difluorophenylalanine (25FPHE) were chosen as a small sampling of possible permutations of bare and fluorinated phenylalanine derivatives to determine if the hypothesized effects existed. To examine these effects, fluoride (F^-), chloride (Cl^-), bromide (Br^-) and trifluoromethanolate (CF_3O^-) ions were chosen to probe a variety of anions both small and large.

4.2 Methods

In order to analyze the results, both computational chemistry, as described in **§2.1,** and infrared multiple photon dissociation (IRMPD) spectroscopy (**§2.2**) are used.

4.2.1 Computational

Potential structures were found using chemical intuition and prior experiments which indicated where the anions of interest might reside in the gas phase. Optimization and frequency calculations were performed at the B3LYP/6-311++G(d,p) level of theory with a scaling factor of 0.968 [23, 24, 35, 36]. After optimization, single point energy (SPE) calculations were run using the higher level of theory MP2/aug-cc-pVTZ. Upon completion of the SPE calculations, Gibbs free energies and enthalpies were calculated using **Eq. 2.1.1** and **Eq. 2.1.2**. Isomers were then reduced using a cut-off of 15 kJ/mol as previously described. Potential structures that fell within this cut-off then had anharmonic calculations run using the same B3LYP/6-311++G(d,p) level of theory as before. For clusters that had anomalous trends or were lacking experimental spectra, anharmonic calculations for a range of isomers were completed. For the anharmonic calculations scaling factors were not utilized as a Lorentzian fit with a full width half max of 15 cm^{-1} is applied to the results, so a scaling factor for these calculations is not necessary.

4.2.2 Experimental

For this investigation only spectra where chloride anions were the ion of interest were generated. The experimental set-up is as described previously in **§2.1**. A solution matrix of 1:1 acetonitrile and water was combined with a 50:50 mixture of the phenylalanine (or FPhe) and sodium chloride to create a final concentration of ~10^{-4} - 10^{-6} M. This solution was

electrosprayed so as to generate ions of interest, which were trapped within the QIT-MS coupled to an IR-FEL at CLIO. The emission beam was set to run between 46-48 MeV with a scanning frequency range of 1000-2000 cm^{-1} [26, 28 - 31, 41]. The experimental spectra were acquired by prior group members of the McMahon lab in 2009.

4.3 Results and Discussion

4.3.1 Chloride ion (Cl$^-$)

Chloride anions are readily available as salts and thus are easy to acquire and test. In addition to ease of use, these anions represent the relative middle ground of the anions to be tested in terms of both electrostatics and overall size. The relatively small size allows the anion to fit in smaller potential cage-like conformations of the phenylalanine complexes as well as not being too strongly basic as to remove hydrogen from the Phe/FPhe derivatives.

- Phenylalanine---Cl$^-$

Phenylalanine in the presence of a chloride anion was found to have five isomers with relative Gibbs free energy values less than 15 kJ/mol higher than the most stable structure. These five isomers along with a higher energy conformation are displayed in **Figure 10**. These isomers are stabilized by hydrogen bonding networks, charge stabilization and/or edgewise interactions with phenyl ring through quadrupole stabilization. The energetics of the first five isomers implies that they are the most likely to be present in the gas phase. With the exception of PheCl_1 and PheCl_2, the isomers show that for the phenylalanine---Cl$^-$ complex, charge solvated/canonical structures are dominant over edgewise interactions. PheCl_1 and PheCl_2 have both edgewise interactions with the ring and a canonical structure thus stabilizing the chloride ion, though they are the only isomers with edgewise interaction. Although the electronic structure calculations

point to the possibility that all five isomers can be present in the gas phase, definite conclusions

cannot be made without comparison between simulated and experimental spectra.
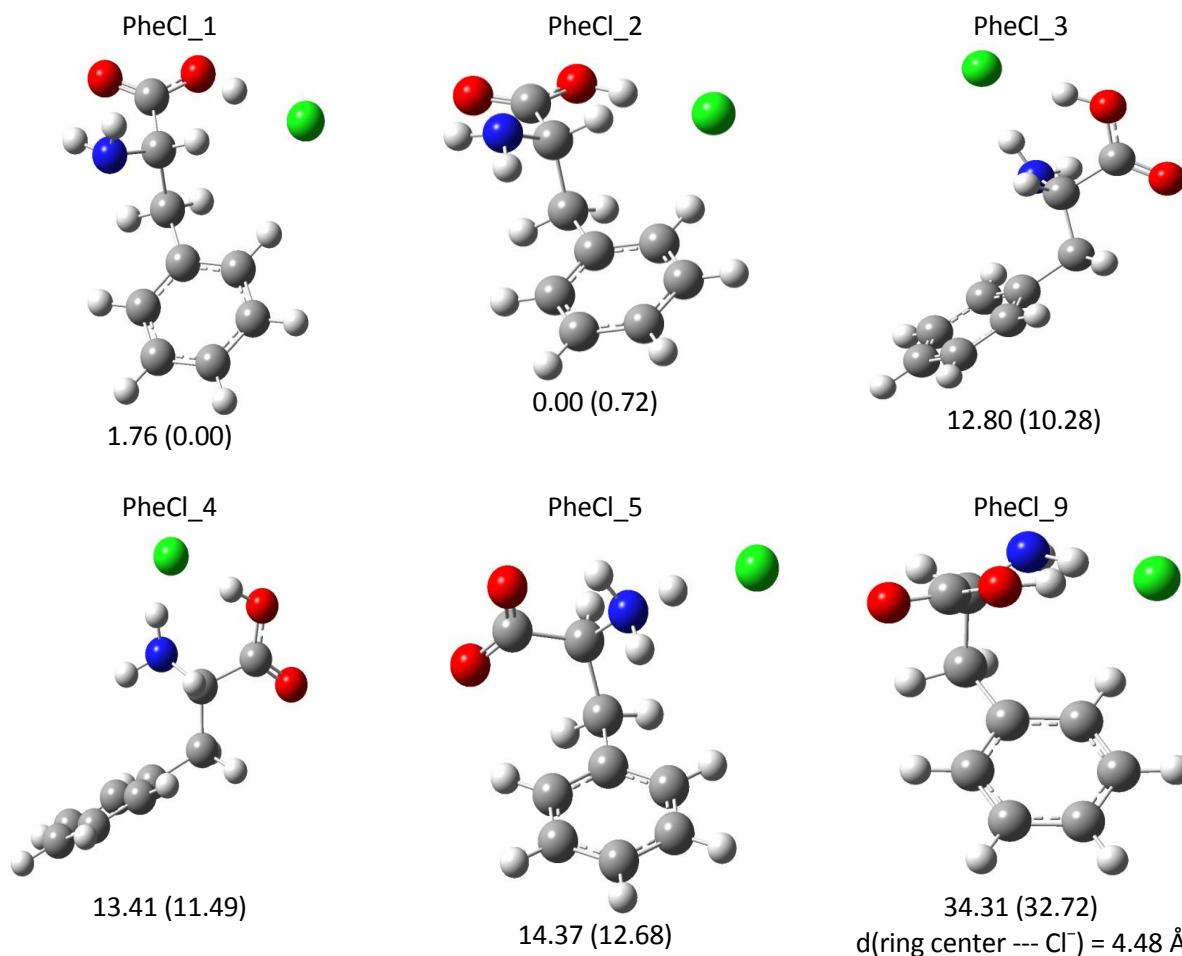
Figure 10: Most Stable Structures of Phenylalanine---Cl⁻. Isomers 1 through 5 are within the 15 kJ/mol cut-off, while Isomer 9 has a good spectral match. Isomers are ordered based on their relative Gibbs free energy values at 298 K. Energetics shown for ΔH (ΔG) in kJ/mol.

Comparison of simulated spectra with the experimental IRMPD spectrum of gaseous

phenylalanine---Cl⁻ complexes identifies which conformations are likely present. Isomers 1, 2 and

4 fail to map the IRMPD vibrations in the 1300-1400 cm^{-1} region. Although these two isomers are

lowest in energy, their failure to map a key region of the gaseous complex suggests that two

cases exist: either higher energy isomers are being generated by the ESI process, or that more

than one isomer is present in the gas phase. Comparison of the IRMPD spectrum to the various

isomers shows that good agreement between spectra exists for isomers 3, 4, and 9. Analysis of the simulated spectra of isomers 3, 4 and 9 show that this region corresponds to bending modes of the ring hydrogens, and bends/rocking of the NH and OH towards the chloride. These modes also exist in the other lowest energy isomers, only shifted to higher wavenumbers (**Table 2**). Isomers 3 and 4 are charge solvated with hydrogen bonding stabilization while isomer 9 has additional ring edge stabilization with both the chloride and the oxygen which is situated above C_1. Although isomers 1 and 2 do not match the 1300-1400 cm^{-1} region they do match the 1650-1800 cm^{-1} region, while isomer 5 fails to accurately fit either region. This would suggest that isomer 5 is likely not present in the gas phase as shifting the simulated spectrum would not improve the fit.

Table 2: Summarized Vibrational Modes of Phenylalanine---Cl⁻ using Wilson and Gardner Notation [63, 64] (Ring stretches of Wilson Notation shown in **Appendix A: Supplementary Information**)

Structure	Vibrational modes (values in cm^{-1})					
IRMPD	**1700 – 1800**	**1600**		**1300 – 1400**		
1	1711	1604		1382		
	C=O stretch	NH₂ Scissor		OH & CH wags, NH₂ twist		
2	1722	1598		1395		
	C=O stretch, NH₂ scissor	Ring stretch (9a)		OH and CH Wags, NH₂ twist		
3	1710	1594		1375		1330
	C=O stretch, COH scissor	Ring stretch (9a)		OH & CH wags, NH₂ twist		
				Ring H wags		
4	1720	1597		1400	1369	1333
	C=O stretch, COH scissor	Ring stretch (9a)		OH & CH wags, NH₂ twist		
				OH & CH wags		
				OH & CH wags, CH₂ twist, Ring H wags		
5	1688	1600	1600	1344		
	Asymmetric O-C=O stretch, HNH₂ scissor	HNH₂ scissor, HN wag		Ring H wags, CH wag		
		Ring stretch (9a)				
9	1716	1602		1374	1351	1339
	C=O stretch, COH scissor, NH₂ scissor, CH wag	Ring stretch (9a)		NH₂ twist, CH wag, Slight CH₂ twist		
				CH₂ rock, CH wag		
				Ring H wags, CH₂ twist		
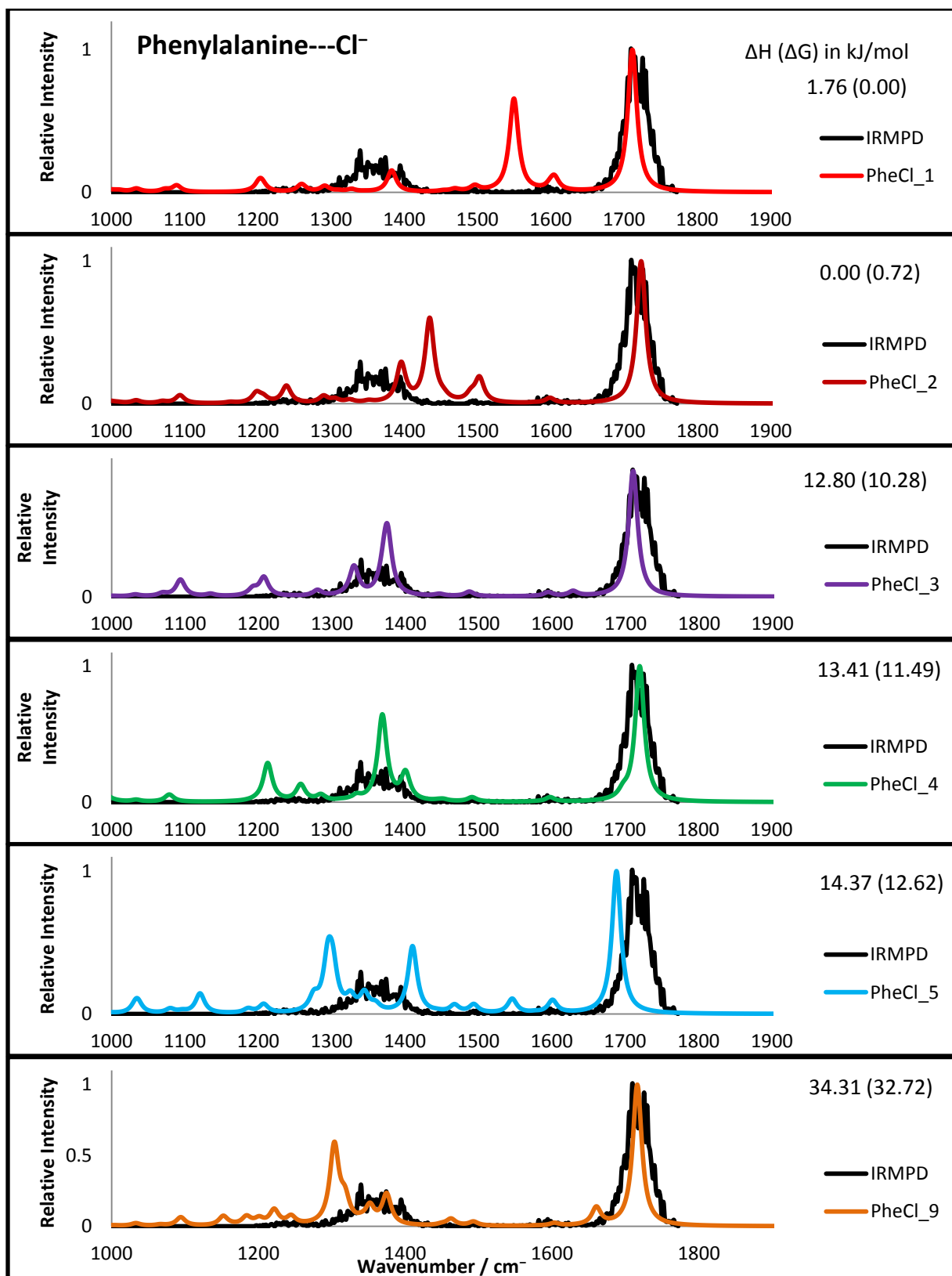
Figure 11: Comparison of computed anharmonic spectra and IRMPD spectrum of Phenylalanine---Cl⁻ for the isomers shown above. Spectra are arranged in increasing relative Gibbs free energy values at 298 K.

Combination of isomeric energetics along with how well the isomers can correctly match the IRMPD spectra illustrates that isomers 3, 4 and 9 are most likely dominant in the gas phase, with isomers 1 and 2 being minor contributions. This shows the importance of both canonical structures as well as edgewise interactions for phenylalanine---Cl⁻ complexes.

- 3-fluorophenylalanine---Cl⁻

As seen in previous chapters, fluorination of the phenyl ring starts the process of inverting the quadrupole moment. Adding one fluorine to the ring will increase the positive charge in the center of the ring slightly, thus increasing the desire for anionic binding with the phenyl ring. Based on the results of **Chapter 3**, it is surmised that although there will be a higher degree of quadrupole-anion interactions, due to the slight increase of positive charge on the ring, edgewise and charge solvated structures should still dominate.

3FPheCl_1
1.05 (0.00)

3FPheCl_2
0.00 (0.91)

3FPheCl_3
12.51 (9.99)

3FPheCl_4
14.16 (12.14)

3FPheCl_5
16.90 (14.97)

3FPheCl_8
30.62 (29.41)
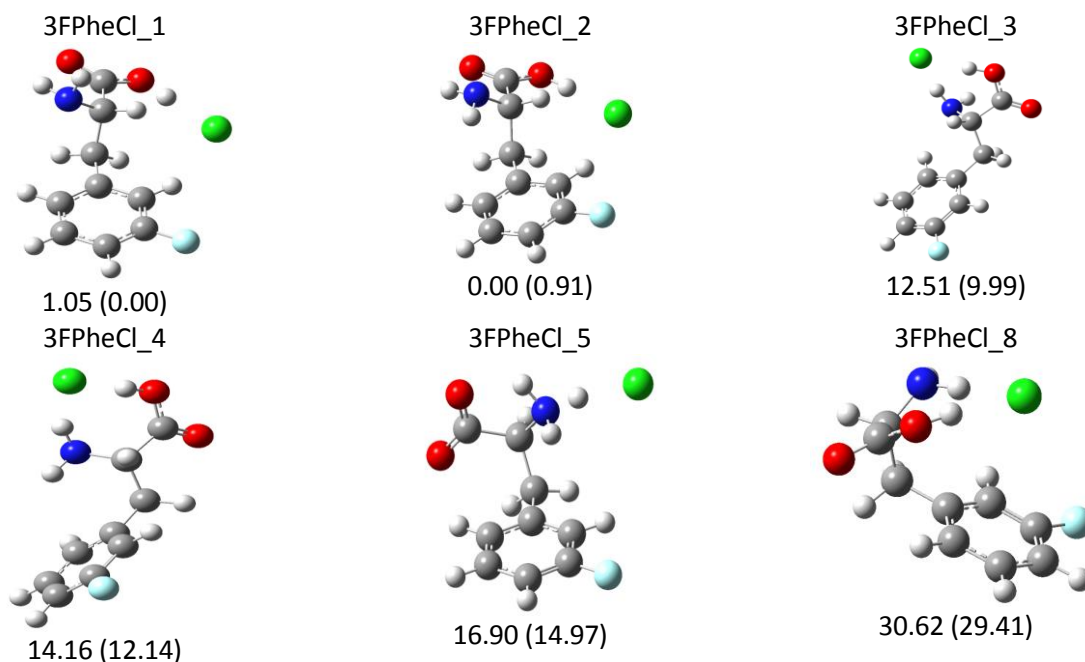
Figure 12: Most stable structures of 3-fluorophenylalanine---Cl⁻ arranged in increasing relative Gibbs free energy (at 298 K). Energetics shown for ΔH (ΔG) in kJ/mol.

Computational calculations showed that there were five unique isomers that all had

energetics below the imposed cut-off value of 15 kJ/mol. These five isomers show the same

structural characteristics as the unfluorinated phenylalanine. This confirms the previous theory

that addition of one fluorine to the ring would not impact the structural conformation to a large

degree. Comparison of the simulated and experimental spectra shows the same trend as the

phenylalanine case. The lowest energy isomers (1 and 2) have good correlation to the higher

energy vibrations of the IRMPD but they fail to match the IRMPD in the lower vibrational regions.

These regions are better mapped with higher energy isomers, specifically isomers 3 and 4 in the

$1300 - 1400$ cm^{-1} region which consists of ring stretches, OH wags and NH$_2$ twists (**Table 3**).

Isomer 8 was included as it shows the evolution of the interactions progressing towards anion-

quadrupole interactions. This higher energy isomer has good correlations between the simulated

and experimental spectra in the 1500 cm^{-1} region, though the spectrum appears shifted. The

1500 cm^{-1} region corresponds to variations of symmetric ring stretches, ring hydrogen wags and a

CH$_2$ wag. These anion-quadrupole interactions appear to influence whether this region can be

accurately mapped. Isomer 5 has poor correlation with all of the peaks seen in the IRMPD

spectrum, though a shift of roughly 100 cm^{-1} would greatly improve the fit. This lack of fit

suggests that isomer 5, and the only isomer below the cut-off that contains a zwitterion, is not

present in the gas phase. Thus, it can be concluded that 3-fluorophenylalanine---Cl$^-$ complexes

do not contain NH$_3$ groups in the gas phase. As isomers 1-4 and 8 combined have excellent

agreement with the IRMPD spectrum it can be inferred that they may all be present in the gas

phase.

Table 3: Summarized Vibrational Modes of 3-fluorophenylalanine---Cl$^-$ using Wilson and Gardner Notation **[63, 64]**
(Ring stretches of Wilson Notation shown in **Appendix A: Supplementary Information**)

IRMPD	1700 – 1780	1600 –1650		1460 – 1500		1330 – 1430		1250 –1278	
	1712	1605	1574	1484	1440	1378	1338	1267	1235
1	C=O stretch, COH scissor, CH wag	NH_2 scissor		Ring H wags		NH_2 twist, CH wag, CH_2 twist, OH wag		Ring H wags, OH & CH wags, CH_2 rock	
		CH_2 twist, Ring stretch (9b)		Ring stretch μ_{24}(b2)		OH wag CH wag		CH_2 rock, Ring breathing (13)	
	1727	1603		1482	1458	1387		1238	
2	C=O stretch, COH scissor, NH_2 scissor	Ring stretch (9a)		Ring H wags		OH & CH wags		CH_2 rock, Ring breathing (13)	
				OH wag, CH wag		NH_2 twist, CH_2 rock			
	1710	1638	1609	1478		1378	1346	1287	
3	OH stretch, COH scissor, CH wag	NH_2 scissor		Ring H wags Slight CH_2 scissor		OH & CH wags, CH_2 rock		Ring H wags, CH wag, CH_2 rock	
		Ring stretch (9a)				OH & CH wags, CH_2 rocking			
	1723	1612	1571	1484		1411	1383	1281	1255
4	C=O stretch, COH scissor	Ring stretch (9a)		Ring H wags		NH_2 twist, OH & CH wags		Ring H & CH & OH wags, CH_2 rock	
		Ring stretch μ_{23}(b2)				OH & CH wags, CH_2 rock		NH_2 twist, Ring H & CH wags, CH_2 twist	
	1681	1607		1481	1460	1402	1330	1273	1234
5	Asymmetric C=O stretch, HNH_2 scissor	Ring stretch (9a)		Ring H wags		HNH_2 scissor		Ring H wags, CH wag, CH_2 rock, NH_3 rock	
				CH_2 scissor		NH_3 umbrella CH_2 rock CH wag		CH_2 rock, Ring breathing (13)	
	1700	1612	1584	1486	1447	1380	1347	1252	
8	C=O stretch, COH scissor, NH_2 scissor	Ring stretch (9a)		Ring H wags		NH_2 twist, CH wag, CH_2 twist		CH_2 rock, OH & CH wags	
		CH_2 twist, Ring stretch (9b)		CH_2 twist, Ring stretch (9b)		CH wag, CH_2 rock			

Vibrational modes (values in cm^{-1})
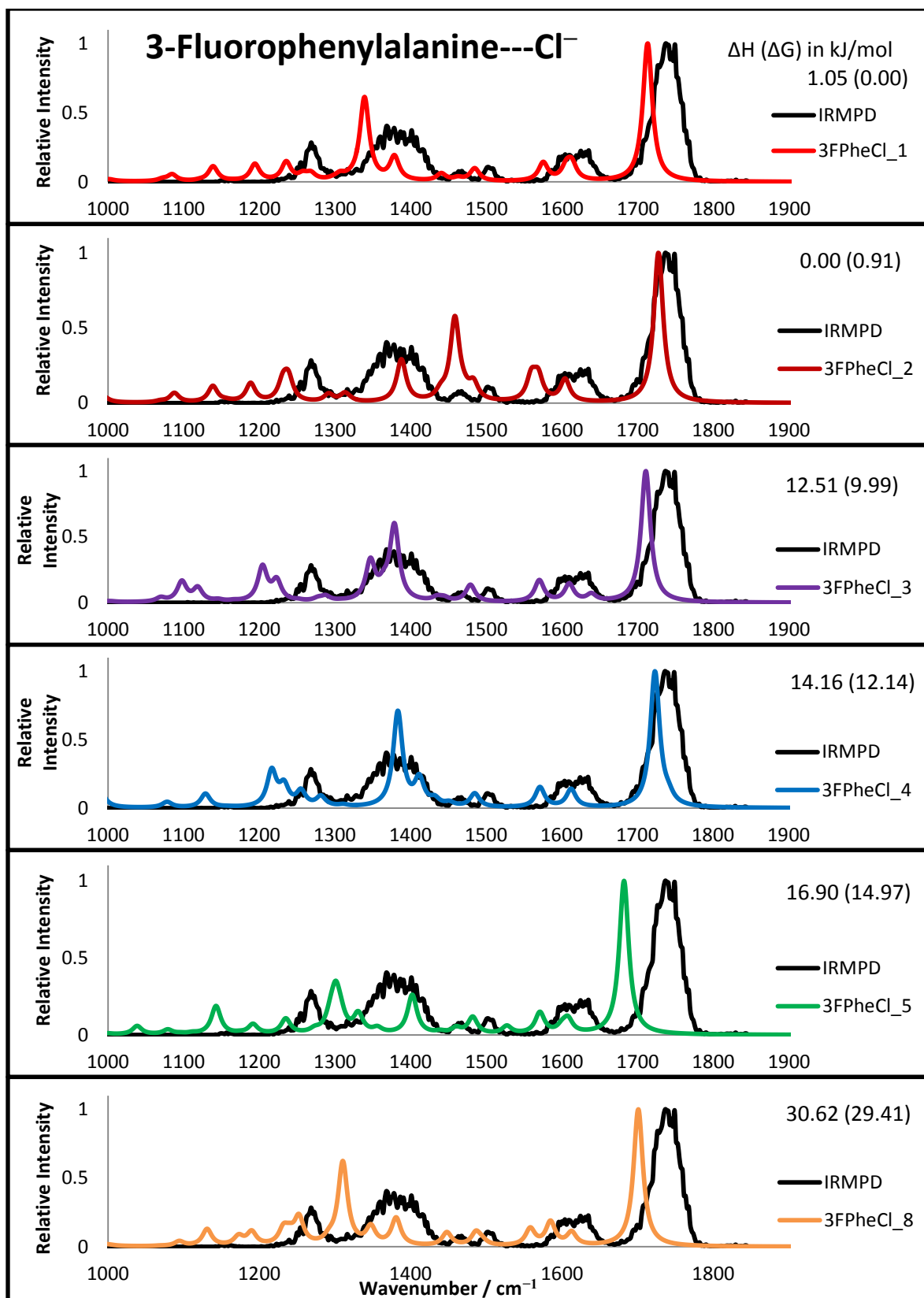
Figure 13: Comparison of simulated anharmonic spectra and experimental IRMPD spectrum of 3-fluorophenylalanine---Cl⁻. Spectra are arranged in increasing relative Gibbs free energy at 298 K.

- 4-fluorophenylalanine---Cl⁻

Fluorination at the 4- position should have the same effect as the previous fluorination at the 3- position. As seen in **Chapter 3**, variation of position of the electron withdrawing substituent does not alter the magnitude of the quadrupole, it only affects the directionality. Thus this alteration should produce isomers that are similar to that of the 3-fluorophenylalanine---Cl⁻ and phenylalanine---Cl⁻ complexes. This indicates that edgewise interactions in addition to charge stabilization should dominate over quadrupole-anion interactions. However, as was also seen in the 3-fluorophenylalanine---Cl⁻ complexes, interactions between the ring and chloride ion better predict the experimental spectrum at lower vibrational frequencies.
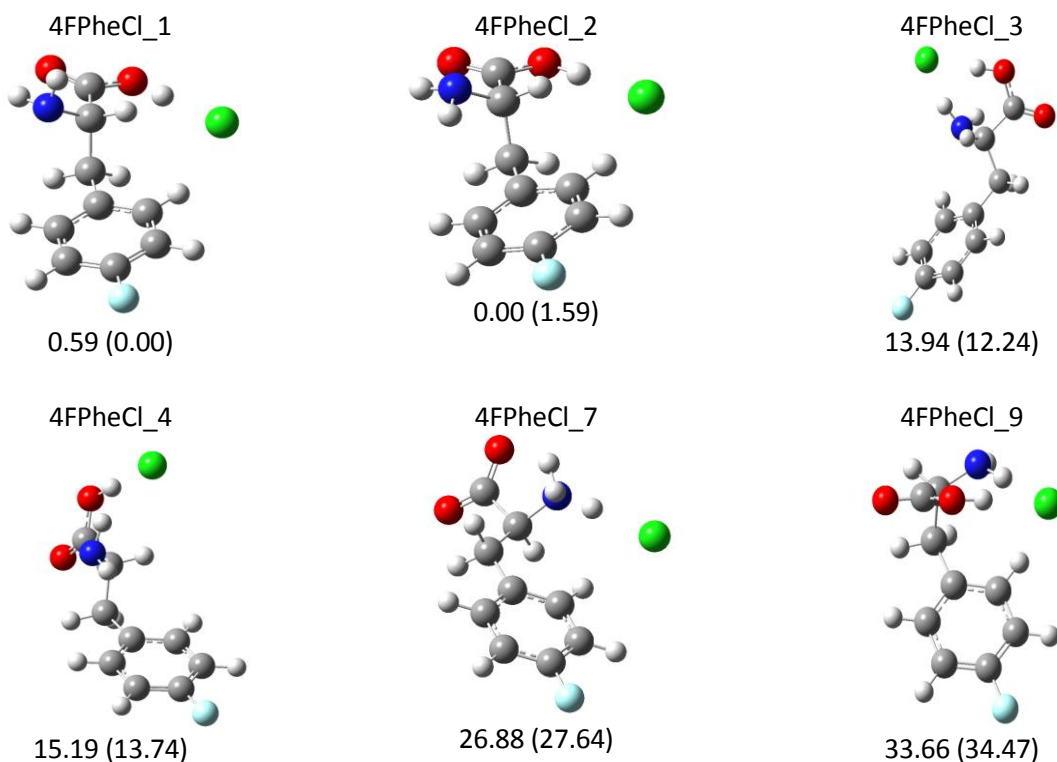
Figure 14: Most stable structures of 4-fluorophenylalanine---Cl⁻, arranged in increasing relative Gibbs free energy at 298 K. Isomers 7 and 9 are included as they have regions of good overlap between the simulated and experimental spectra. Energetics shown for ΔH (ΔG) in kJ/mol.

Electronic structure calculations found that only four isomers fell below the 15 kJ/mol cut-off. These four isomers all mimic the previously observed isomers for the prior two phenylalanine species. Analysis of the fits between simulated and experimental spectra illustrates the same trend as before. The lower energy isomers fit the higher vibrational frequencies but miss the vibrations associated with ring breathing modes, various hydrogen modes including ring hydrogens, carboxyl hydrogen and amine hydrogen wags, twists, bends and scissors. These modes are still present, but are not as strong as the higher energy isomers. This indicates that the chloride presence is greatly affecting these vibrational regions. None of the isomers can accurately reproduce the breathing modes of the ring located around 1250 cm^{-1}, though some isomers come close, specifically isomers 2, 4, 7 and 9. These isomers show weak peaks in this region. These isomers all differ in how the chloride interacts with 4-fluorophenylalanine, though they share one commonality. Each of these isomers has one hydrogen pointing towards the ring edge for edgewise interactions. This implies that the lower vibrational bands stem from edgewise ring interactions.

Table 4: Summarized Vibrational Modes of 4-fluorophenylalanine---Cl⁻ using Wilson and Gardner Notation **[63, 64]**
(Ring stretches of Wilson Notation shown in **Appendix A: Supplementary Information**)

Vibrational modes (values in cm^{-1})

IRMPD	1680 – 1750	1600	1500 – 1530		1313 – 1415				1220 – 1250		1165
1	1715	1606	1502		1384				1208		1152
	C=O stretch, OH & CH wags, NH$_2$ scissor	NH$_2$ scissor	Ring stretch (8a)		NH$_2$ twist, OH & CH wags				OH & CH wags, ring breathing (13)		Slight ring breathing (13)
2	1728	1596	1524	1501	1396	1338	1313		1242		1156
	NH$_2$ scissor, C=O stretch, OH & CH wags	Ring stretch (9a)	NH$_2$ scissor	Ring stretch (18a)	OH & CH wags, NH$_2$ twist CH$_2$ rock / OH & CH & ring H wags NH$_2$ twist / CH$_2$ rock, CH wag, Ring stretch (15)				CH$_2$ & NH$_2$ twists, OH & CH wags		Ring stretch (8a)
3	1710	1599	1499		1375	1346			1196		1152
	C=O stretch, COH scissor	Ring stretch (9a)	Ring H wags		CH$_2$ rock, OH & CH wags, NH$_2$ twist / CH$_2$ rock OH & CH & ring H wags				OH & CH wags, Ring breathing (13)		Ring H wags
4	1723	1592	1498		1409	1383			1255	1214	1153
	C=O stretch, OH & CH wags	Ring stretch (9a)	Ring stretch (8a)		OH & CH wags, NH$_2$ twist CH$_2$ rock				CH wag, NH$_2$ & CH$_2$ twist	CH & OH wags, NH$_2$ twist, CH$_2$ rock	CH$_2$ & NH$_2$ twists, OH & CH wags, Ring stretch (15)
7	1705	1597	1508		1385	1409	1358	1315	1248	1205	1158
	NH$_3$ umbrella, Asymmetric C=O stretch	Ring stretch (9a)	Ring stretch (8a)		NH$_3$ umbrella / NH$_3$ umbrella, CH$_2$ scissor Ring stretch μ$_{23}$(b2) / Ring H & OH wags CH$_2$ rock, HNH$_2$ rock / Ring stretch μ$_{23}$(b2)				Ring H wag, NH$_3$ umbrella, CH$_2$ rock	Ring breathing (13), Asymmetric NH$_3$ umbrella, CH$_2$ rock, CH wag	Ring stretch (9a)
9	1714	1601	1502		1378	1348			1251	1231	1150
	C=O stretch, NH$_2$ scissor, OH & CH wags	Ring stretch (9a)	Ring H wag		NH$_2$ twist, CH wag, CH$_2$ scissor / CH$_2$ rock OH wag				CH$_2$ rock, OH & CH wags	OH & CH wags CH$_2$ twist	CH$_2$ & NH$_2$ twist, OH & CH wags

Figure 15: Anharmonic Spectra of 4-Fluorophenylalanine---Cl⁻ arranged in increasing relative Gibbs free energy at 298 K.

Higher energy vibrational bands (1500, 1600 and 1700 – 1800 cm^{-1}) come from OH stretches, HOC and NH$_2$ scissors as well as various ring vibrations (**Table 4**). Isomer 3 has the best overall spectral match to the IRMPD spectrum, though some shifting is observed for the higher frequency IRMPD peaks. As the lower energy isomers match the higher vibrations, and the higher energy isomers can better predict the low energy vibrational regions, it can be inferred that a mixture of these isomers likely exists in the gas phase.

- 2,5-difluorophenylalanine---Cl$^-$

Addition of a second electron withdrawing group to the phenyl ring pushes the electrostatic charge of the phenyl ring to be more positive, thus increasing the ability for anion stabilization. Computational calculations found six unique isomers all within the energetic cut-off of 15 kJ/mol. Unlike past Phe and FPhe derivatives that were observed, an isomer that has direct interaction between the phenyl ring and the chloride anion is within the cut-off (isomer 6); while edgewise interactions with the ring are still favoured (isomer 5). This increase in stability of an isomer with direct ring interactions illustrates the increasing strength of the quadrupole moment. The addition of the second fluorine to the ring is still not enough to invert the quadrupole charge and thus a strong prevalence of charge solvated or canonical structures are observed.
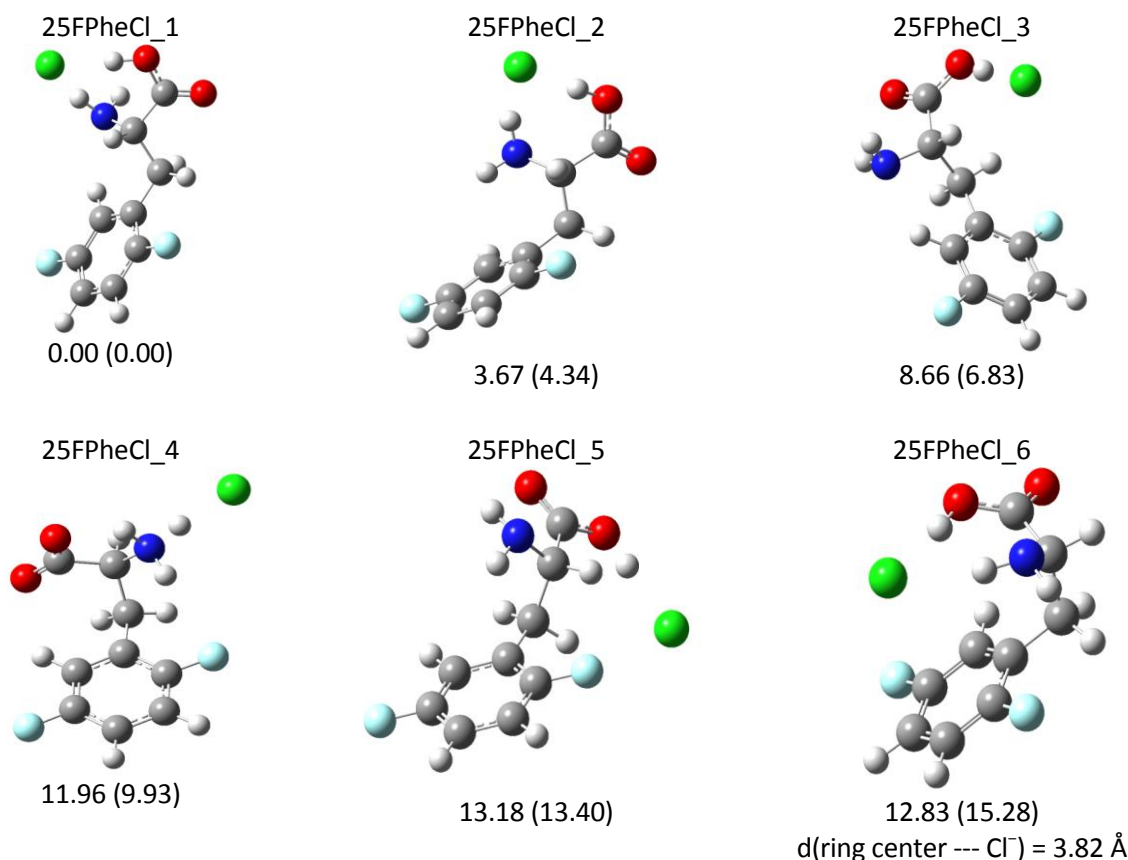
Figure 16: Most Stable Structures of 2,5-difluorophenylalanine---Cl⁻ ordered with increasing relative Gibbs free energy at 298 K. All six isomers are within or on the border of the 15 kJ/mol cut-off. Energetics shown for ΔH (ΔG) in kJ/mol.

Analysis of the simulated spectra and IRMPD spectrum (**Figure 17**) demonstrates that the lower energy isomers, whose stability is dominated by charge solvation, are getting better at predicting the lower energy vibrational regions. As previously observed, the higher vibrational regions correspond to CO stretches, CO_2H and NH_2 scissors, and ring rocking and various ring modes, while the lower modes correspond to ring stretches, hydrogen wags, and scissors and bends of hydrogens involved in the amino backbone. Isomers 1 and 2 show good correlation with all peaks present in the IRMPD spectrum. This indicates that unlike prior cases where lower regions were not well reproduced, addition of the second fluorine increases the fit of the simulated spectra for the lower energy isomers. Isomer 3 fits poorly in the region associated with ring and hydrogen modes (1300-1400 cm^{-1}), while the remaining isomers 4-6 show peaks that

appear shifted to lower frequencies (**Table 5**). Isomers 3-6 would have a better fit if their spectra were slightly blue shifted. Blue shifting the spectra would result with isomers 3 and 4 having good agreement with experiment, isomer 5 would better fit the lower vibrational regions and shifting isomer 6 would result in better fitting with 1700-1800, 1300-1400, and the 1200 cm^{-1} regions while at 1500 cm^{-1} would have worse overlap. This implies that the likely isomers present in the gas phase are isomers 1 and 2. Thus the canonical structures are still dominant for 2,5-difluorophenylalanine---Cl$^-$ complexes.

Table 5: Summarized Vibrational Modes of 2,5-difluorophenylalanine---Cl⁻ using Wilson and Gardner Notation [63, 64]
(Ring stretches of Wilson Notation shown in **Appendix A: Supplementary Information**)

Vibrational modes (values in cm^{-1})

IRMPD	1680 – 1760	1583 – 1634	1480 – 1530	1330 – 1420	1247 – 1330	1206 – 1247
1 (freq)	1713	1628, 1577	1484	1386, 1369, 1325	1286, 1248	1201
1 (assign)	COH scissor, C=O stretch, NH$_2$ scissor, CH wag	NH$_2$ twist, Slight ring stretch (9a) / CH$_2$ twist, Ring stretch μ$_{23}$(b2)	CH$_2$ twist Ring stretch (18a)	NH$_2$ twist, CH$_2$ rock, OH & CH wags / NH$_2$ twist, CH$_2$ rock, OH & CH wags, OH stretch / CH$_2$ rock, OH & CH wags	CH$_2$ wag, OH & CH wags, Ring stretch (15) / NH$_2$ & CH$_2$ twists, OH & CH wags, Ring breathing (13)	OH & CH wag, C-O stretch, NH$_2$ twist, CH$_2$ wag,
2 (freq)	1718	1621, 1584	1487	1400, 1375	1262	1215
2 (assign)	C=O stretch, COH scissor, OH wag	Ring stretch (9a) / Ring stretch (9b)	Ring stretch (18a), CH$_2$ twist	NH$_2$ twist, CH$_2$ rock, OH & CH wags, CO stretch / OH & CH wags, CH$_2$ rock	CH wag, NH$_2$ & CH$_2$ twists, ring stretch μ$_{24}$(b2)	Slight ring stretch μ$_{24}$(b2), NH$_2$ twist, CH$_2$ rock, OH & CH wags, CO stretch
3 (freq)	1707	1632, 1583	1479	1396, 1361	1312	1209
3 (assign)	C=O stretch, COH scissor, OH wag,	NH$_2$ scissor / Ring stretch (9b)	CH$_2$ rock, Ring stretch (18a)	CH wag, NH$_2$ & CH$_2$ twists / CH$_2$ rock, OH & CH wags	OH & CH wags, CH$_2$ twist, ring stretch μ$_{25}$(b2)	C-O stretch, OH & CH wags, CH$_2$ rock
4 (freq)	1713	1618	1483	1396, 1355	1322, 1312, 1300	1237, 1197
4 (assign)	Asymmetric CO$_2$ stretch, NH$_3$ umbrella	Ring stretch (9a)	CH$_2$ twist, ring stretch (18a)	CH$_2$ scissor, NH$_3$ umbrella / CH$_2$ rock, CH wag, NH$_3$ umbrella	Symmetric CO$_2$ stretch, CH$_2$ rock, CH wag, NH$_3$ umbrella / Symmetric CO$_2$ stretch, CH$_2$ rock, CH wag, NH$_3$ umbrella, ring stretch (15) / Symmetric CO$_2$ stretch, CH$_2$ rock, CH wag, NH$_3$ rock	Ring breathing (2), CH$_2$ rock, CH wag / Ring stretch (7b), CH$_2$ twist, CH wag, NH$_3$ umbrella
7 (freq)	1713	1617, 1584	1487	1372	1320, 1289, 1248	1205
7 (assign)	C=O stretch, COH & NH$_2$ scissor, OH wag	Ring stretch (9a) / NH$_2$ scissor, CH$_2$ twist, ring stretch (9b)	CH$_2$ scissor, ring stretch (18a)	NH$_2$ twist, symmetric CO$_2$ stretch, OH & CH wags	CH$_2$ scissor, OH & CH wags / CH$_2$ rock, OH & CH wags, NH$_2$ twist / Ring breathing (2), CO$_2$ symmetric stretch, NH$_2$ twist, OH wag	Ring stretch (7b), OH wag, CH$_2$ twist
9 (freq)	1703	1627, 1591	1532, 1491	1424, 1383, 1348	1306, 1263, 1242	1175, 1161
9 (assign)	C=O stretch COH & NH$_2$ scissors CH wag	Ring stretch (9a) / Ring stretch μ$_{23}$(b2)	NH$_2$ scissor / CH$_2$ twist, Ring stretch (18a)	Ring stretch (18a), CH$_2$ twist, CH wag / NH$_2$ and CH$_2$ twist, CH & OH wag / CH$_2$ rock, CH wag	OH & CH wag, C-O stretch, CH$_2$ rock / OH & CH wag, CH$_2$ twist, Ring H wags / OH & CH wags, CH$_2$ rock, ring H wags	OH & CH wag, NH$_2$ & CH$_2$ rock, Ring stretch (7b) / OH stretch, CH wag, NH$_2$ & CH$_2$ twist, Ring stretch (7b)
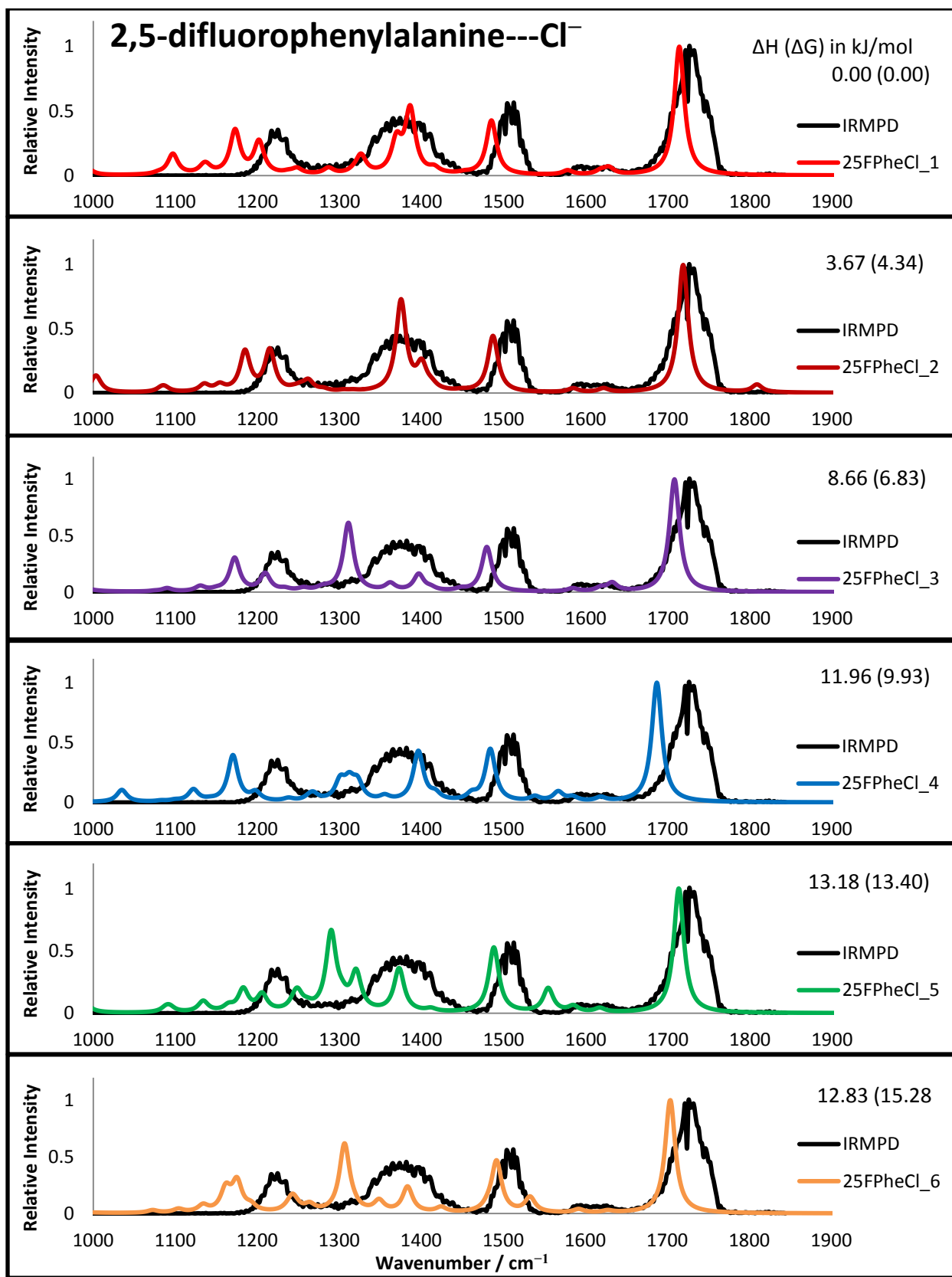
Figure 17: Anharmonic Spectra of 2,5-difluorophenylalanine---Cl⁻. Spectra are ordered with increasing relative Gibbs free energy at 298 K.

4.3.2 Fluoride ion (F⁻)

The fluoride anion is a more compact and thus harder anion than chloride due to its smaller ionic radius. Hard ions have small ionic radii so the electrons are held closer to the nucleus creating a compact ion. The smaller ionic radius should result in increased interactions with both the ring edge as well as the amino terminus. This will also increase the possibility of creating zwitterions in the gas phase. As there is currently no experimental IRMPD spectrum available, only energetics can be compared. As seen with the chloride case, energetics alone are not enough to determine which species are present in the gas phase. This section will aid in future determinations of which structures are present in the gas phase as all calculations prior to acquiring experimental data have been completed. Simulated anharmonic spectra for the lowest energy isomers are included for completeness in **Appendix A: Supplementary Information**.

- Phenylalanine---F⁻

For phenylalanine---F⁻ complexes, seven isomers had energetics below the 15 kJ/mol cut-off. All of the seven isomers show interesting properties between the fluoride anion and either the carboxylic acid or an amine hydrogen. Abstraction of a proton has occurred in all seven isomers. These proton transfer (PT) clusters have vibrations where the hydrogen is oscillating between the fluoride and the phenylalanine at 1600 - 1700 cm^{-1} and around 1900 – 2000 cm^{-1}. The lower of the two modes is easily accessible by IRMPD while the upper vibrations may be accessible depending on the specific isomer.

PheF_1

0.00 (0.00)
d(H---F) = 1.04
d(O---H) = 1.36

PheF_2

1.43 (3.18)
d(H---F) = 1.04
d(O---H) = 1.36

PheF_3

7.26 (8.73)
d(H---F) = 1.04
d(O---H) =1.34
d(N-H--F) = 2.07

PheF_4

7.26 (8.75)
d(H---F) = 1.04
d(O---H) = 1.34
d(N-H--F) = 2.07

PheF_5

11.18 (12.97)
d(H---F) = 1.03
d(O---H) = 1.47

PheF_6

13.65 (12.98)
d(H---F) = 1.06
d(O---H) = 1.32
d(N-H--F) = 2.09

PheF_7

14.72 (14.47)
d(H---F) = 1.04
d(O---H) =1.34
d(N-H--F) = 2.09
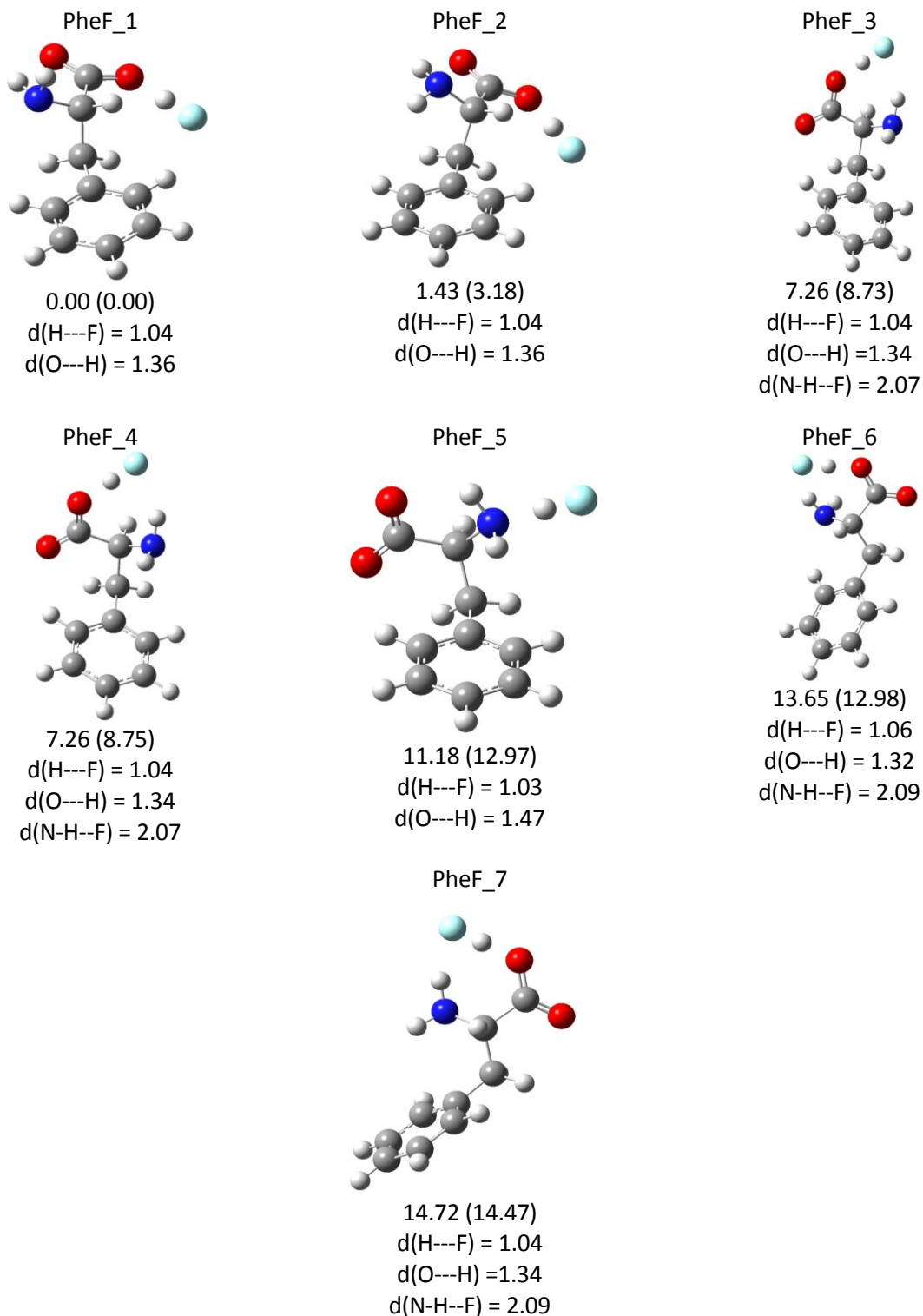
Figure 18: Most Stable Structures of Phenylalanine---F⁻. Isomers are arranged in increasing relative Gibbs free energy at 298 K. Distances between the fluoride and respective hydrogens all show proton transfers occurring. Energetics ΔH (ΔG) in kJ/mol with distances in Å.

The six unique isomers below the cut-off show the same trends seen with the chloride anion, where edgewise interactions with the ring are observed. The energetics predict that in the gas phase, when a fluoride anion is present, proton transfers leading to proton abstraction will dominate over charge solvated structures, as all structures within the 15 kJ/mol cut-off are demonstrating transfers. The most stable structures, isomers 1 and 2, show proton transfer (PT) between the carboxyl group and the fluoride anion, with the fluoride being close to the ring plane. This implies that edgewise stabilization as described by Jackson *et al.* is playing a factor [14]. The chloride complex investigations would suggest that the orientation of the NH_2 group plays an important part in spectral comparisons and as isomer 2 has the NH_2 group pointing down towards the ring, it is likely that isomer 2 would have a better spectral fit than isomer 1.

As previously mentioned, without an experimental spectrum to compare with, one can only speculate as to which species are present in the gas phase. As the lowest energy isomers are all relatively close in energy, it is possible that many of these structures are present in the gas phase. Using the conclusions made from the phenylalanine---Cl^- complexes as a guide, it is likely that isomer 5 would have a poor spectral match due to the absence of a NH_3 group and is likely not present in the gas phase. Isomers 2, 3, 4 and 7 should have good overlap due to additional interactions of hydrogen atoms pointing towards the ring. It is difficult to anticipate which patterns seen with a chloride anion are present in the fluoride anion case as chloride was stabilized by charge solvation, while the fluoride anion produced proton transfers and thus, a completely different class of compounds. As all of the lowest energy isomers are relatively close in both energetics and structure, it is not possible to determine exactly which species are present in the gas phase with any certainty without experimental data. In preparation for an

experimental IRMPD spectrum, anharmonic calculations of all isomers have been completed. The

calculated spectra for the lowest energy isomers shown in **Figure 18** are included in **Appendix A**.

- 3-fluorophenylalanine---F⁻

As only one electron withdrawing substituent does not alter the electrostatics enough for

quadrupole-anion interactions to be dominant, it is expected that the previously observed PT

structures will dominate with potential for weak edgewise interactions with the hydrogen

fluoride species. Electronic structure calculations produced six unique isomers within the 15

kJ/mol cut-off as seen in **Figure 19**. These structures are different from previously seen isomers

in that isomer 2 has the amino backbone rotated so that the NH_2 group is slightly above the plane

of the ring. Based on energetics alone, isomers 1-3 should be present in the gas phase as they

only differ by 5.11 kJ/mol. However, as was seen with the complexes involving a chloride anion,

higher energy isomers may better match experimental spectra, thus energetics can only act as a

guideline for which conformations may be present.

3FPheF_1

0.00 (0.00)
d(H---F) = 1.04
d(O---H) = 1.36
d(ring C_2-H---F) = 2.41

3FPheF_2

5.11 (0.39)
d(H---F) = 1.47
d(O---H) = 1.09

3FPheF_3

2.42 (4.58)
d(H---F) = 1.04
d(O---H) = 1.35

3FPheF_4

12.48 (12.22)
d(H---F) = 1.02
d(O---H) = 1.35

3FPheF_5

14.49 (13.96)
d(H---F) = 1.06
d(O---H) = 1.32
d(N-H--F) = 2.08

3FPheF_6

16.18 (14.09)
d(H---F) = 1.03
d(O---H) = 1.36
d(N-H--F) = 2.15
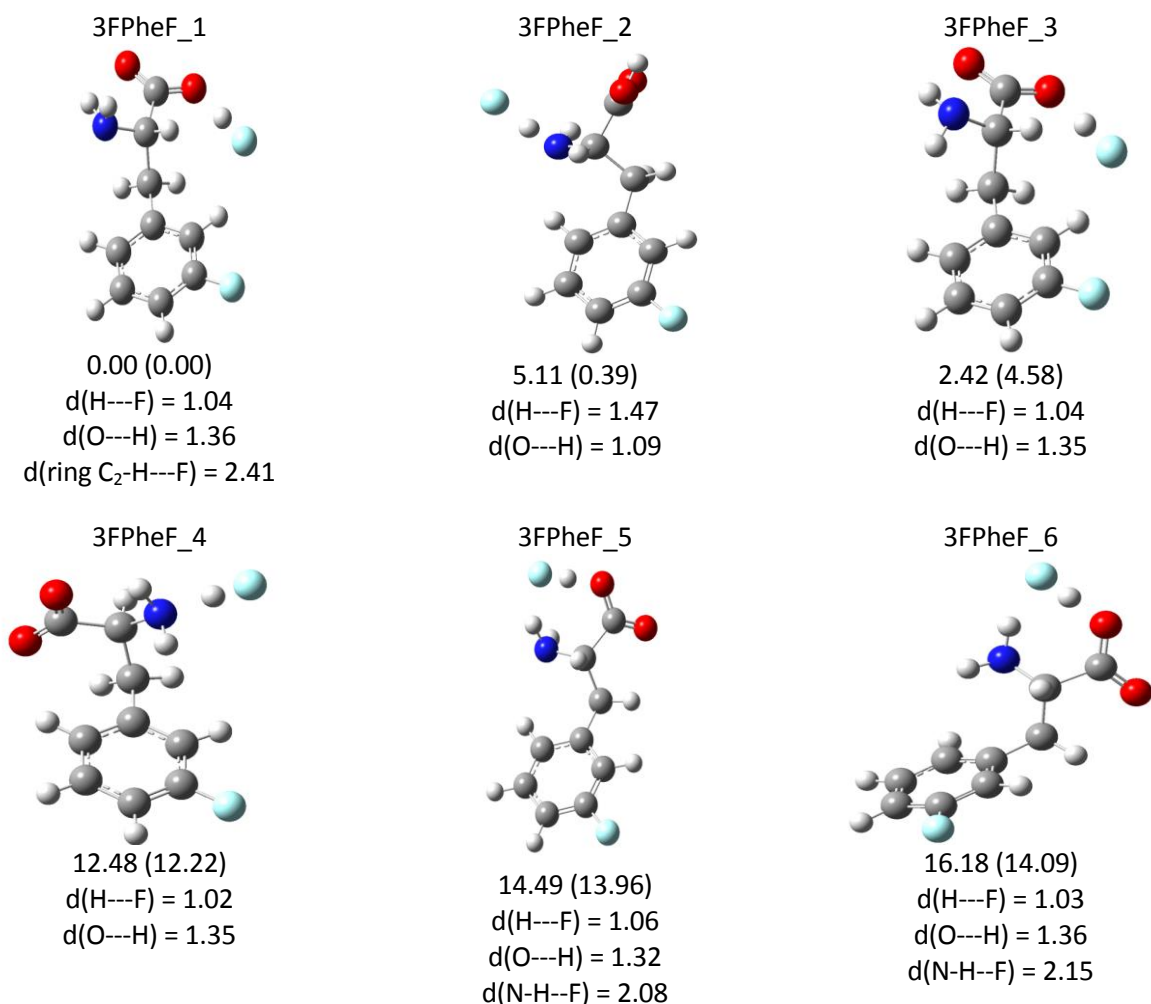
Figure 19: Most Stable Structures of 3-fluorophenylalanine---F⁻. Conformations are arranged in increasing relative Gibbs free energy at 298 K. Proton transfers are occurring in all isomers below the 15 kJ/mol cut-off. Energetics shown for ΔH (ΔG) in kJ/mol with distances in Å.

Based on the trends that were seen with the chloride anion, it is likely that isomers 2, 3 and 6 may yield better spectral matches as they consist of hydrogens that are interacting with the ring system. This additional interaction has proven to aid in the fitting of vibrations at lower frequencies.

- 4-fluorophenylalalnine---F⁻

Alteration of the fluorine location has been shown to alter the direction of the quadrupole moment. Electronic structure calculations produced seven unique isomers, with one of these isomers (isomer 7) being slightly above the 15 kJ/mol cut-off with 15.06 kJ/mol for the relative

Gibbs free energy. The influence of altering 3-fluoro to 4-fluorophenylalanine can be observed most notably by looking at the stable structures for the 4-fluorophenylalanine---F$^-$ complexes. None of the seven lowest energy conformations have a structure in which nitrogen is close to the plane of the ring. This type of structure was seen to be the second most stable isomer of the 3-fluorophenylalanine---F$^-$ complexes. The stable 4-fluorophenylalanine---F$^-$ complexes show the typical conformations that were seen for the chloride cases. Just as previous fluoride investigations have seen, all of the isomers below the cut-off experience proton transfers. Isomers where the fluoride is in the ring plane are lowest in energy, while isomers where ring interactions are less are higher in energy. This suggests that ring interactions are providing added stability to these complexes.
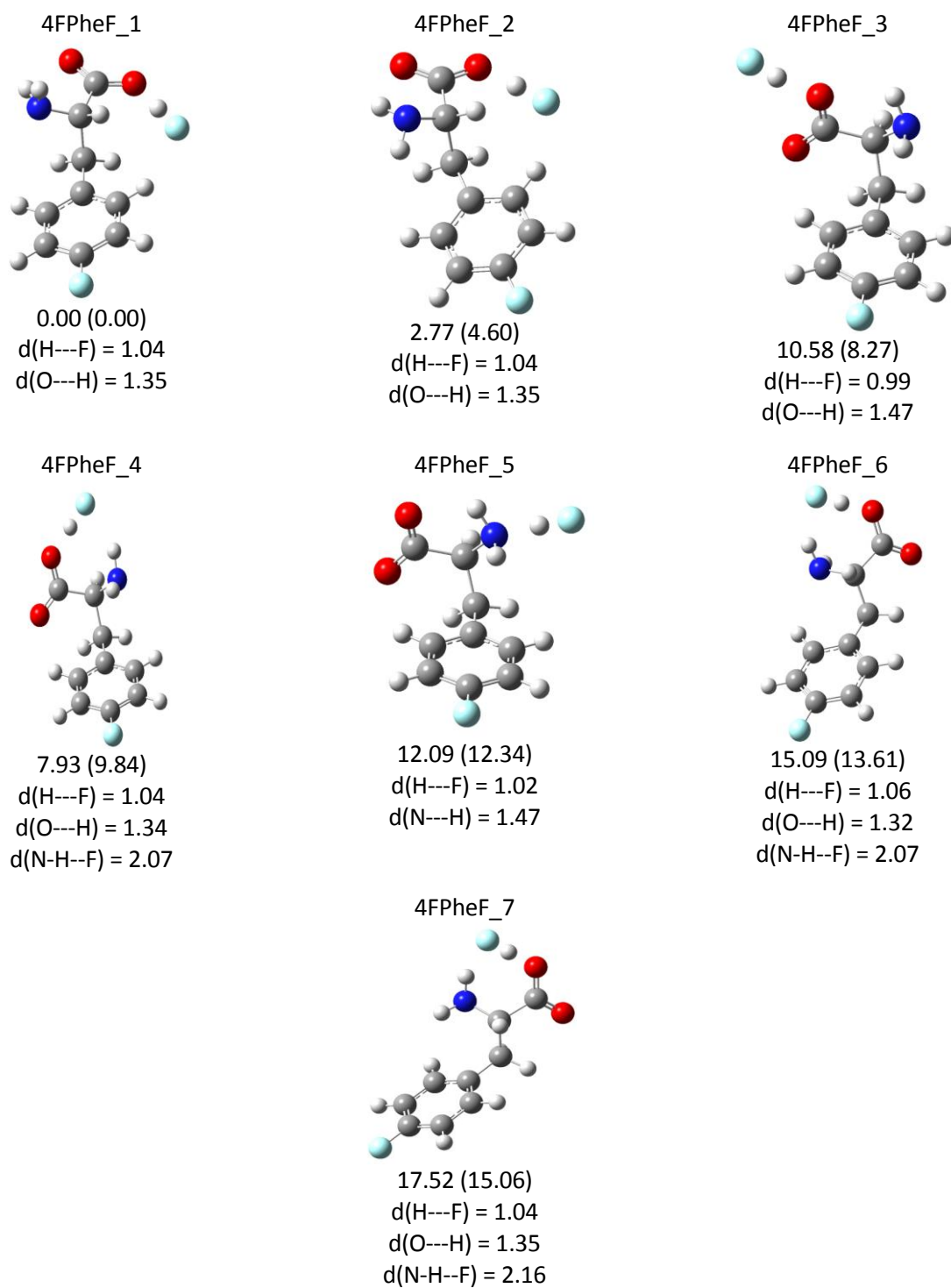
Figure 20: Most Stable Structures of 4-fluorophenylalanine---F⁻. All isomers within or borderline to the 15 kJ/mol cut-off exhibit proton transfers. Isomers are arranged in increasing relative Gibbs free energy (298 K). Energetics shown for ΔH (ΔG) in kJ/mol with distances in Å.

It has also been observed previously in the chloride cases that overlap between simulated

spectra and an experimental spectrum is better when there are additional interactions between

the ring edge and hydrogens when the fluorination degree of the ring is small. This would imply that the lower energy isomers that have hydrogen atoms pointing towards the ring/interacting with the ring edge will have a better fit. Thus isomers 2, 4 and 6 should have good overlap with an experimental spectrum once acquired. Final conclusions about which species are present in the gas phase will be relatively quick as simulated spectra for all isomers (both below and above the 15 kJ/mol cut-off) have already been produced to ensure both completeness and as a preventative measure if higher energy isomers above this cut-off have been generated during experimental IRMPD measurement.

- 2,5-difluorophenylalanine---F$^-$

Addition of a second fluorine to the phenyl ring will increase the strength of the quadrupole moment, thus improving quadrupole-anion binding. However, only two electron withdrawing substituents on the ring will not change the electrostatics of the ring enough to observe an anion centered over the ring plane. Computational chemistry calculations found six unique isomers lower than the 15 kJ/mol cut-off, all with conformations allowing transfer of a proton to the fluoride. Isomers 1 and 5 look similar, but differ in Gibbs energy by about 15 kJ/mol. The difference lies in the orientation of both the ring and NH$_2$ group. Isomer 5 has both the ring and NH$_2$ groups rotated 180° relative to isomer 1. This rotation allows isomer 1 to have HF stabilized by the ring hydrogen. Isomers 1 and 2 are also the only isomers within the cut-off to have anions slightly above the ring plane.

25FPheF_1

0.00 (0.00)
d(H---F) = 1.05
d(O---H) = 1.34
d(ring C$_2$-H---F) = 2.31

25FPheF_2

14.41 (11.93)
d(H---F) = 1.06
d(O---H) = 1.32
d(N-H--F) = 2.11
d(C-H---F) = 2.93

25FPheF_3

17.72 (13.42)
d(H---F) = 1.02
d(O---H) = 1.37
d(N-H--F) = 2.25

Nit (4)

14.77 (14.06)
d(H---F) = 1.03
d(O---H) = 1.36
d(N-H--F) = 2.13

78 (5)

18.52 (15.20)
d(H---F) = 1.01
d(O---H) = 1.41

106 (6)

15.89 (15.20)
d(H---F) = 1.02
d(O---H) = 1.50
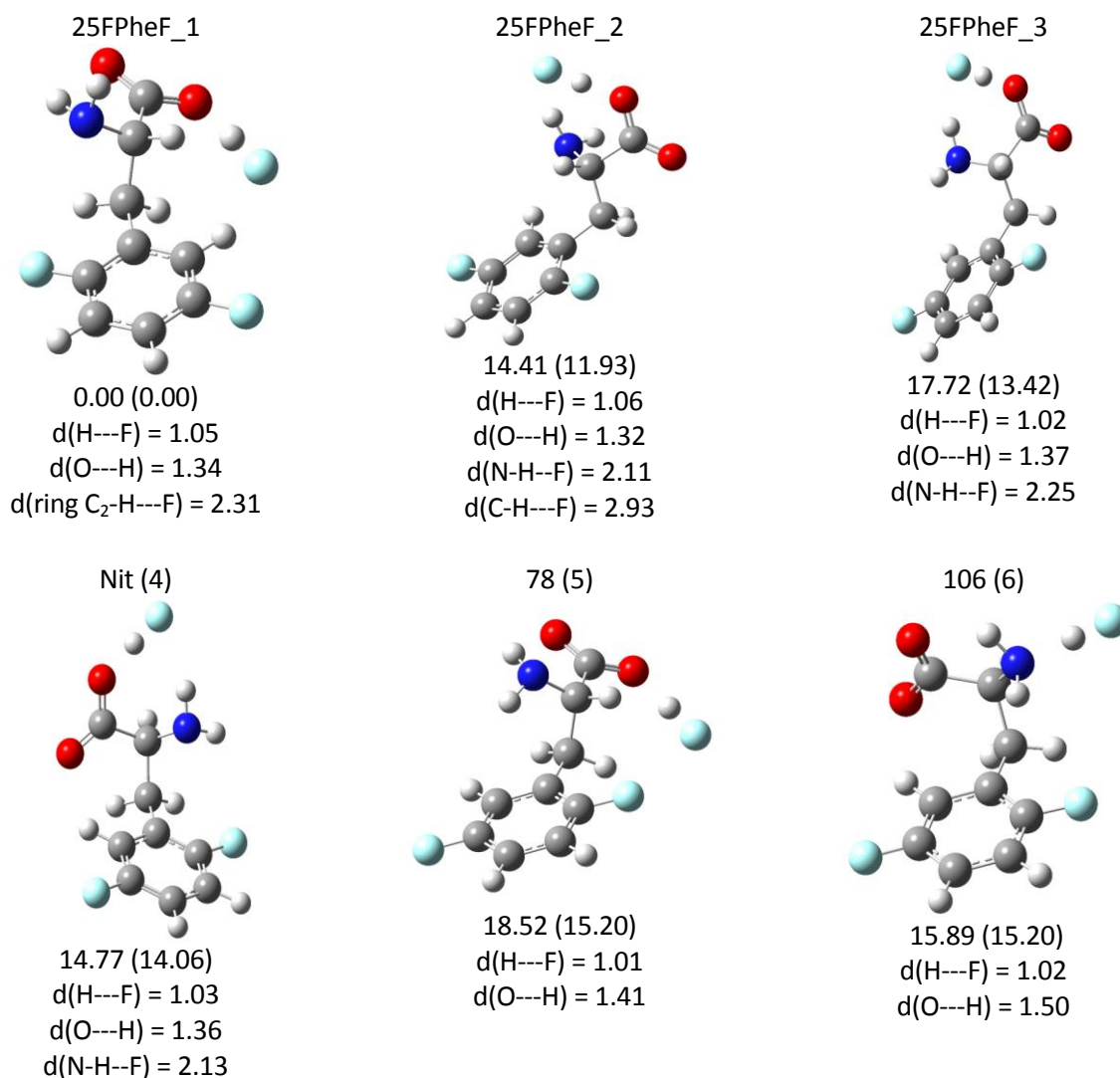
Figure 21: Most Stable Structures of 2,5-difluorophenylalanine---F⁻ ordered by relative Gibbs free energy (298 K). Energetics shown for ΔH (ΔG) in kJ/mol with distances in Å.

As seen in the chloride cases, complexes that have hydrogens interacting with the still negative ring edge better predict the experimental spectrum. If this relationship holds true for these 2,5-difluorophenylalanine---F⁻ complexes, it denotes that isomers 1, 2, 3 and 5 should display a good fit to some or all of the experimental peaks. As isomer 1 has ring interaction, it can be speculated that the simulated spectra will fit the experimental data. Simulated spectra of the lowest energy isomers are included in **Appendix A: Supplementary Information** so that rapid conclusions can be made when an IRMPD spectrum becomes available.

4.3.3 Bromide ion (Br⁻)

The bromide anion is an interesting case as it is a larger anion than previously studied. Although bromide is a larger ion than chloride, it has more electrons that are easily dispersed thus it is a softer anion with respect to chloride. Soft ions are where the ionic radius is large with the electrons diffused through the ionic radius. The increased size means that the nucleus feels less of an effect from the dispersed electrons, allowing diffusion of the electrons throughout the radius. This dispersion means that bromide is softer than the previously tested hard fluoride. This plays an important role as size is now a factor in anion stabilization. Bromide has a larger electron cloud therefore increased interactions with the ring are expected, as the overall size of the anion has not yet become too large to fit above the center of the ring

- Phenylalanine---Br⁻

Computational calculations found six unique isomers within the 15 kJ/mol cut-off (**Figure 22**). Of the six unique isomers of the phenylalanine---Br⁻ complexes, three have the ability for edgewise bonding, isomers 1, 2 and 6. The remainder of these six isomers have the bromide anion located far from the ring edge or ring plane. As well as potential binding between the ring edge and bromide, all isomers except for isomer 2 have the potential for ring interactions with hydrogen atoms. As seen in both the chloride and fluoride cases for phenylalanine an intricate network of hydrogen bonds is aiding the stabilization of these complexes. Of these six, two isomers fall on the border of the 15 kJ/mol cut-off (isomers 5 and 6); however, the Gibbs free energy indicates that these structures should still be included. Based on the energetics, as well as how the phenylalanine---Cl⁻ complexes behaved, it is likely that isomer 5 is absent in the gas phase based on conformation. The chloride complexes demonstrated that species containing an

NH$_3$ group failed to properly fit all regions of the IRMPD spectrum, thus it is likely that a bromide complex containing NH$_3$ would also fail to match these regions. It is also possible that higher energy conformers are present, as was the case with PheCl_9 from the chloride investigation due to carrier gas stabilizations.

PheBr_1

0.00 (0.00)

PheBr_2

2.58 (0.67)

PheBr_3

10.62 (10.59)

PheBr_4

14.09 (12.32)

PheBr_5

16.25 (14.95)

PheBr_6

17.98 (15.72)

Figure 22: Most Stable Structures of Phenylalanine---Br⁻ arranged in increasing relative Gibbs free energy at 298 K. Energetics for ΔH (ΔG) in kJ/mol.

In order to accurately determine which species are present in the gas phase, simulated anharmonic spectra need to be compared with experimental spectra. The simulated spectra show vibrations involving the anion to fall outside the limits that are typically accessible in the FEL experiment. The vibrations mainly fall in the 2900 – 3100 cm^{-1} region with vibrations near the bromide occurring in regions that can be captured. The regions that may give a glimpse into the location of the bromide are located around 1600 – 1800, and 1450 cm^{-1}. These regions capable of being probed by IRMPD involve stretches, bends and scissors where hydrogen atoms move

closer to the bromide ion. Depending on which vibrations are seen in the experimental spectrum, this will allow narrowing of the potential structures present in the gas phase. Simulated spectra are available in **Appendix A: Supplementary Information**.

- 3-fluorophenylalanine---Br$^-$

As bromide is a softer and larger anion it should be able to interact with slight changes in electrostatics of the ring. As previously mentioned, addition of one electron withdrawing group is not enough to invert the quadrupole, thus cation stabilization above the ring should still dominate. This means that the bromide should have edgewise interactions with the ring as well as interactions with the hydrogen network of the amino backbone as previously seen.

3FPheBr_1	3FPheBr_2	3FPheBr_3
1.72 (0.00)	0.00 (0.79)	9.29 (8.45)
3FPheBr_4	3FPheBr_5	3FPheBr_6
9.23 (8.46)	13.21 (11.16)	14.74 (13.01)

Figure 23: Most stable structures of 3-fluorophenylalanine---Br$^-$ shown in increasing relative Gibbs free energy at 298 K. Energetics shown for ΔH (ΔG) in kJ/mol.

Electronic structure calculations found six unique isomers with energy less than the imposed 15 kJ/mol cut-off. Isomers 1 and 2 are similar in structural conformation. Both have the bromide ion located in the ring plane near the carbonyl group with the CH hydrogen also directed towards the bromide. The variation between the two isomers lies in the orientation of the amine group. Isomer 1 has the amine hydrogens pointing away from the ring while isomer 2 has the hydrogens pointing towards the ring. This slight variation yields an enthalpy difference between isomers 1 and 2 of 1.72 kJ/mol and a Gibbs free energy difference of -0.79 kJ/mol. Thus, the two isomers are determined to be equivalent as the energetics are extremely close. Prior results for the chloride anion have shown that better spectral matches for 3-flurophenylalanine-anion complexes occur when the amino group is interacting, even if only slightly, with the quadrupole moment. Therefore, isomer 2 should have a better fit with an experimental spectrum.

Isomers 3 and 4 have similar variation of the amino group; slight rotation is the cause for the energy difference. These isomers show the same conformation as the lowest energy chloride isomers. The increased size of the anion makes it more difficult to fit in the claw formed by the amino terminus, thus increasing the energetics. As there is currently no experimental spectrum, only hypotheses can be made about the spectral matches. It is thought that isomers 1 and 2 should have good spectral agreement with experiment as the rotation of the amine group has been shown to increase matching. An experimental IRMPD spectrum will distinguish if the chloride patterns between structure and IRMPD spectrum exist for bromide.

- 4-fluorophenylalalnine---Br$^-$

Fluorination at the 4- position results in some of the same structures as fluorination at the 3- position for isomers with relative energies less than 15 kJ/mol. All isomers are common to

61

both mono-fluorinated locations. Isomers 1 and 2 have bromide located in the ring plane, with an almost flat amino backbone. The alteration between the two is the rotation of the amine, just like in the 3-fluoro case. Isomers 3 and 4 differ in the rotation of the backbone. Isomer 3 has the CH group pointing away from the ring while isomer 4 has CH pointing towards the ring. These slight rotation variations account for the energy differences between isomers 1 and 2, and isomers 3 and 4. Isomer 5 is the highest in energy of the cut-off structures; however it is similar in structure to isomer 4. Just like isomers 3 and 4, isomers 4 and 5 are also connected by alteration of the amino terminus. If the ring lay in the xy plane, isomer 5 would be a rotation about the x axis by roughly 90°. This rotation removes the ring interactions with the amine group, thus decreasing the stability.

4FPheBr_1

1.24 (0.00)

4FPheBr_2

0.00 (0.38)

4FPheBr_3

10.87 (10.43)

4FPheBr_4

15.32 (13.45)

4FPheBr_5

16.41 (13.91)
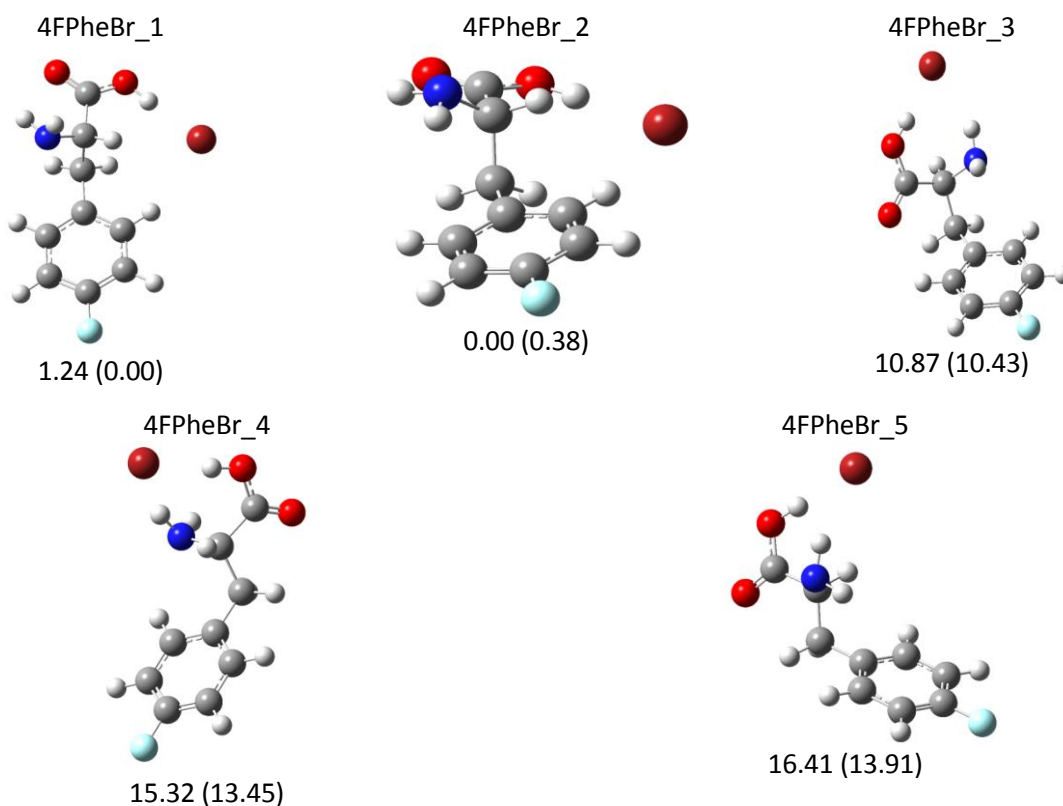
Figure 24: Most stable structures of 4-fluorophenylalanine---Br⁻ within a 15 kJ/mol cut-off arranged in increasing relative Gibbs free energy (298 K). Energetics shown for ΔH (ΔG) in kJ/mol.

It is likely that the two lowest energy isomers, isomers 1 and 2 will be present in the gas phase. Based on the chloride results it is also possible that better spectral fits will exist with isomers 3 and 4. Without an experimental spectrum, it can be speculated that at least isomers 1 and 2 are likely present in the gas phase.

- 2,5-difluorophenylalanine---Br^-

Addition of a second fluorine to the phenyl ring should slightly increase quadrupole-anion interaction. Unlike the previous investigations, only two isomers fall within the imposed energetic cut-off. The third lowest energy conformation is shown in **Figure 25** to illustrate the jump in energy. The three isomers shown in **Figure 25** increase by approximately 12 kJ/mol. These energetic jumps confirm that isomer 1 should be the only isomer present in the gas phase. Experimental IRMPD will confirm if isomer 1 and possibly isomer 2 are present in the gaseous complexes.

25FPheBr_1   25FPheBr_2   25FPheBr_3

0.00 (0.00)   13.91 (12.99)   22.69 (21.47)
d(ring center --- Br^-) = 4.35 Å
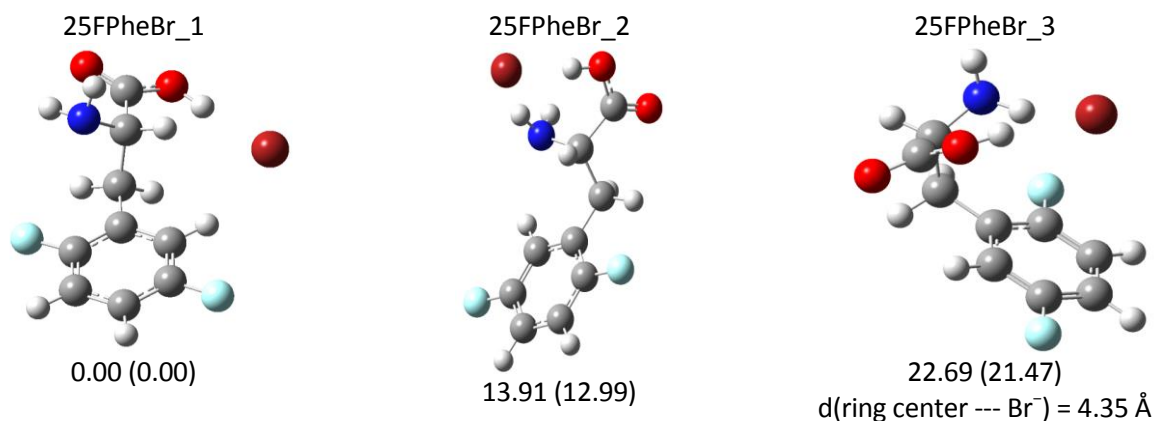
Figure 25: Most stable structures of 2,5-difluorophenylalanine---Br^-. Only two structures fall within the 15 kJ/mol cut-off with energy jumps of roughly 12 kJ/mol occurring between the each of the three lowest energy conformations. Isomers are listed in increasing relative Gibbs free energies at 298 K. Energetics shown for ΔH (ΔG) in kJ/mol.

4.3.4 Trifluoromethanolate ion (CF$_3$O$^-$)

Trifluoromethanolate (CF$_3$O$^-$) combines the high charge density regions of fluoride with the size considerations that were seen with the larger bromide. The large size of the CF$_3$O$^-$ ion

makes it difficult for anion-quadrupole interactions with the ring face, thus edgewise interactions, or canonical interactions should be dominant. It is plausible that due to the charge density, CF_3O^- will produce similar structures as the fluoride cases. However, the charge is located on the oxygen instead of the fluorides, thus the likelihood that proton transfer will be produced is lower than fluoride yet higher than chloride. It is favourable that interactions will involve CF_3O^- oriented to interact with the charged oxygen as opposed to the fluorine atoms.

- Phenylalanine---CF_3O^-

The phenylalanine complexes contain a normal quadrupole, thus cation-π interactions will dominate. Anion interactions will be with the amino backbone and/or the ring edge. Electronic structure calculations produced five unique lowest energy conformations (**Figure 26**). Trifluoromethanolate interactions with the amino backbone, ring edge, NH_2 and CH are the two lowest energy isomers. These two isomers have a network of hydrogen interactions with both the anion and ring edge which lowers the energy of these isomers. Moving CF_3O^- away from the ring produces isomers 3 and 5. These two isomers have fewer hydrogen interactions. Due to the gap in energy, and the unknown experimental spectrum, it is determined that isomers 1 and 2 are likely the only isomers present in the gas phase. Simulated anharmonic spectra have been generated and are included in **Appendix A: Supplementary Information**. Vibrations between the carbonyl hydrogen and the oxygen of the anion occurs around 2900 cm^{-1}, thus it cannot be captured in our standard range. However, vibrations involving the anion fall within the target range at ~1450 cm^{-1}. Inclusion of all simulated spectra will aid in rapid comparison when an experimental IRMPD spectrum becomes available.
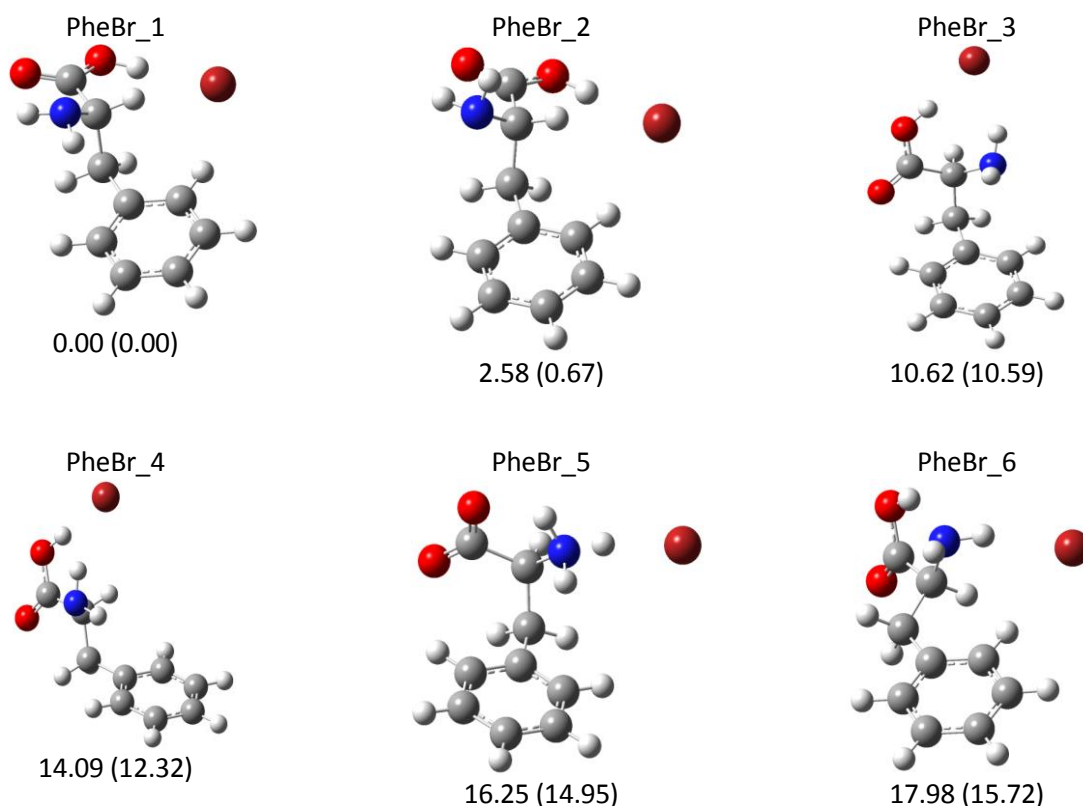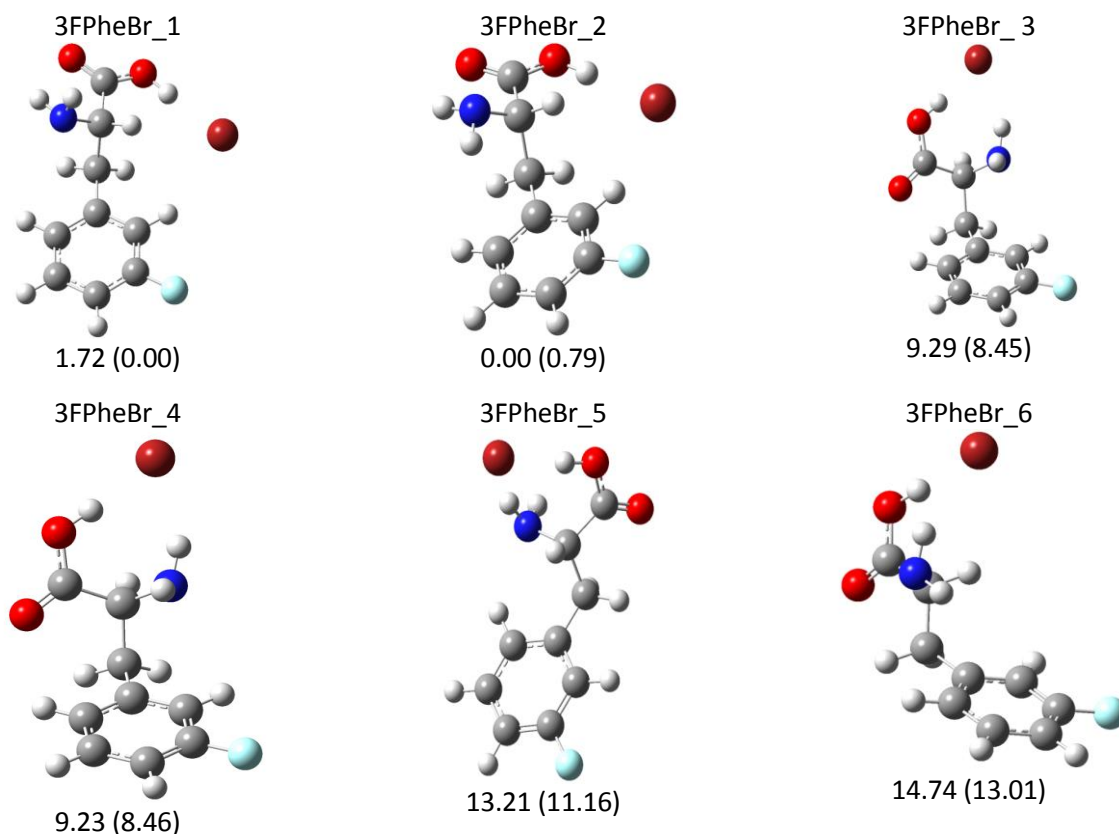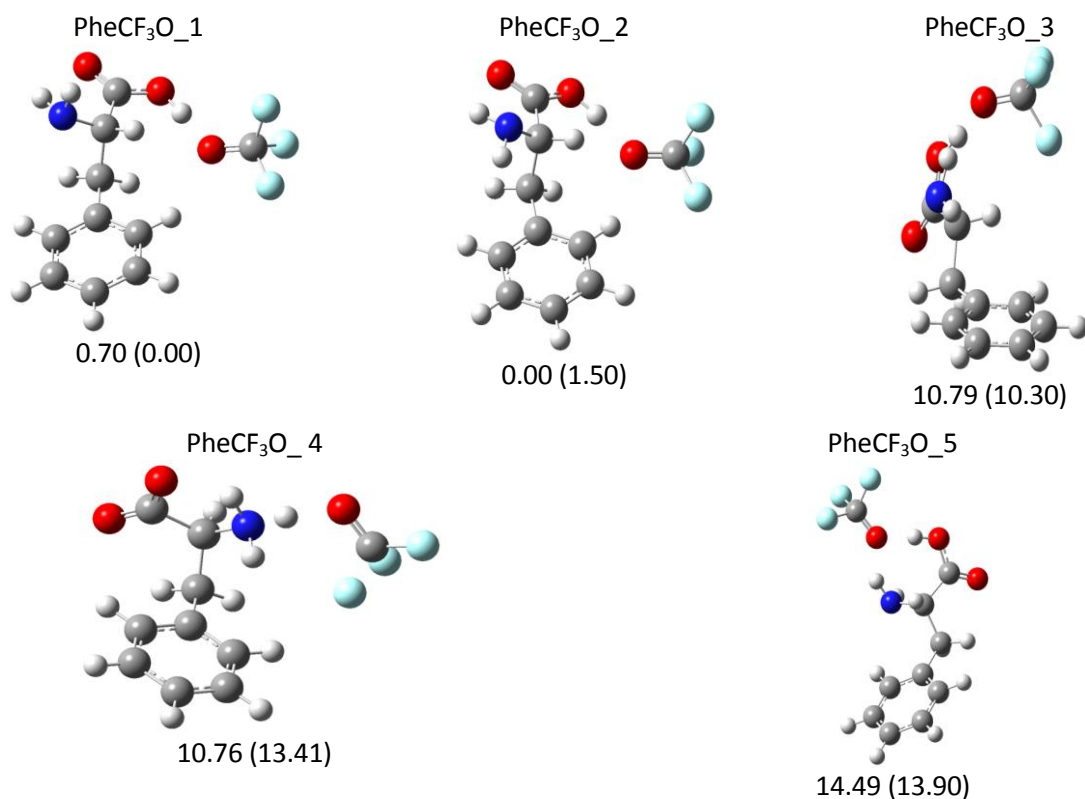
Figure 26: Most stable structures of phenylalanine---CF_3O^- arranged in increasing relative Gibbs free energy (298 K). Energetics shown for ΔH (ΔG) in kJ/mol.

- 3-fluorophenylalanine---CF_3O^-

As seen in prior experiments, addition of one fluorine to the ring does not greatly alter the quadrupole and therefore there will not be any large changes to the most stable structures. Computational calculations produced five unique isomers. Isomers 1-4 are the same observed structures as the Phenylalanine---CF_3O^- complexes. Isomer 5 has interactions between the anion oxygen and the carbonyl hydrogen and slight interaction between the anion fluoride and the ring edge/plane.
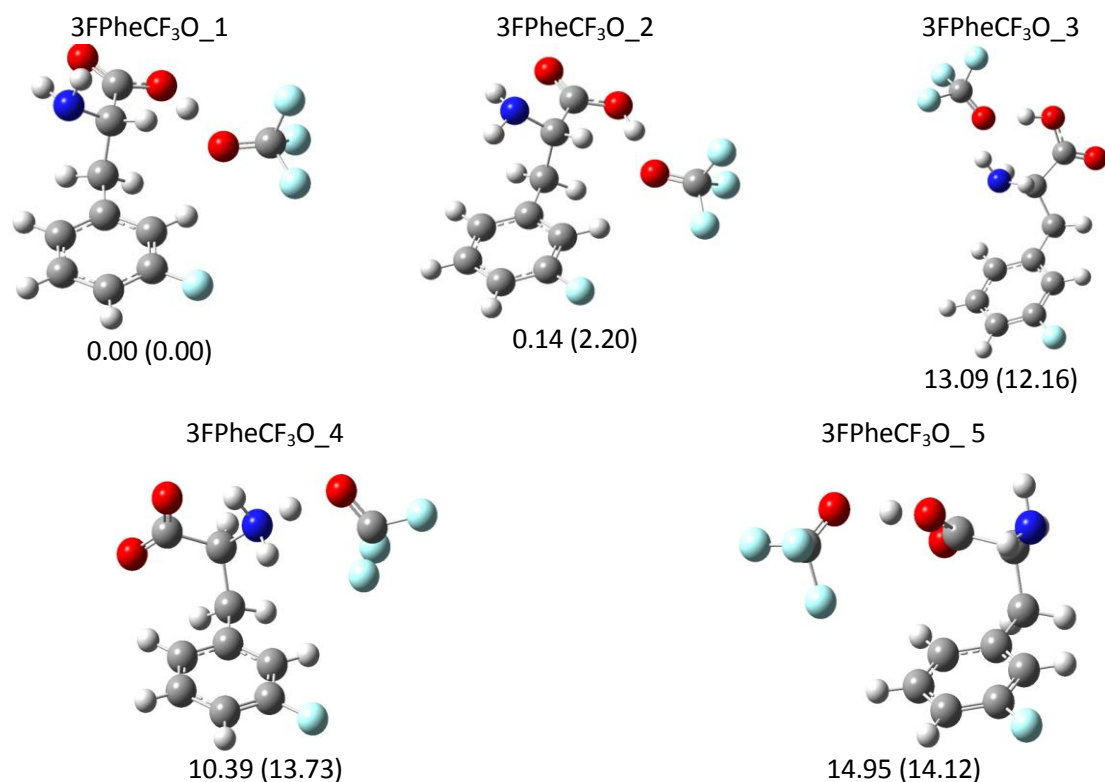
Figure 27: Most stable structures of 3-fluorophenylalanine---CF$_3$O$^-$ within a cut-off of 15 kJ/mol ordered in increasing relative Gibbs free energy calculated at 298 K. Energetics shown for ΔH (ΔG) in kJ/mol.

It is believed that isomers 1 and 2 with their hydrogen bonding network are the isomers most likely present in the gas phase. Comparison between simulated spectra and IRMPD spectrum will confirm or disprove this hypothesis.

- 4-fluorophenylalalnine---CF$_3$O$^-$

Computational investigations produced four unique structures with relative energetics less than 15 kJ/mol. Fluorination at the fourth position, yielded the top four isomers that were present in the 3-fluorophenylalanine---CF$_3$O$^-$ complexes. Isomers 3 and 4 of 4-fluorophenylalanine---CF$_3$O$^-$ are isomers 4 and 3 of the 3-fluorophenylalanine complexes respectively. The lowest energy isomers (isomers 1 and 2) have CF$_3$O$^-$ slightly closer to the ring plane than the 3-fluorophenylalanine complexes. This is due to the position of the ring fluorination. Fluorination at the 4- position of the ring allows the CF$_3$O$^-$ to get closer to the ring

plane as only attractive forces are now present, whereas fluorination of the third position would

have fluorine-anion repulsive interactions. Based on electronic energies alone, isomers 1 and 2

are expected to exist in the gas phase, in equal proportions.

4FPheCF$_3$O_1

4FPheCF$_3$O_2

4FPheCF$_3$O_3

0.00 (0.00)

0.68 (3.46)

11.40 (9.89)

4FPheCF$_3$O_4

15.85 (15.35)
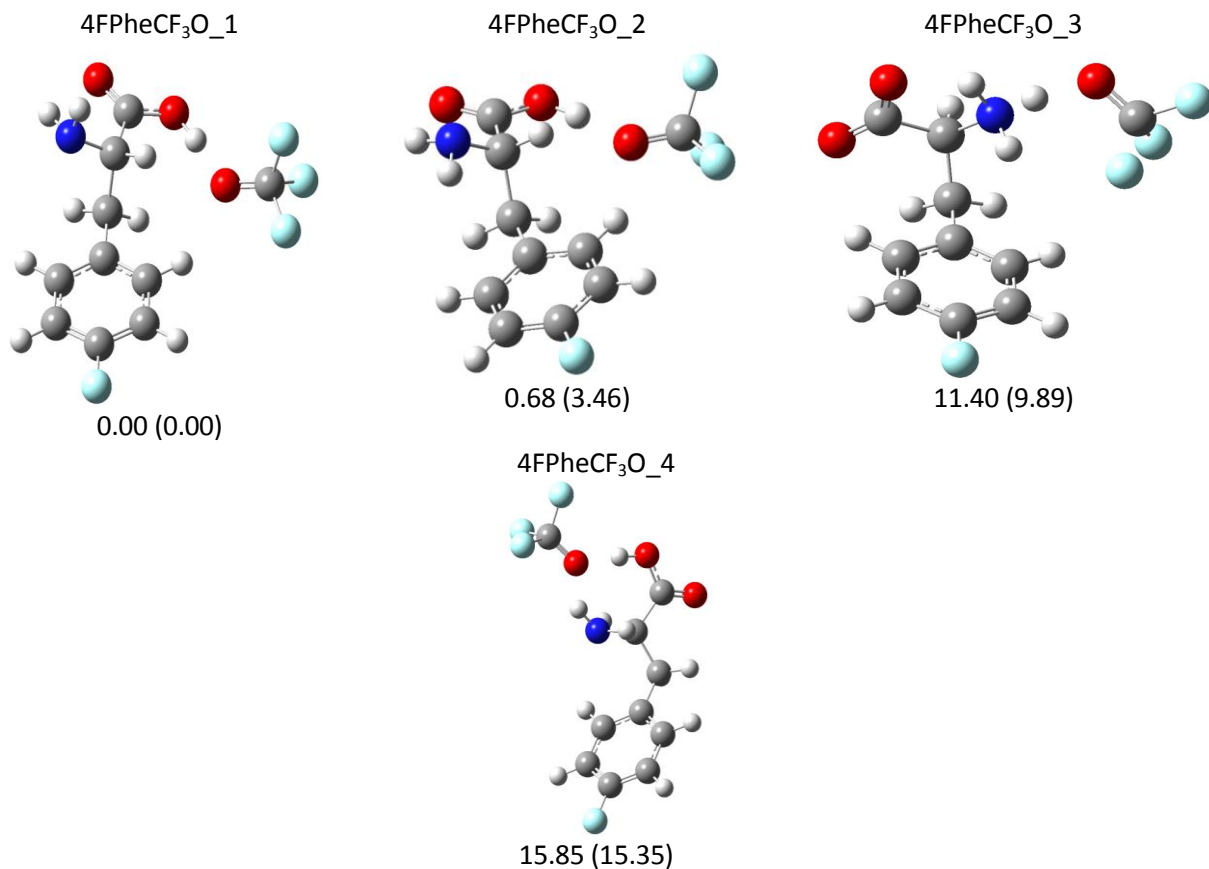
Figure 28: Most stable structures of 4-fluorophenylalanine---CF$_3$O$^-$ arranged in increasing relative Gibbs free energy calculated at 298 K. Energetics for ΔH (ΔG) in kJ/mol.

- 2,5-difluorophenylalanine---CF$_3$O$^-$

Fluorination at positions two and five produce an interesting scenario in which the anion

cannot interact with the ring plane without incurring strong repulsive forces. Without any kind of

rotation, this forces CF$_3$O$^-$ away from the ring plane, only allowing interactions with the amino

backbone and thus limiting the number of possible isomers. Electronic structure calculations

proved this theory by only locating two isomers with energies less than 15 kJ/mol. Isomer 1 is the

same lowest energy conformation that has been observed in the other complexes. In order for isomer 1 to adopt the same conformation, the ring had to rotate 180°. This rotation allows the hydrogen bonding network to include the ring. Isomer 2 has a hydrogen bonding network that involves the entire amino terminus, but lacks any ring interactions. The energetic jump implies that the ring interactions play an important role in stabilization.

25FPheCF$_3$O_1

25FPheCF$_3$O_2

0.00 (0.00)

13.71 (10.83)
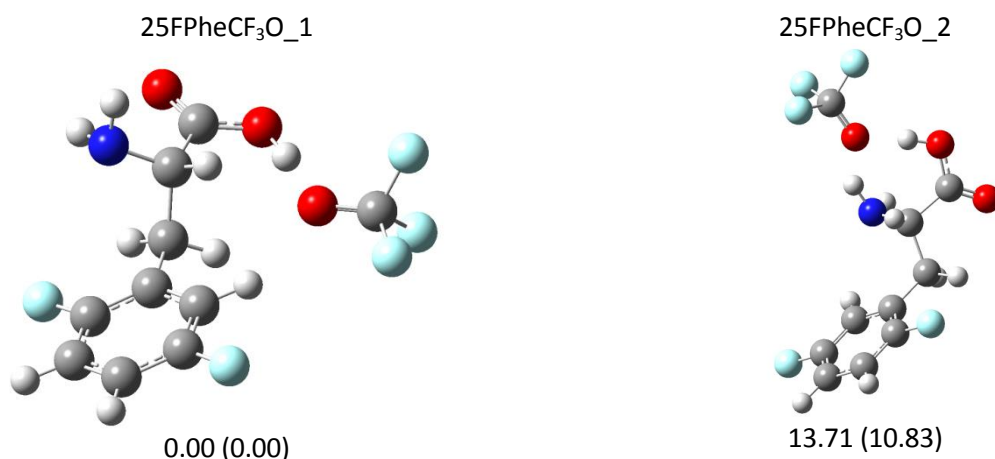
Figure 29: Most stable conformations of 2,5-difluorophenylalanine---CF$_3$O$^-$ arranged in increasing relative Gibbs free energy at 298 K. Energetics shown for ΔH (ΔG) in kJ/mol.

The two lowest energy conformations as seen in **Figure 29**, illustrate that increasing the fluorination reduces the edgewise interactions. This is due to repulsive interactions of the ring fluorine atoms. Rotation of the ring allows some interactions with CF$_3$O$^-$ which produces the lowest energy isomer. As the energy gap between the two isomers is ~12 kJ/mol, isomer 1 is likely the only isomer present in the gas phase.

4.4 Conclusions

The effects of fluorination are not entirely evident in this study as fluorination degrees past difluorination were not studied. What is clear is that for the fluorination degrees studied, different anions adopt similar structures. These structures have anions that are close to the ring plane, while still interacting with the amino terminus, specifically the carbonyl group. The

investigation involving chloride showed that occasionally higher energy isomers may better match experimental spectra in one or all vibrational regions. Thus higher energy conformations need anharmonic spectra generated. The prevalence of higher energy conformations being present in the experimental IRMPD data may mean that the clusters are interacting with the carrier gas or that higher energy conformations are being produced and trapped. The carrier gas interactions may be stabilizing the higher energy conformers thus changing the experimental ordering, which will then be different from the ordering of the computationally discovered isomers.

It is this additional unknown stabilization that proves difficult to properly predict which isomers are present in the gas phase based solely on computational electronic structure calculations. Anharmonic spectral generation is required to be able to definitively identify which species are present. Upon acquisition of IRMPD spectra for the phenylalanine, 3-fluorophenylalanine, 4-fluorophenylalanine and 2,5-difluorophenylalanine clusters with fluoride, bromide and trifluoromethanolate ions, comparison with the simulated spectra will be done. This spectral matching should be fast as the anharmonic spectra have already been generated in anticipation of future experimental data.

4.5 Future Work

Future work will consist of acquiring IRMPD spectral data for the remaining phenylalanine and phenylalanine derivatives with bromine, fluorine and trifluoromethanolate anions so as to confirm experimentally which conformations are present in the gas phase.

Chapter 5

Systematic Investigation of Quadrupole-Anion Interactions of Phenylalanine and fluorinated derivatives of Phenylalanine

5.1 Introduction

Following the results of **Chapter 4**, it was decided that the systematic nature of **Chapter 3** needed to be analyzed for the anion-quadrupole systems for all possible permutations and degrees of ring fluorination. It has been observed that increasing fluorination will slowly invert the quadrupole so as to promote anion-quadrupole interactions. **Chapter 4** saw that different anions typically produced similar conformations, however, only fluorination up to the second degree was analyzed. To inspect the influence of increasing fluorination and the effects this has on anion stability, higher fluorination needs to be investigated. **Chapter 3** illustrated that fluorination location affected the direction, not the magnitude of the quadrupole. It was observed in **Chapter 4** that the location of the fluorine substitutions affects how the anion binds. Thus, both quadrupole strength and fluorination location are important considerations for anion-quadrupole interactions. To study these interactions, three of the previously studied anions will be included. Chloride, bromide and fluoride will be investigated for all fluorination degrees and permutations. By investigating the fluorination degree, the influence of the quadrupole will be better understood, while permutations of fluorination will provide insight as to which permutations promote anion-quadrupole interactions.

5.2 Methods

Computational chemistry as described in **§2.1** was used. Unique structures with the three anions that were discovered in **Chapter 4**, independent of ring fluorination were chosen to be

analyzed and are the original conformations for this study. Fluorination of these structures was then performed so all fluorination degrees and permutations of fluorine around the ring were represented. When all of the fluorination starting structures had been created they were optimized using B3LYP/6-311++G(d,p). After the optimization and frequency calculations are completed, single point energy calculations are performed at MP2/aug-cc-pVTZ. After completion of the single point energy calculation, enthalpies are calculated to find the lowest energy isomers.

5.3 Results and Discussion

Isomers for all permutations were tested and labelled alphabetically. Ordering of the letters is based on the phenylalanine results. Phenylalanine with each anion was calculated and arranged from lowest to highest enthalpy, with the lowest energy being labelled as A. The structures that the lettering stems from are hereby known as the base structures. For simplicity the three lowest energy isomers in each fluorination degree/permutation are shown.

5.3.1 Cl⁻
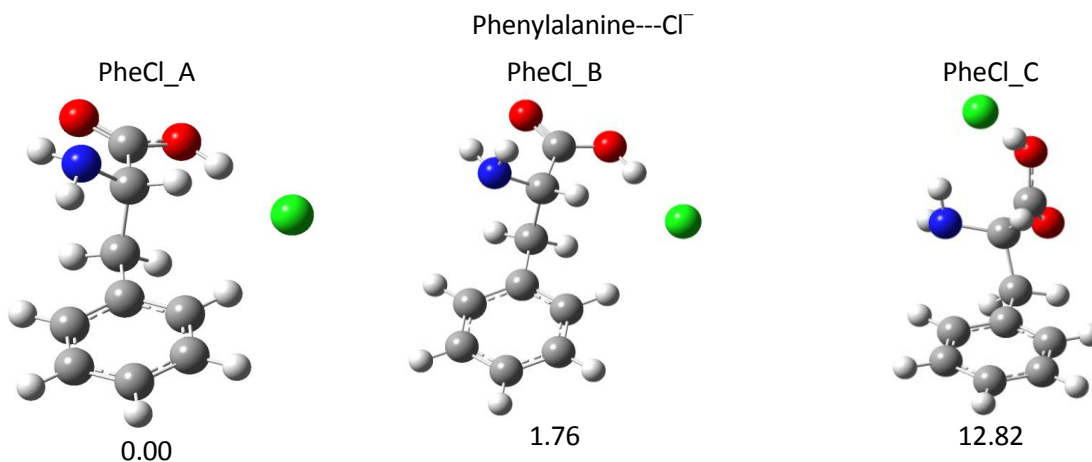
Figure 30: Phenylalanine clustered with chloride arranged in increasing relative enthalpy. These structures are the three lowest enthalpy base structures, thus determining the ordering of the clusters containing chloride labels. Energetics shown for ΔH in kJ/mol.

Optimization of phenylalanine in the presence of chloride produced sixteen unique conformations, labelled A-P with A being the lowest in enthalpy. These structures are the same as those found in **Chapter 4**, and form the foundation of the fluorination study of phenylalanine clustered with chloride. The three lowest energy isomers as described by enthalpy are shown in **Figure 30**. The first two isomers show the chloride ion slightly above the ring plane and off to the side of the ring. This allows interactions between the chloride and hydroxyl, ring, CH_2 and CH hydrogens. These interactions help to stabilize the anion. In addition to anion stabilizations, ring interactions exist with the amine group. The difference between the two lowest isomers is that PheCl_A has the hydrogens directed towards the ring, while the amine hydrogens in PheCl_B are pointed away from the ring. PheCl_C has adopted a claw-like formation in which the amino group is directed towards the chloride forming a claw, with the CH group pointing more towards the ring. As all interactions are between the amino group and the anion, there are no ring interactions for PheCl_C.
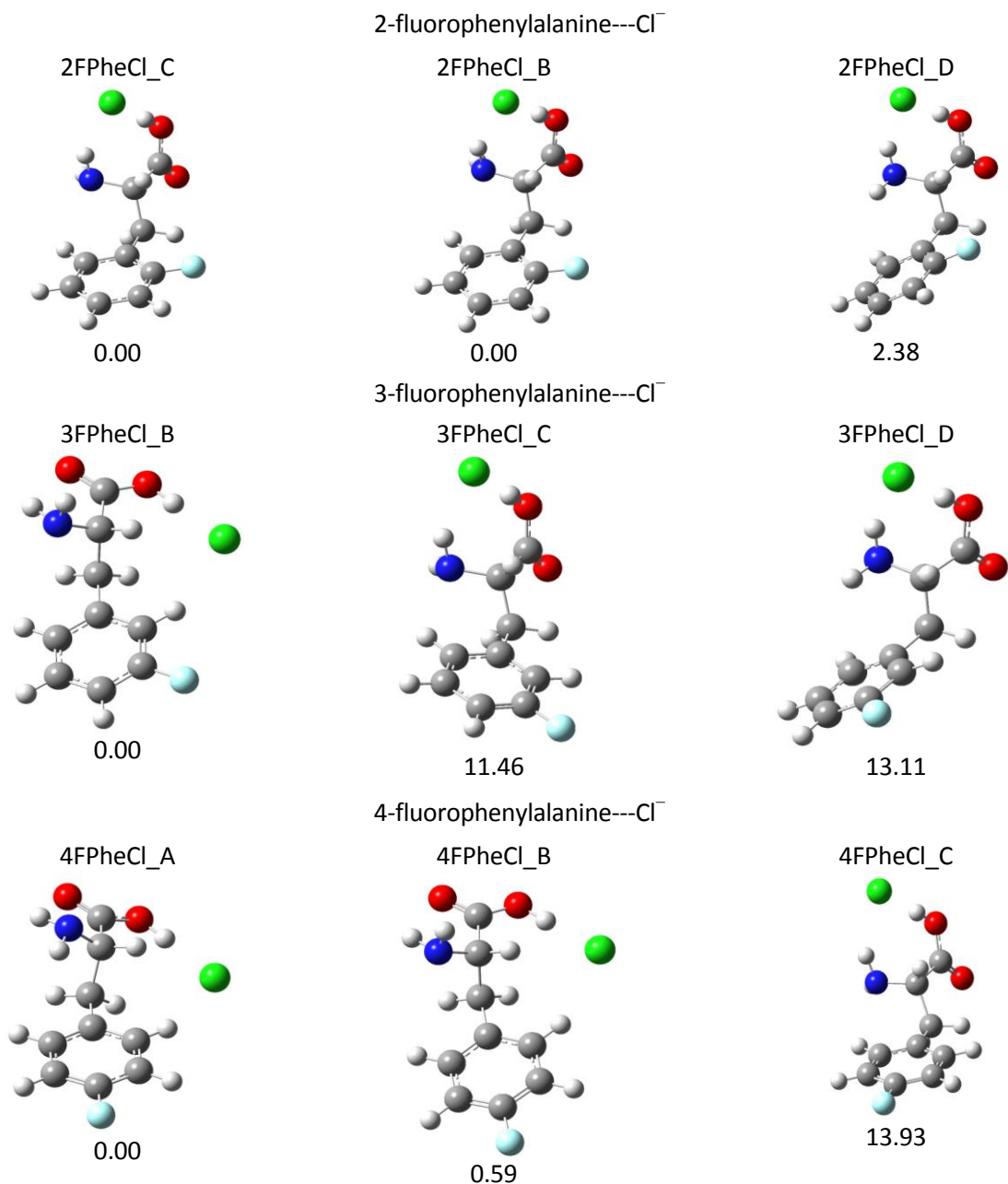
Figure 31: Monofluorinated Phenylalanine clustered with chloride. Three permutations for monofluorinated phenylalanine clusters exist. For each permutation, the three lowest isomers are ordered with increasing relative enthalpy. Relative enthalpy listed in kJ/mol.

Addition of one fluorine to the ring had previously been observed to have little influence on the total conformation; **Chapter 3** and **Chapter 4** indicated that location of fluorine would have little to no effect. The results shown in **Figure 31** disprove these conclusions. Fluorination at the 2- position forces the three lowest energy conformations to adopt the claw-like structure

that was previously seen in PheCl_C. Fluorination at the 3- position shows the emergence of the

structures that were present in the unfluorinated clustering of phenylalanine and chloride. The

ordering of the unfluorinated case is recreated with fluorination at the 4- position. This denotes

that the previous notion that fluorination would have little effect on the structural conformation

is incorrect. Fluorination location will dictate which structures form. As fluorination moves away

from the amino backbone to the opposite side of the phenyl ring, the chloride moves away from

the claw-like formation, into the ring plane. This suggests that symmetry around the ring and

position relative to the amino backbone is significant.

2,3-difluorophenylalanine---Cl⁻

23FPheCl_B

0.00

23FPheCl_C

16.57

23FPheCl_D

19.28

2,4-difluorophenylalanine---Cl⁻

24FPheCl_B

0.00

24FPheCl_C

16.79

24FPheCl_D

19.61
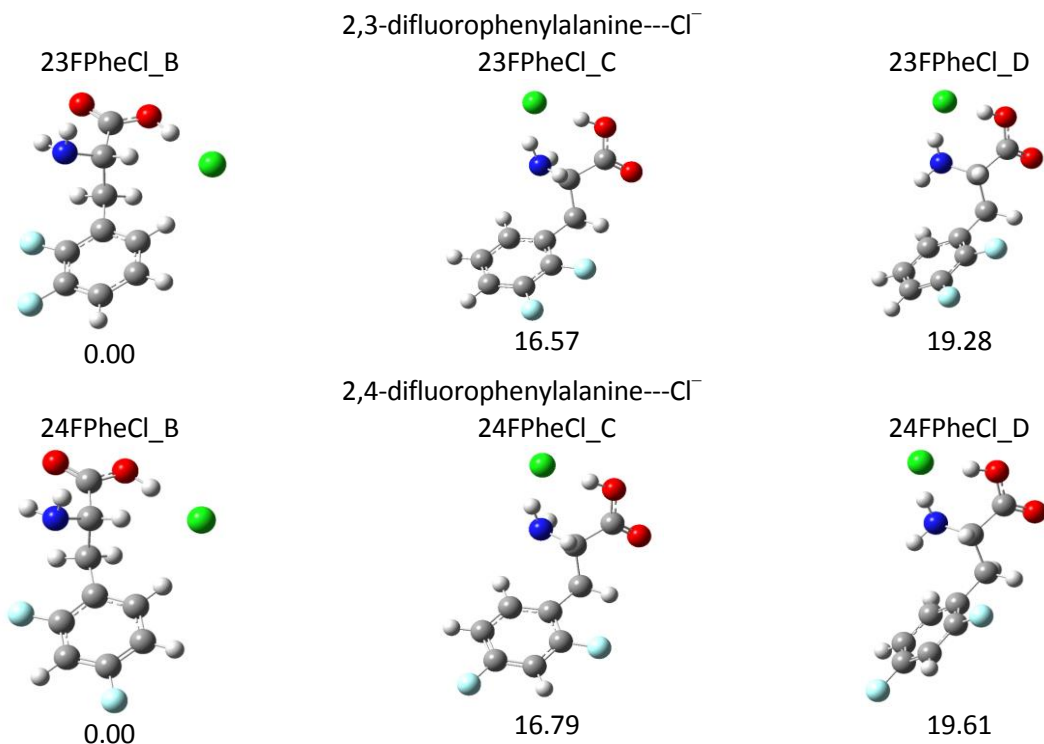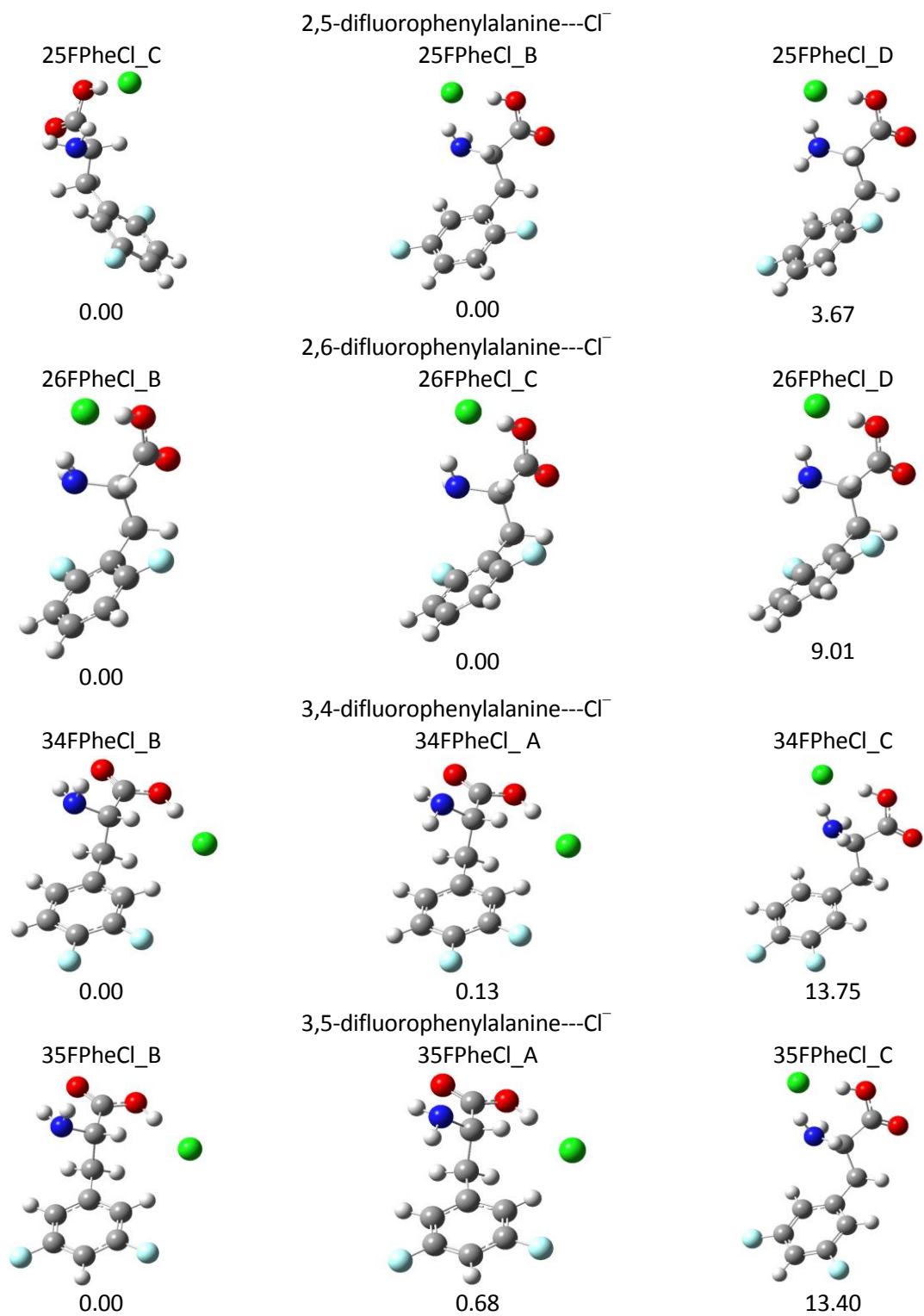
Figure 32: Difluorinated phenylalanine clustered with chloride. Six permutations for fluorination location exist for the difluorinated clusters. Ordering within each permutation is based on increasing relative enthalpy. ΔH in kJ/mol.

Addition of a second fluorine (**Figure 32**) improves the understanding of how the symmetry of the fluorine atoms influences the structural conformations. As was seen in **Chapter 3**, the second fluorine has little effect on the quadrupole moment. When the two fluorine atoms are the furthest from the amino backbone, at the 3,4- and 3,5- positions, the three lowest energy conformations mimic that of the unfluorinated case. In these two cases, there is inversion of the two lowest energy conformations, A and B. However, their energy difference is less than 0.7 kJ/mol which is close to the experimental errors for the computational methods. Thus, the ordering of these isomers is insignificant.

When the charge density, or fluorination location, is close to the amino backbone and symmetric across the ring with respect to the amino backbone (fluorines at 2,5 and 2,6 positions), the isomers all adopt the claw-like formation. When one fluorine is close to the backbone (at the 2- position) and the other is located either opposite to, or on the same side of the phenyl ring as the backbone (positions 2,4- and 2,3- respectively) the lowest energy isomer adopts a PheCl_B formation with the amine group pointing away from the ring with the chloride in the ring plane, while the next two lowest energy isomers adopt claw formations. In this case, the jump in energy is quite large between the lowest energy isomer and the next two conformations. For difluorinated phenylalanine clustered with chloride, edgewise interactions are greatest when the fluorine atoms are located opposite the backbone, or when they are weighted to one side of the ring.

2,3,4-trifluorophenylalanine---Cl⁻

234FPheCl_B

0.00

234FPheCl_C

0.00

234FPheCl_D

9.27

2,3,5-trifluorophenylalanine---Cl⁻

235FPheCl_B

0.00

235FPheCl_C

16.71

235FPheCl_D

20.95

2,3,6-trifluorophenylalanine---Cl⁻

236FPheCl_C

0.00

236FPheCl_D

9.88

236FPheCl_B

11.49

2,4,5-trifluorophenylalanine---Cl⁻

245FPheCl_C

0.00

245FPheCl_D

4.95

245FPheCl_B

7.18
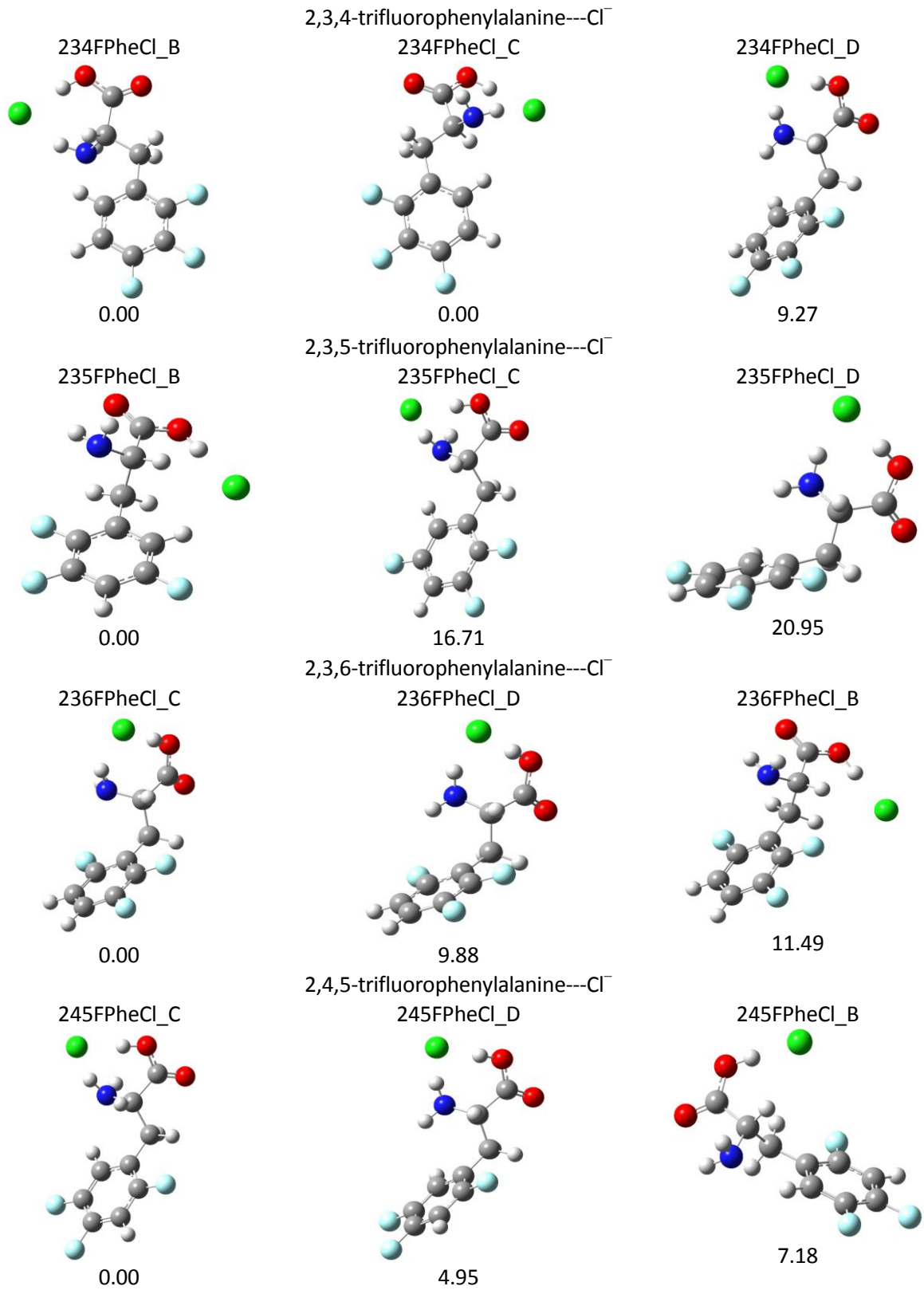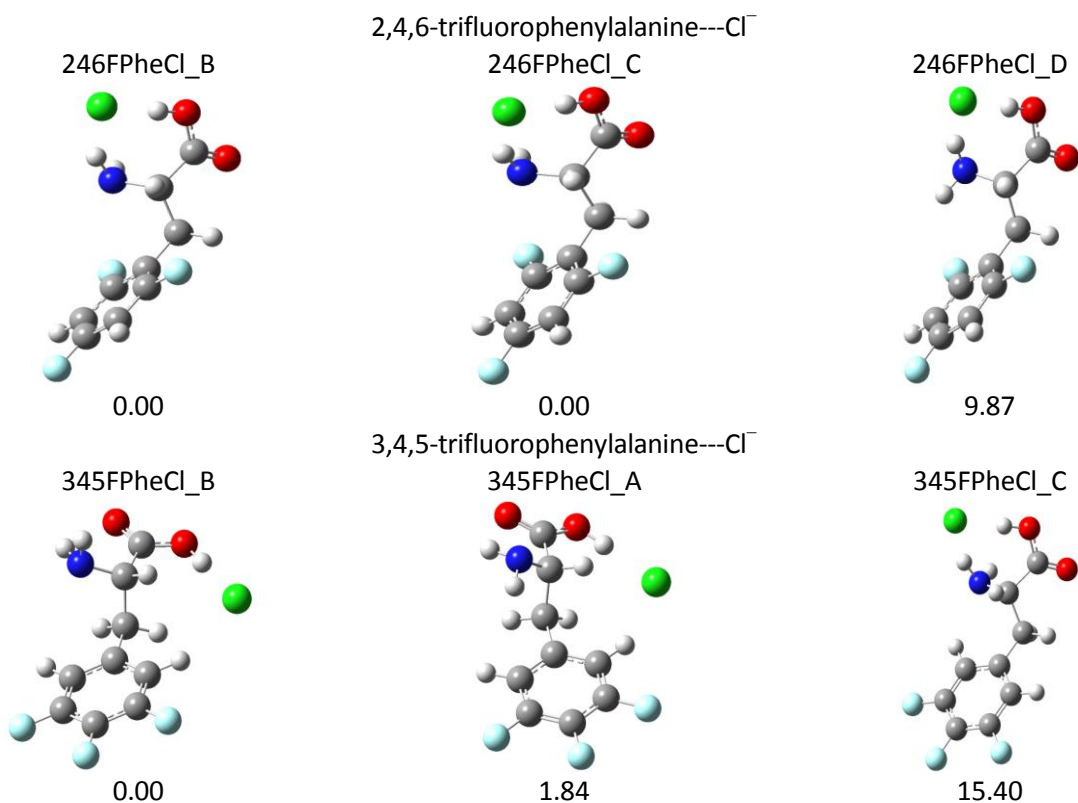
Figure 33: Trifluorinated phenylalanine clustered with chloride. Six permutations of fluorine locations exist for the trifluorinated clusters. Isomers are listed in increasing relative enthalpy for each fluorination permutation. Relative enthalpy listed in kJ/mol.

Figure 33 illustrates the structural conformations that result when trifluorophenylalanine

species are clustered with a chloride ion. From the trifluorophenylalanine cases it can also be

seen that the lowest energy isomers are being dictated by the locations. This is most evident

when looking at positions two and six of the phenyl ring. If neither of these positions has a

fluorine substitution (3,4,5-trifluorophenylalanine), then the isomers will adopt the same

conformation as the unfluorinated cases. This is due to interactions between the backbone and

phenyl ring. The backbone can bend close to the phenyl ring thus allowing the chloride to

interact with both ring and amine terminus. If both of these positions are fluorinated (2,3,6- and

2,4,6-trifluorophenylalanine) the claw-like formation is dominant. When the fluorine charge is

predominately around the backbone with some charge opposite the backbone (2,4,6-

trifluorophenylalanine) the lowest three isomers are all in the claw formation, whereas if the charge is entirely around the backbone the two lowest conformations will be the claw formations and a jump in energy will produce a planar formation of the third isomer.

If only one of these positions (two or six) is fluorinated, then the structural conformation of the lowest three isomers will be predicted by positions five and three, respectively. That is to say, if position two is fluorinated and position six is not, then the conformation will be dictated by the fluorination of position five. If a fluorine substituent is lacking at position five with fluorination at position two (2,3,4-trifluorophenylalanine) then extreme plane formations will exist. These extreme plane formations are where the entire backbone is twisted in such a way that the carboxyl portion of the backbone and the chloride are in the ring plane. If fluorination exists at either secondary position (2,3,5- or 2,4,5-trifluorophenylalanine) the structure is dependent on where the charges lie. For 2,3,5-trifluorophenylalanine, the lowest energy structure is with the chloride in the ring plane, like with the unfluorinated phenylalanine. The second lowest energy isomer is a bent version of the claw formation. This structure is tilted so that the amine group is approaching the ring plane while still maintaining the claw formations. This is due to the charge being localized on one side of the phenyl ring, forcing the backbone to bend. 2,4,5-trifluorophenylalanine has the charge more dispersed across the ring away from the backbone. This promotes the two lowest energy conformations to adopt the claw-like formation. The least stable of the three has the nitrogen directly on the ring plane, with the amino terminus completely flat. This allows interactions between the ring hydrogen and the amine group.
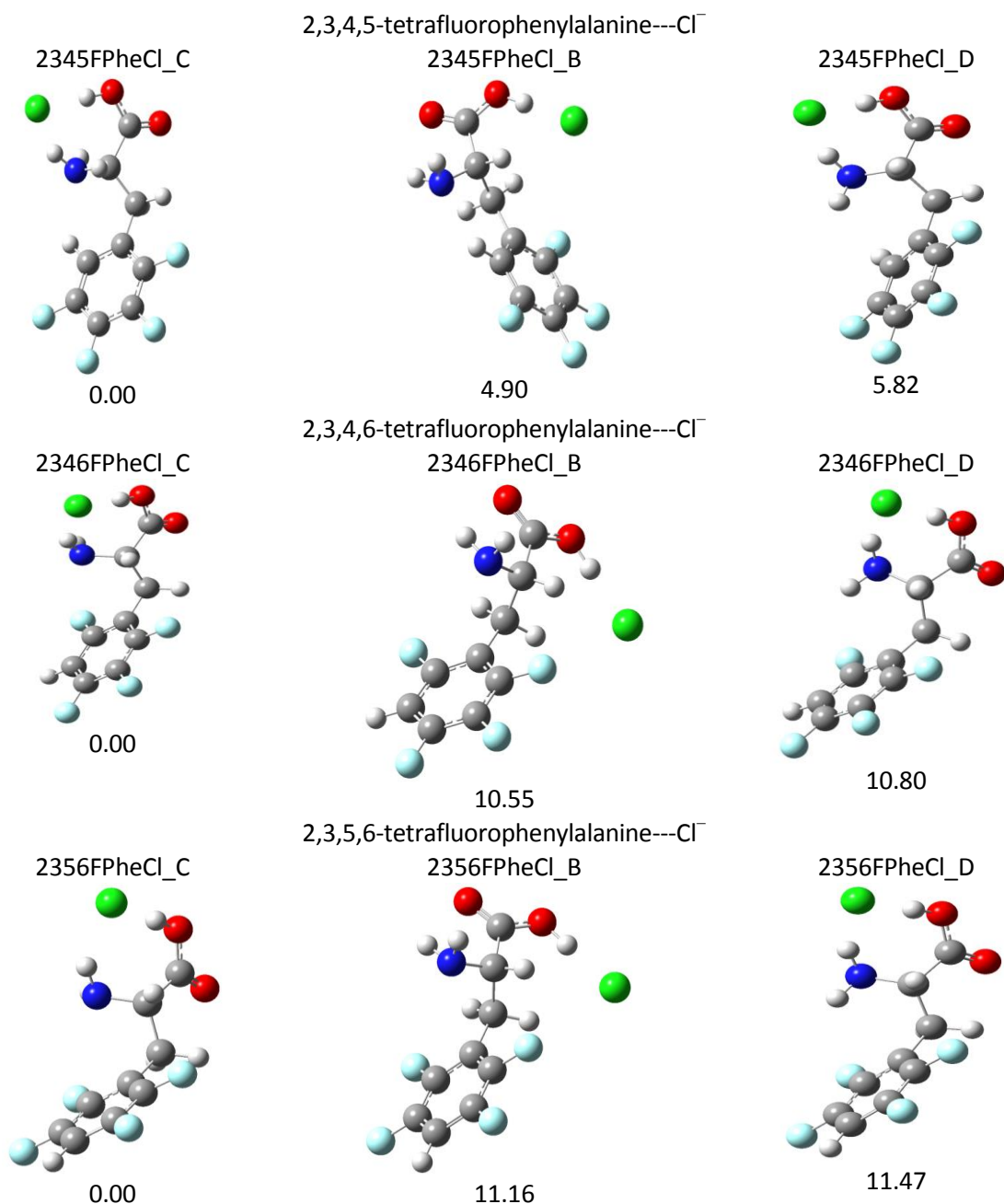
Figure 34: Tetrafluorinated phenylalanine clustered with chloride. Three fluorine permutations exist for the tetrafluorinated phenylalanine clusters. The isomers in each permutation are ordered from lowest to highest relative enthalpy. ΔH shown in kJ/mol.

Addition of a fourth fluorine to the ring increases the quadrupole moment and should increase the quadrupole-anion interactions, however, **Figure 34** shows otherwise. For all fluorination locations for tetrafluorophenylalanine, none of the three lowest energy isomers have interactions with the ring center. This denotes that for chloride, the hydrogen bonding network is

having a stronger influence on where the anion is stabilized. When the fluorines are symmetric around the ring (2,3,5,6-tetrafluorophenylalanine) the claw formation is dominant, with a jump in energy to the next stable isomer which is in the plane formation. When the fluorine atoms are sequential around the ring with the unsubstituted location at the sixth position (2,3,4,5-tetrafluorophenylalanine), variations of the claw and planar formations are dominant. The two lowest energy isomers adopt the formations as previously seen in the trifluorophenylalanine conformations. The lowest energy isomer adopts the conformation seen in isomer C of 2,3,5-trifluorophenylalanine, and the second lowest energy isomer adopts the conformation seen in isomer B of 2,4,5-trifluorophenylalanine. The lowest energy isomer of 2,3,4,5-tetrafluorophenylalanine adopts the standard claw formation. The last possible permutation of tetrafluorophenylalanine exists for 2,3,4,6-tetrafluorophenylalanine. This fluorination permutation has the claw conformation as the lowest energy and third most stable isomer. The second most stable isomer adopts a variation of the plane formation. The chloride is slightly below the ring plane and the amino terminus is bent to point towards it, thus bending it slightly when compared to the plane formation.

2,3,4,5,6-pentafluorophenylalanine---Cl⁻

PentFPheCl_C	PentFPheCl_B	PentFPheCl_D
0.00	9.51	12.30
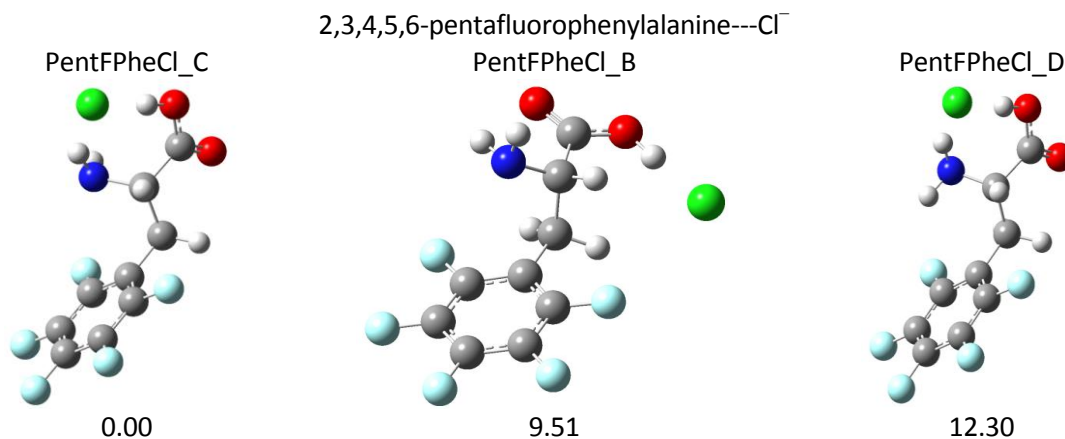
Figure 35: Pentafluorinated phenylalanine clustered with chloride. Isomers are ordered with increasing enthalpy. Relative enthalpy shown in kJ/mol.

The fully fluorinated ring sees the isomers returning to the conformations that were present in the unfluorinated cases though in a different order. The ordering of the three isomers from lowest energy to highest energy is claw, planar chloride and claw formation again.

The overall trend from the chloride case is that the fluorine location around the ring plays an important role in which isomers are the most stable. When the fluorine substituents are close to the backbone the claw formation dominates. If a fluorine substituent exists near the backbone and the remaining substituents are symmetric around the ring, chloride prefers to be stabilized by the amine terminus in the claw. If the charge density around the ring lies far from the amino backbone then the chloride will lie outside the ring, but in the same ring plane thus being stabilized by a hydrogen framework which includes the ring.

5.3.2 F^-

The high charge density of the fluoride anion has been seen to prefer conformations that allow proton transfers. The reason for analyzing fluorination degree and location for fluoride is to see whether or not transfers are preferred for all strengths of the quadrupole moment. Computational calculations found fourteen unique isomers. The three lowest energy isomers for each fluorination degree are shown in the following six figures (**Figures 36-41**). These three isomers represent the conformations that the fluorination permutations are likely to take.

Phenylalanine---F⁻

PheF_A	PheF_B	PheF_C
0.00	1.42	7.26
d(H---F) = 1.04	d(H---F) = 1.04	d(H---F) = 1.04
d(O---H) = 1.36	d(O---H) = 1.36	d(O---H) = 1.34
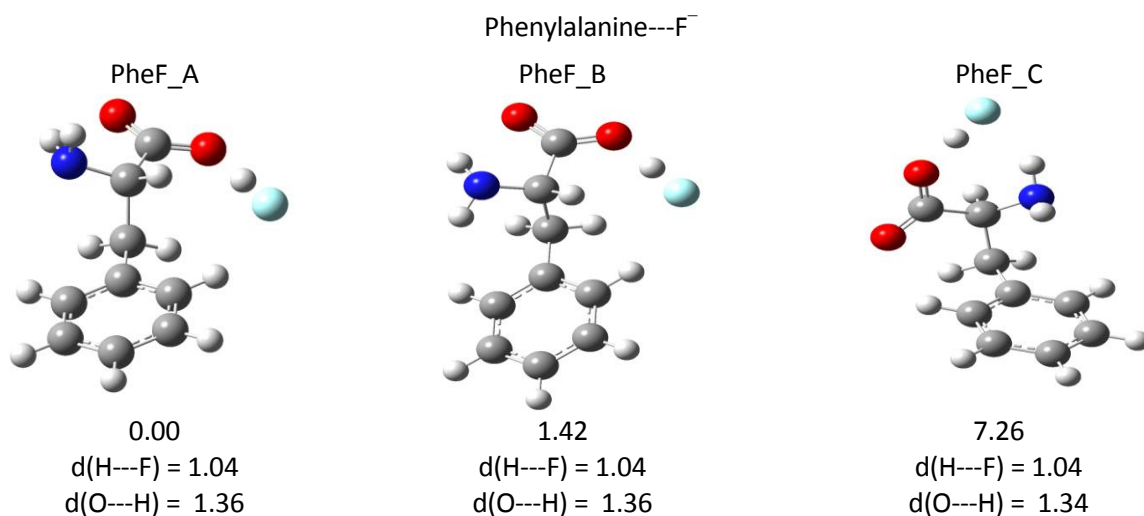
Figure 36: Phenylalanine clustered with fluoride base structures. Isomers are ordered from lowest to highest relative enthalpy. All three isomers show a preference for proton transfers, with HF being weakly bound to Phe. Relative enthalpies in kJ/mol with distances in Å.

The three lowest energy isomers for phenylalanine clustered with fluoride are shown in Figure 36. The most stable conformations for the fluoride anion are the same conformations as was seen with the chloride anion. However, while the chloride has no proton transfer (PT) properties with the base phenylalanine, all three lowest energy isomers for the fluoride ion show transfers occurring. The lowest energy isomer has the fluoride in the ring plane undergoing PT with the hydroxyl group. PheF_A has the amine group pointing away from the ring towards the carboxyl oxygen that is not interacting with the fluorine. The second lowest energy isomer, PheF_B, has the amine group pointing towards the ring, and PheF_C has adopted a formation where the fluoride is above the junction of the amino terminus allowing transfers with the hydroxyl oxygen in a Y like formation where CH is directed away from the ring.

2-fluorophenylalanine---F⁻

2FPheF_K

0.00
d(H---F) = 1.04
d(O---H) = 1.35
d(N-H---F) = 2.08

2FPheF_ C

0.00
d(H---F) = 1.04
d(O---H) = 1.35
d(N-H---F) = 2.08

2FPheF_A

7.46
d(H---F) = 1.01
d(O---H) = 1.41

3-fluorophenylalanine---F⁻

3FPheF_A

0.00
d(H---F) = 1.04
d(O---H) = 1.36

3FPheF_B

2.42
d(H---F) = 1.04
d(O---H) = 1.35

3FPheF_D

12.48
d(H---F) = 1.02
d(N---H) = 1.48

4-fluorophenylalanine---F⁻

4FPheF_A

0.00
d(H---F) = 1.04
d(O---H) = 1.35

4FPheF_B

2.77
d(H---F) = 1.04
d(O---H) = 1.35

4FPheF_N

10.59
d(H---F) = 0.99
d(O---H) = 1.47
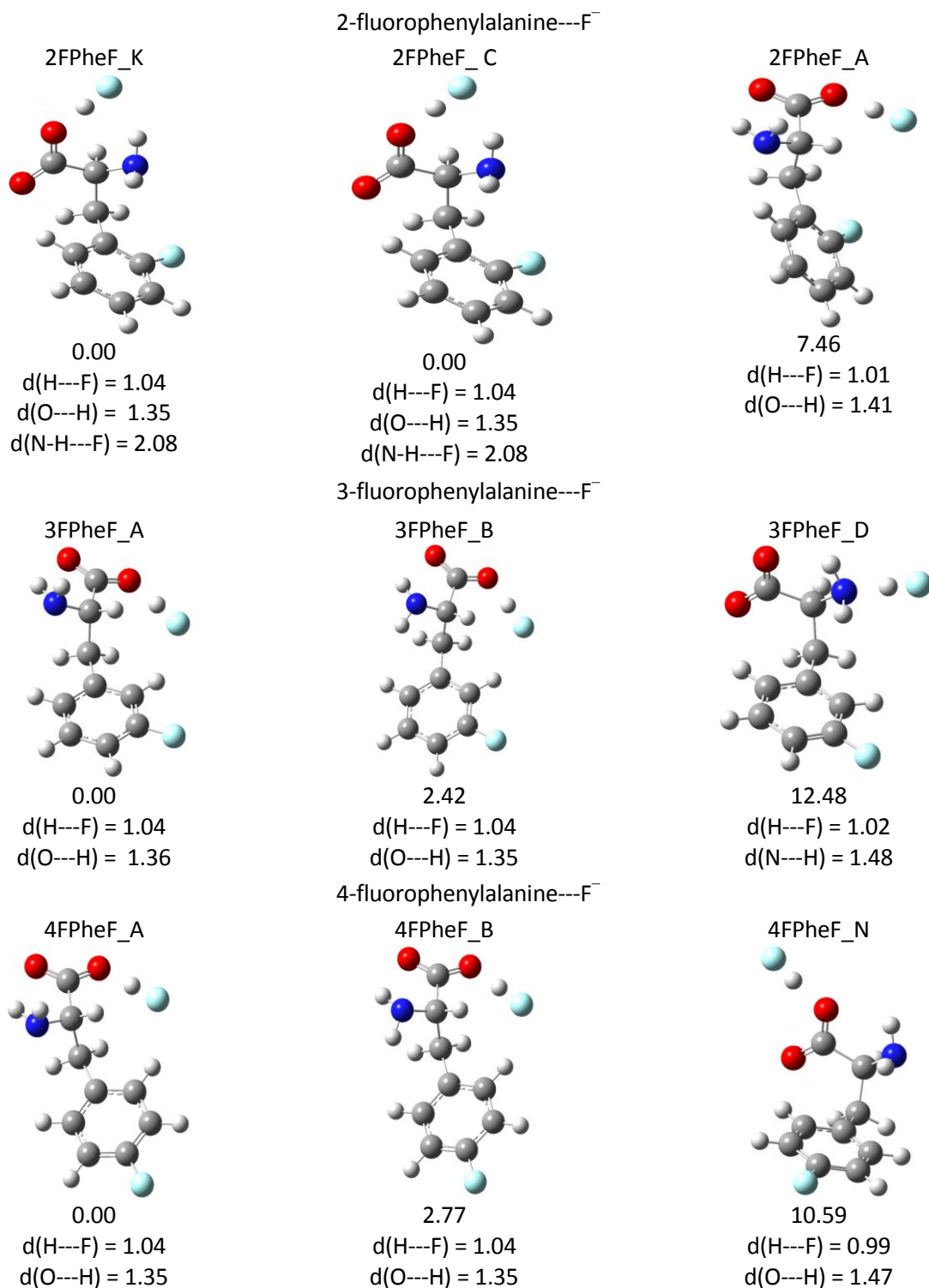
Figure 37: Monofluorinated phenylalanine clustered with fluoride. Three permutations of fluorine location around the phenyl ring exist for monofluorinated phenylalanine clusters. Isomers within each permutation are ordered in increasing enthalpy. Relative enthalpies listed in kJ/mol with distances in Å.

Fluorination of the phenyl ring shown in **Figure 37** illustrates the dependence on fluorination location. Fluorination at the *ortho* position prevents the HF from interacting with the ring. The two most stable structures are in the Y formation with the anion centered above the amino backbone with CH directed away from the ring creating a PT with the hydroxyl hydrogen. When the fluorine is moved to the *meta* position it allows interactions between the *ortho* hydrogen and the fluoride. This results in the ability for the fluoride to move into the ring plane, allowing additional hydrogen stabilizations. Fluorination *para* to the backbone has been observed to mimic the unfluorinated case with chloride anions. Fluorination at the *para* position clustered with fluoride follows this trend and shows that the two most stable isomers match those found in the unfluorinated case, however the third isomer differs. For 4-fluorophenylalanine, the HF is located near the carboxyl group creating a higher energy isomer, not the Y formation as was seen previously. Therefore the combination of anion and fluorination position appears to be dominating which structures are most stable.

2,3-difluorophenylalanine---F⁻

23FPheF_A
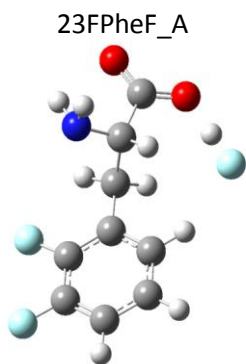
0.00
d(H---F) = 1.05
d(O---H) = 1.34

23FPheF_K

9.86
d(H---F) = 1.04
d(O---H) = 1.35

23FPheF_E
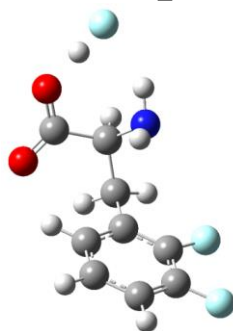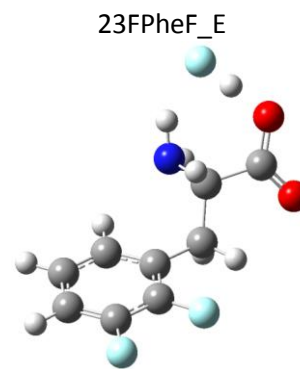
16.35
d(H---F) = 1.06
d(O---H) = 1.32

2,4-difluorophenylalanine---F⁻

24FPheF_K
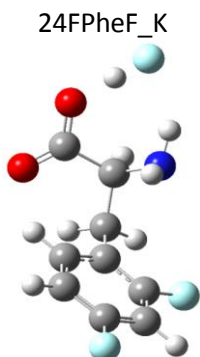
0.00
d(H---F) = 1.04
d(O---H) =1.35

24FPheF_E

5.65
d(H---F) = 1.01
d(O---H) =1.41

24FPheF_A

7.96
d(H---F) = 1.06
d(O---H) = 1.32

2,5-difluorophenylalanine---F⁻

25FPheF_K
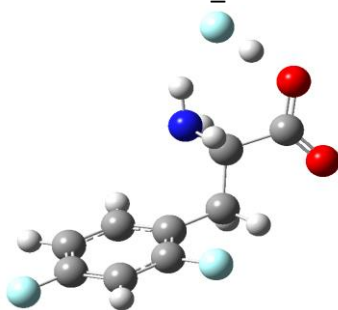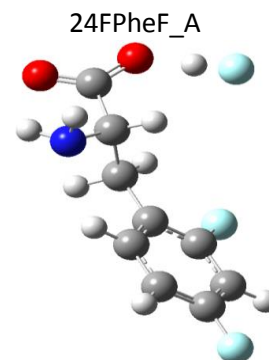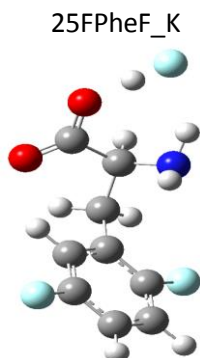
0.00
d(H---F) = 1.04
d(O---H) = 1.35

25FPheF_N

3.10
d(H---F) = 0.99
d(O---H) = 1.48

25FPheF_E
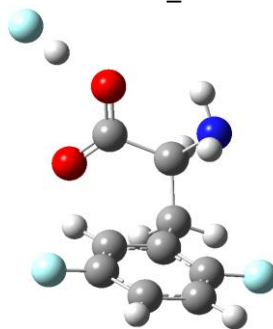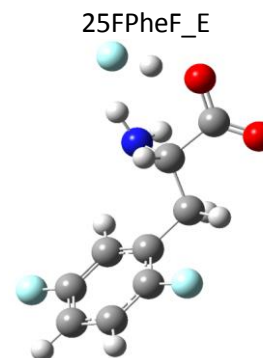
4.67
d(H---F) = 1.06
d(O---H) = 1.32
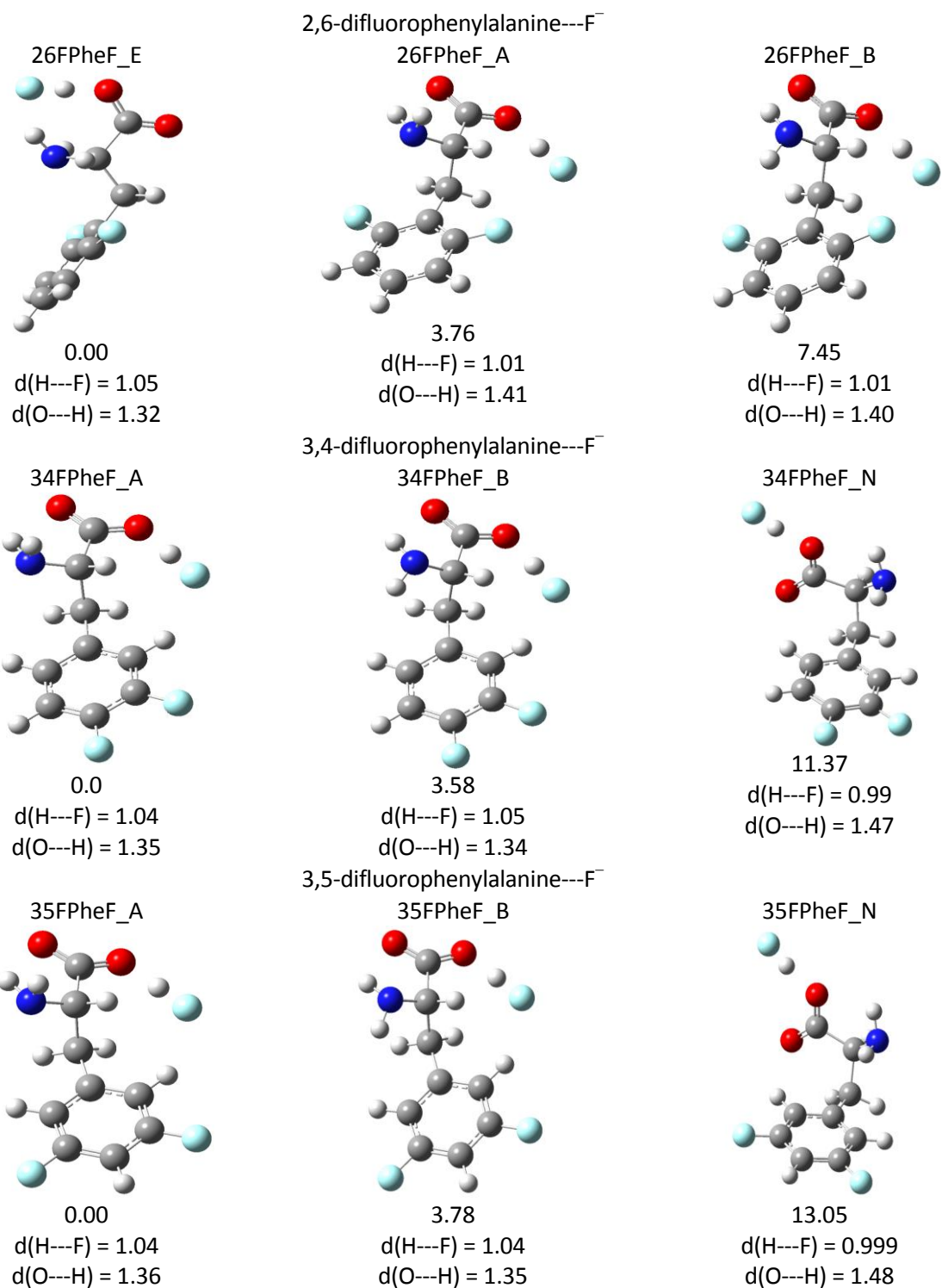
Figure 38: Difluorinated phenylalanine clustered with fluoride has six possible fluorine location permutations. The three lowest isomers as dictated by relative enthalpy are shown in increasing enthalpy. Relative enthalpies shown in kJ/mol with distanced listed in Å.

Secondary fluorination of the phenyl ring shown in **Figure 38** slightly increases the quadrupole moment. The difluorinated phenylalanine structures when clustered with chloride showed that there exist three main classes based on fluorination location. The three classes of fluorination around the ring are: 1) both position 2 and 6 are fluorinated 2) neither position 2, nor 6 are fluorinated 3) either position 2 or position 6 is fluorinated. Class 3 has two subclasses, A and B. Class 3A is where there exists a fluorination at a secondary carbon across the ring, that is to say, if position 2 is fluorinated, position 5 is also fluorinated. The reverse is also true for positions 3 and 6. Class 3B is where the secondary positions are not fluorinated.

Analysis of the class 1 structure (2,6-difluorophenylalanine) shows a similar claw-like structure as seen in the chloride cases where the amino backbone forms a claw with CH directed towards the ring. The remaining two isomers adopt the plane formations, where fluoride is in the ring plane with the amino terminus, specifically the CH and carboxyl groups.

The class 2 structures (3,4- and 3,5-difluorophenylalanine) typically produce isomers similar to the unfluorinated case. This is due to the electronegativity being far from the amino backbone allowing anion interaction with nearby ring hydrogens. Both isomers (3,4- and 3,5-difluorophenylalanine) show preferential anion location to be close to the ring plane interacting with ring hydrogens which is comparable to the unfluorinated case. The variation between unfluorinated and fluorinated class 2 structures exists in the third lowest energy isomer. While the unfluorinated case has the open Y formation with CH pointing away from the ring, the fluorinated derivative has fluoride located near the carboxyl terminus forming hydrogen fluoride (HF). Thus, excluding isomers that are closer to bond formation than PT with the fluoride, the structures found in class 2 duplicate the unfluorinated case as expected.

Class 3 isomers consist of two subclasses that are dependent on secondary fluorination. Subclass 3A (2,5-difluorophenylalanine) shows that all three isomers are close in energy. The most stable isomer is with the anion in the Y formation as previously seen, while the remaining two are with the anion near the carboxyl group as seen in class 2 isomers and with the anion in the claw formation. Removal of isomer N shows the possible two lowest energy isomers existing in the Y and claw-like formations. This ordering is different from the chloride case where all isomers were in the claw formation. The chloride case illustrated that the classes 2 and 3A predicted structures that were dominant for higher fluorination degrees. This implies that the claw or Y formations are likely present in the higher fluorinated phenylalanine clusters. As the trends observed in the chloride clusters are not being strictly followed, it can be surmised that the cause of the variations is due to the harder fluoride anion. Class 3B (2,3- and 2,4-difluorophenylalanine) illustrates the impact of having the charge localized predominately on one side of the phenyl ring. Localization of the charge produces structures that are in between classes 1 and 2 as only one of the primary fluorination sites is fluorinated. The two class 3B fluorination permutations show a similar ordering. 2,3-difluorophenylalanine shows ordering of unique isomers from lowest to highest energy as being in the plane (with the anion in the ring plane), Y, and claw formations, while 2,4-difluorophenylalanine has the ordering of Y, claw and a plane-like formation with NH_2 approaching the ring plane and the anion near the carboxyl group.

2,3,4-trifluorophenylalanine---F⁻

234FPheF_K
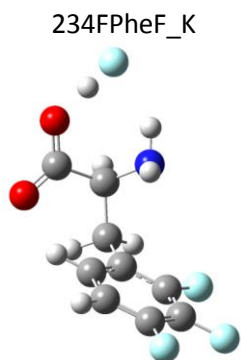
0.00
d(H---F) = 1.04
d(O---H) = 1.35

234FPheF_E

5.61
d(H---F) = 1.06
d(O---H) = 1.31

234FPheF_A
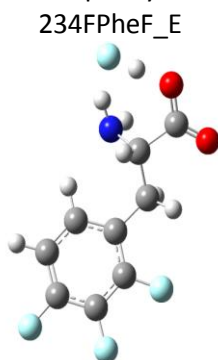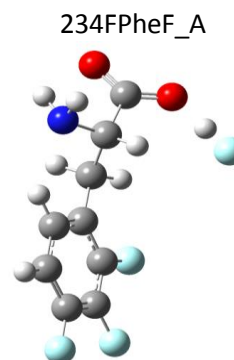
7.90
d(H---F) = 1.01
d(O---H) = 1.41

2,3,5-trifluorophenylalanine---F⁻
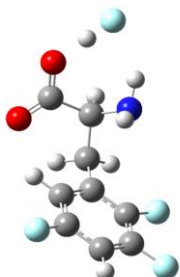
235FPheF_K

0.00
d(H---F) = 1.04
d(O---H) = 1.35
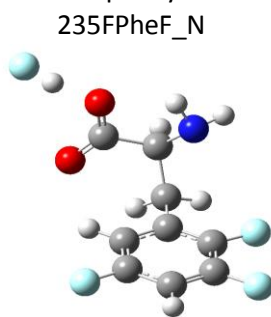
235FPheF_N

3.68
d(H---F) = 0.99
d(O---H) = 1.49

235FPheF_E
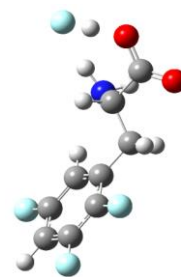
6.02
d(H---F) = 1.05
d(O---H) = 1.32

2,3,6-trifluorophenylalanine---F⁻
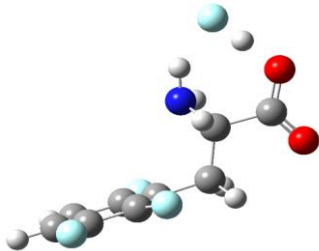
236FPheF_E

0.00
d(H---F) = 1.05
d(O---H) = 1.33

236FPheF_A
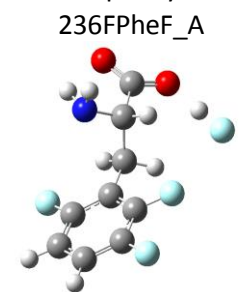
3.65
d(H---F) = 1.01
d(O---H) = 1.40

236FPheF_B
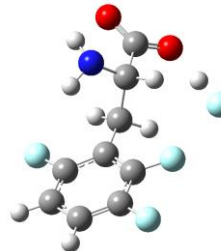
8.41
d(H---F) = 1.01
d(O---H) = 1.40
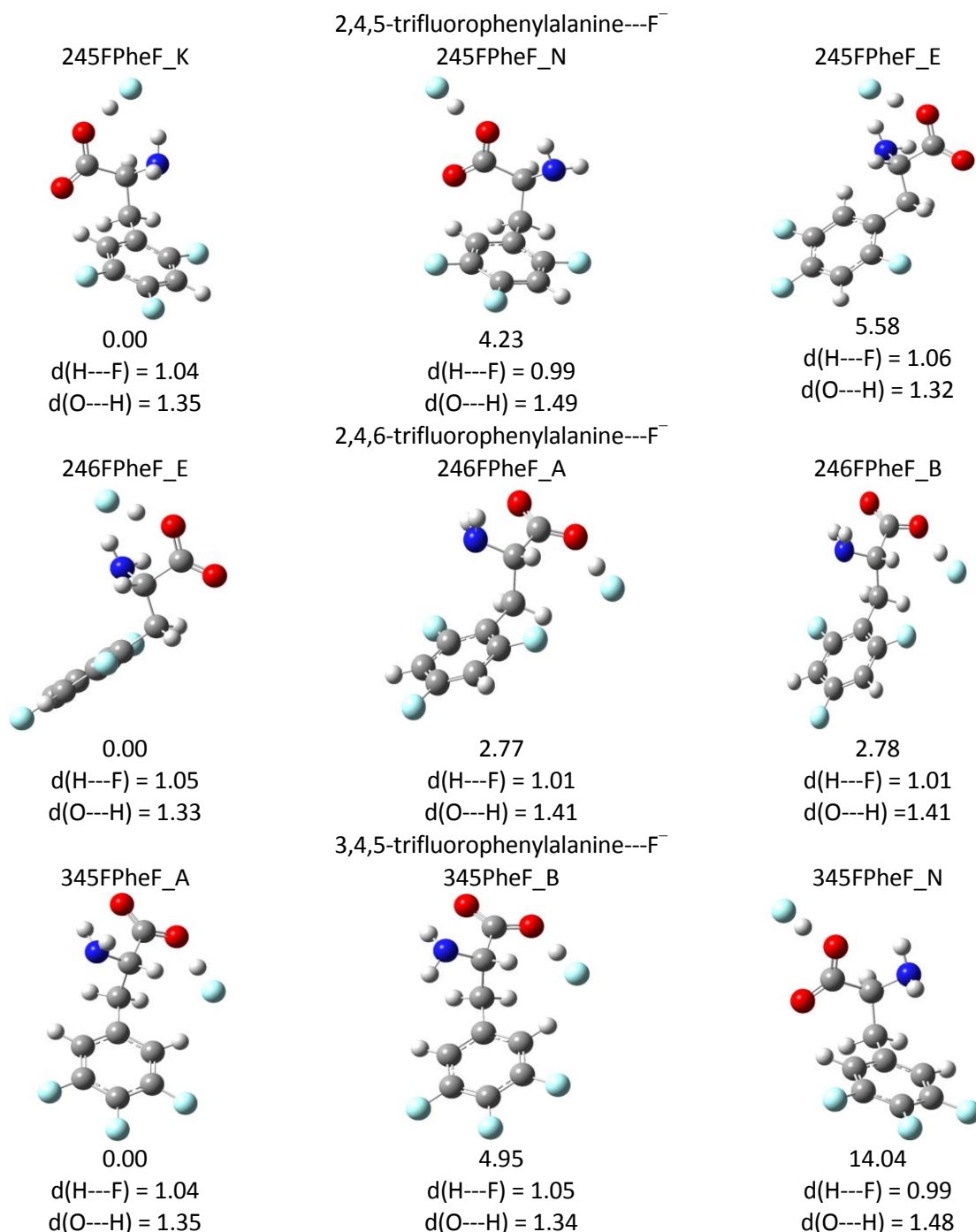
Figure 39: Trifluorinated phenylalanine clustered with fluoride has six fluorine location permutations. Isomers are ordered in increasing relative enthalpy for each permutation. ΔH in kJ/mol with distances in Å.

Addition of a third fluorine to the ring as seen in **Figure 39** also yields the three classes of

fluorination permutations. Class 1 structures (2,3,6- and 2,4,6-trifluorophenylalanine) show a

dominance of the claw formation. Both permutations within class 1 have the claw formation

being the lowest in energy followed by two planar formations where the fluoride anion is located in the plane of the ring interacting with CH_2 and carboxyl hydrogens. The claw formation is preferred in these two permutations as ring interactions are repulsive due to the ring fluorination location being near the amino backbone. Class 2 isomers are present in 3,4,5-trifluorophenylalanine clusters. These structures adopt mainly planar conformations with the exception of the third lowest energy structure which sees the anion moving away from PT and towards two distinct molecules. Excluding this last conformation, 3,4,5-trifluorophenylalanine adopts similar conformations as the unfluorinated entity. Class 3 structures illustrate the same lowest energy conformation independent of subclass. All three structures show that the lowest energy conformation is with the anion located in the Y formation. The class 3A permutations (2,3,5- and 2,4,5-trifluorophenylalanine) have identical structures. They both have the anion within the joint of the amino backbone (Y formation) as the lowest energy conformation, followed by the previously excluded carboxyl interaction isomer, with the claw formation being the least stable of the three. Excluding isomer N based on the previously discussed rationale leaves the Y and claw formations as the most likely to exist in the gas phase. Class 3B (2,3,4-trifluorophenylalanine) produces the same three isomers as well as energetic ordering as 2,4-difluorophenylalanine clustered with fluoride (**Figure 38**). This implies that the addition of a fluorine at the *meta* position has little effect on conformation for the clusters with fluoride.

2,3,4,5-tetrafluorophenylalanine---F⁻

2345FPheF_N

0.00
d(H---F) = 0.99
d(O---H) = 1.49

2345FPheF_A

3.26
d(H---F) = 1.01
d(O---H) =1.41

2345FPheF_E

3.30
d(H---F) = 1.01
d(O---H) = 1.32

2,3,4,6-tetrafluorophenylalanine---F⁻

2346FPheF_E

0.00
d(H---F) = 1.05
d(O---H) =1.33

2346FPheF_F

0.00
d(H---F) = 1.05
d(O---H) =1.33

2346FPheF_A

2.51
d(H---F) = 1.01
d(O---H) = 1.40

2,3,5,6-tetrafluorophenylalanine---F⁻

2356FPheF_E

0.00
d(H---F) = 1.05
d(O---H) = 1.33

2356FPheF_F

0.00
d(H---F) = 1.05
d(O---H) = 1.33

2356FPheF_A

2.97
d(H---F) = 1.01
d(O---H) = 1.41

Figure 40: Tetrafluorinated phenylalanine clustered with fluoride. Three permutations of fluorine location exist for the tetrafluorinated phenylalanine clusters.   Isomers are arranged in increasing relative enthalpy for each permutation. ΔH in kJ/mol with distances in Å.

Additional fluorination of the phenyl ring shown in **Figure 40** alters the quadrupole so that

anion interactions are favourable. However, the hardness of the fluoride has been seen to prefer

proton transfer over ring stabilization. When the ring fluorination leaves a hydrogen near the

amino backbone (2,3,4,5-tetrafluorophenylalanine) interactions between the hydrogen and either the anion or amine will dominate the overall conformation. The lowest energy isomer for 2,3,4,5-tetrafluorophenylalanine is with the anion interacting with the carboxyl hydrogen in such a way that hydrogen fluoride formation is likely. Exclusion of this structure leaves two plane-like conformations in which the amine group is approaching the ring plane. This leaves the carboxylic acid group open for interactions with the fluorine. Relocation of ring fluorination to 2,3,4,6-tetrafluorophenylalanine as well as 2,3,5,6-tetrafluorophenylalanine replaces the hydrogen closest to the amino backbone with a fluorine. This shifting of fluorination removes the ability of hydrogen interactions with the backbone. These two fluorination permutations yield the same three lowest energy conformations. The most stable structures are with the fluoride creating a claw-like formation with the amino backbone utilizing a hydrogen framework for additional stabilization. As all three structures differ in energy by less than 3 kJ/mol, it is concluded that all three are likely present in the gas phase. The third lowest energy conformations in both of these fluorination permutations see the fluoride slightly below the ring plane. This rotation allows the potential for interactions with the CH_2 hydrogens of the amino backbone.

2,3,4,5,6-pentafluorophenylalanine---F⁻

PentFPheF_E	PentFPheF_A	PentFPheF_B

0.00	2.07	2.07
d(H---F) = 1.05	d(H---F) = 1.01	d(H---F) = 1.01
d(O---H) = 1.34	d(O---H) = 1.40	d(O---H) = 1.40
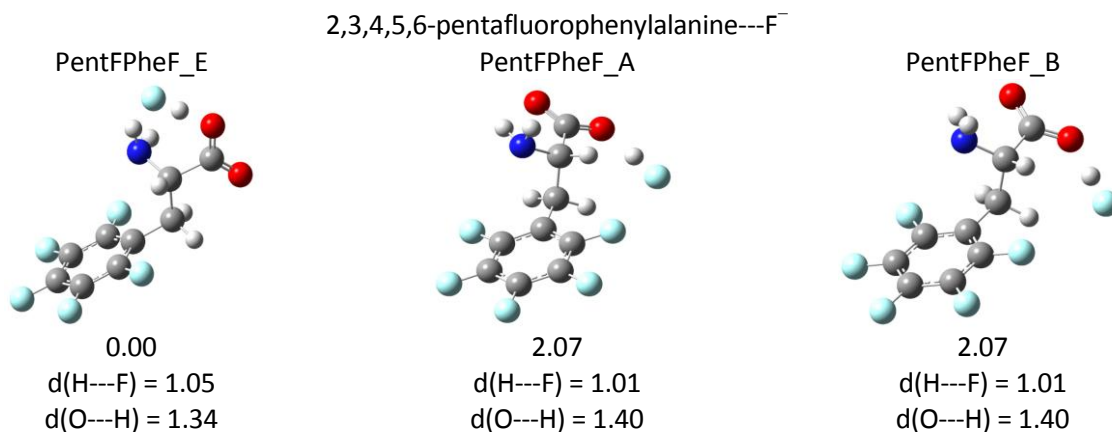
Figure 41: Pentafluorinated phenylalanine clustered with fluoride. Isomers are shown in increasing relative enthalpy. Relative enthalpies in kJ/mol with distances in Å.

Complete fluorination of the phenyl ring in theory will have inverted the quadrupole creating a positive center capable of anion stabilization. As seen in **Figure 41**, none of the lowest energy isomers have interactions with the ring center. This is due to the characteristics of the anion. As fluoride is a hard ion it will be difficult to approach the ring center without experiencing repulsive forces. The three lowest energy isomers that are produced through electronic structure calculations are in the claw and planar formations. This is due to fluoride's desire to induce proton transfer. The claw formation creates a PT between the carboxyl hydrogen and the fluoride; if the anion were any closer to the ring, a PT with the amine would likely result. This ability to produce a proton transfer chain upon migration of fluorine helps to stabilize the structure.

Prior fluorination permutations and degrees have shown the prevalence of the claw, Y and plane formations due to the combination of a proton transfers occurring and additional hydrogen stabilizations. Thus it is likely that at least one of these three conformations will be present in the gas phase depending on fluorination degree and location.

5.3.3 Br$^-$

It was previously observed that the hardness/softness of the chosen anion may either prevent or promote interactions with the ring. As bromide is a softer anion, it is likely that ring interactions will be present and have a larger role in which isomers are the lowest in energy. Electronic structure calculations found fourteen unique isomers of phenylalanine clustered with bromide. The three lowest energy isomers for each fluorine degree and permutation around the phenyl ring are displayed in **Figures 42-47**.
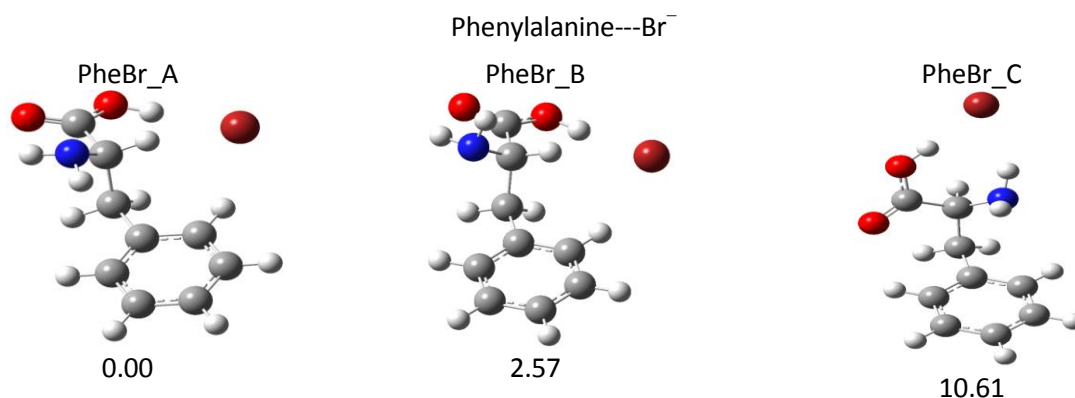
Figure 42: Phenylalanine clustered with bromide base structures. Conformations are ordered in increasing enthalpy listed in kJ/mol.

The unfluorinated phenylalanine clustered with bromide shown in **Figure 42** depicts the three lowest energy isomers. The first two structures, A and B, show a familiar conformation with the anion in the plane of the phenyl ring with the hydroxyl and CH groups bending towards it. This promotes stabilization through an intricate hydrogen network. The third lowest energy isomer has bromide located in the Y formation allowing interactions with the entirety of the amino backbone.
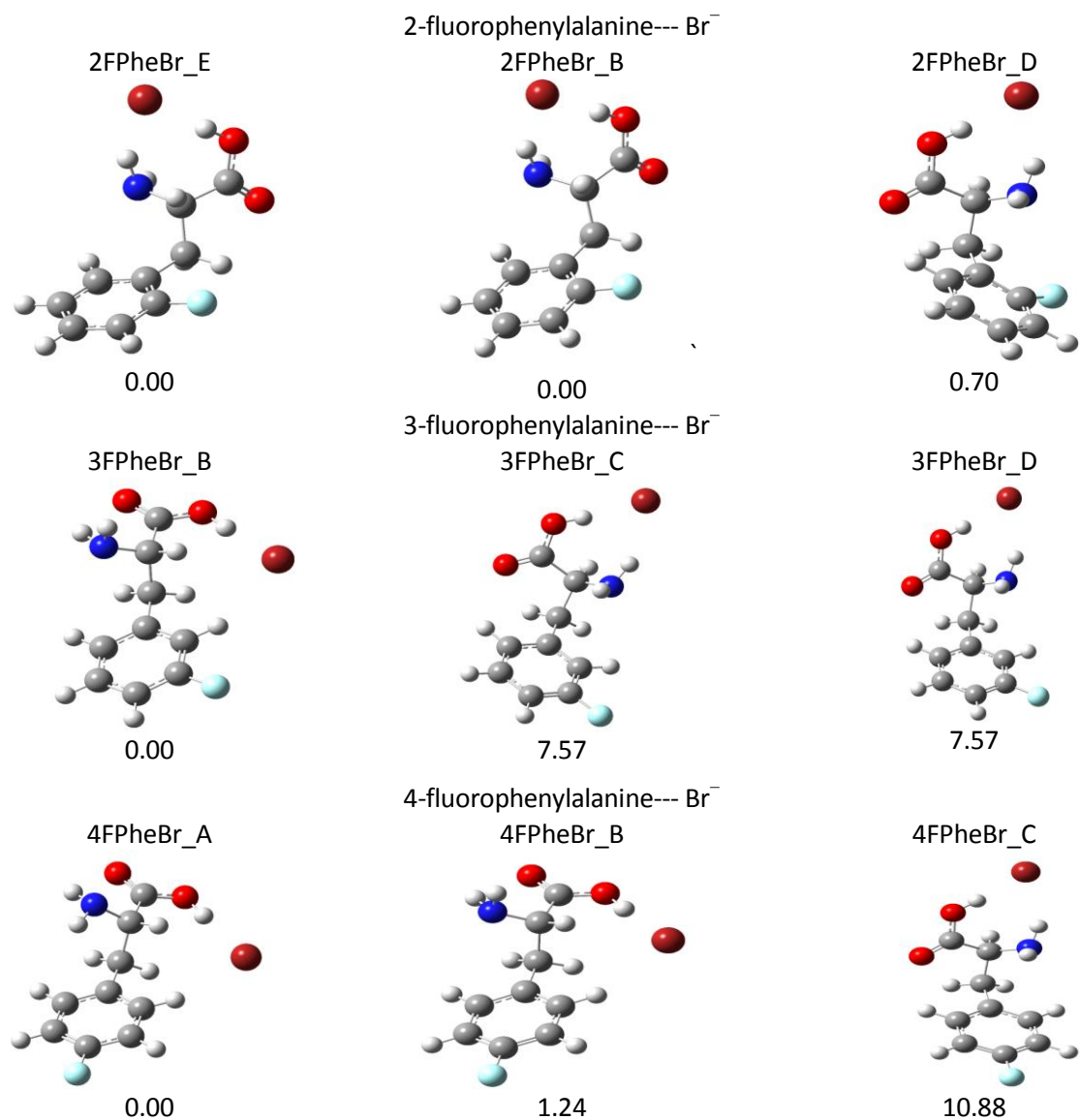
Figure 43: Monofluorinated phenylalanine clustered with bromide. Three permutations of fluorine location around the phenyl ring exist for monofluorinated phenylalanine clusters. Isomers are arranged in increasing relative enthalpy in kJ/mol for each permutation.

Fluorination of the phenyl ring shown in **Figure 43** begins the process of quadrupole moment inversion. The addition of one fluorine on the phenyl ring alters the quadrupole slightly, but not enough to see dominant anion-quadrupole interactions. The trends that have been previously identified due to fluorination location also exist for the bromide case. When the fluorine substituent is closer to the amino backbone (*ortho* substitution), greater quadrupole

effects are felt. The anion will come closer to the ring. As the normal quadrupole remains for

monofluorinated phenylalanine, bromide will form the claw and Y formations as the lowest

energy structures.   Moving the fluorination to the *meta* position provides a mixture of

interactions.   Thus, both plane and Y formations will exist.   *Para* fluorination creates an

atmosphere similar to the unfluorinated phenylalanine situation, and therefore the same

structures observed in the unfluorinated phenylalanine will be observed.

2,3-difluorophenylalanine---Br⁻

23FPheBr_H	23FPheBr_B	23FPheBr_E
0.00	1.05	1.07

2,4-difluorophenylalanine---Br⁻

24FPheBr_C	24FPheBr_B	24FPheBr_E
0.00	0.60	0.60

2,5-difluorophenylalanine---Br⁻

25FPheBr_B	25FPheBr_E	25FPheBr_F
0.00	0.00	4.10
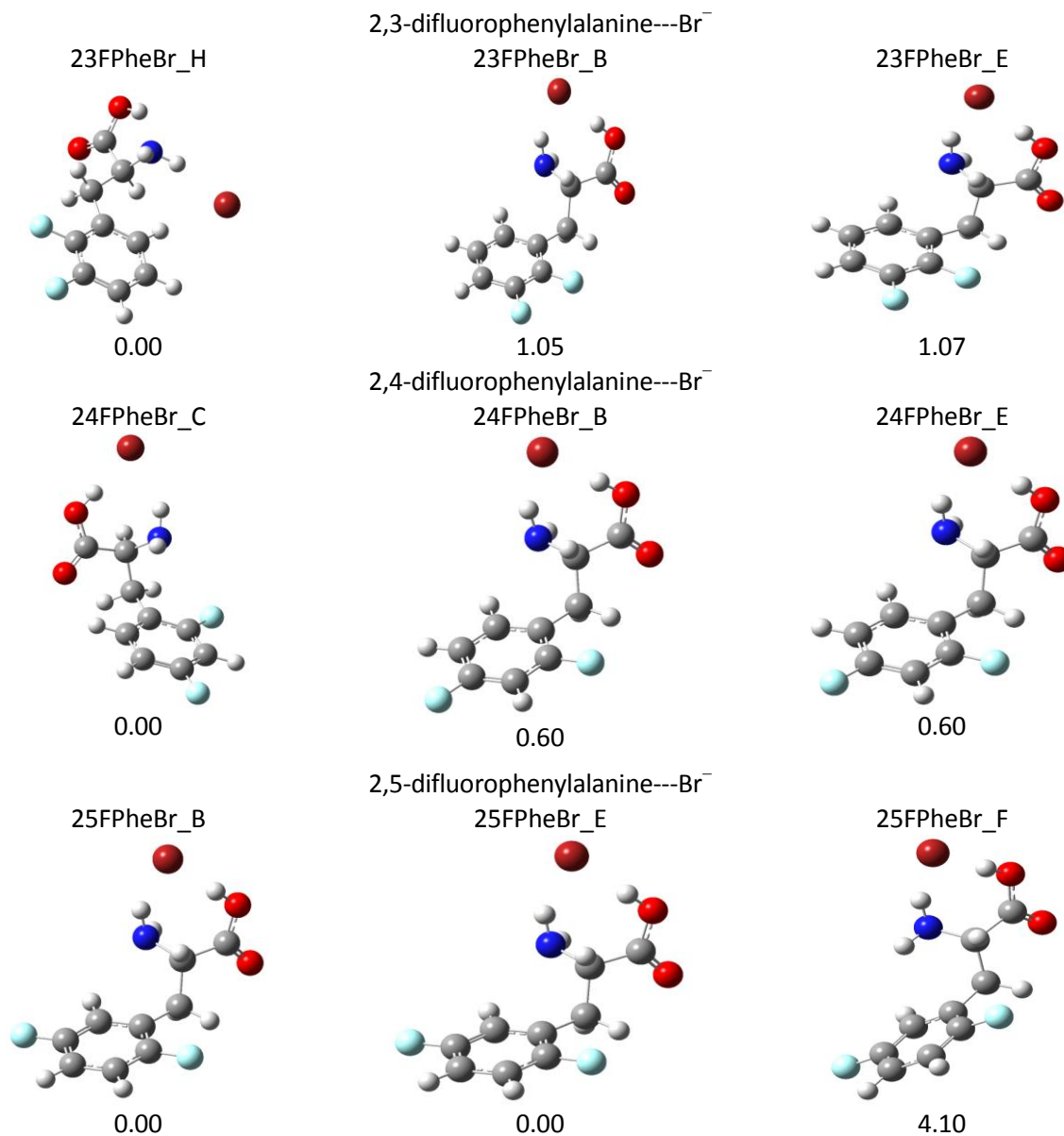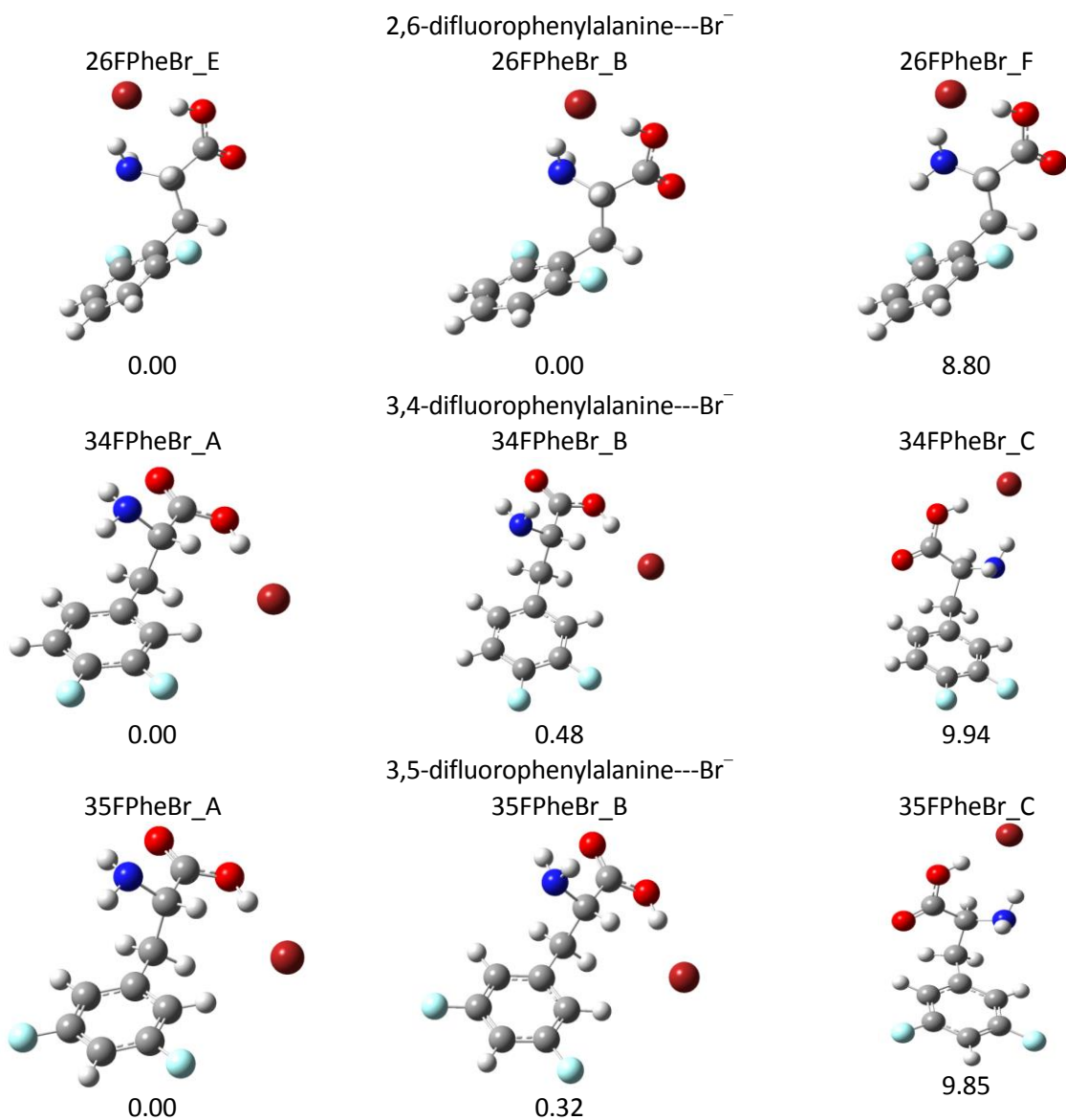
Figure 44: Difluorinated phenylalanine clustered with bromide has six permutations of ring fluorine location. Each permutation is arranged in increasing relative enthalpy in kJ/mol.

Additional fluorination shown in **Figure 44** increases the ability of the quadrupole moment to stabilize an anion. The strength of this interaction is still relatively weak so it is unlikely that ring interactions will be observed for the difluorinated isomers. The class 1 isomers (2,6-difluorophenylalanine) all adopt the claw formation. Class 1 isomers have a stronger influence of the quadrupole moment; therefore the anion prefers to be closer to the ring. This allows the anion in the claw formation to get closer to the ring than other conformations for difluorinated

phenylalanine. Class 2 permutations (3,4- and 3,5-difluorophenylalanine) produce identical isomer orders, with the lowest two configurations adopting the planar orientation. The least stable of the three is in the Y formation. In both of these Y formations, bromide is furthest away from the phenyl ring. Class 3A (2,5-difluorophenylalanine) results show a strong preference for the claw formation, replicating the class 1 isomers. For the class 3B structures, one variation exists between the two permutations (2,3- and 2,4-difluorophenylalanine). The lowest energy isomer for 2,3-difluorophenylalanine clusters is a distorted plane formation, where the bromide as well as all amino backbone carbons lie in the ring plane. While in the ring plane the remainder of the amino backbone remains in the claw-like formation. The most stable isomer for 2,4-difluorophenylalanine is in the Y formation. The remaining isomers for class 3B are all in the claw formation. As the isomers in 2,3-difluorophenylalanine and 2,4-difluorophenylalaine are within 1.10 and 0.60 kJ/mol respectively of each other, the variations are negligible as all three likely exist in the gas phase, with conversions between the three readily occurring.

2,3,4-trifluorophenylalanine---Br⁻

234FPheBr_B

0.00

234FPheBr_H

16.84

234FPheBr_C

18.19

2,3,5-trifluorophenylalanine---Br⁻

235FPheBr_E

0.00

235FPheBr_B

1.21

235FPheBr_F

6.07

2,3,6-trifluorophenylalanine---Br⁻

236FPheBr_E

0.00

236FPheBr_B

1.53

236FPheBr_D

9.45
d(ring center---Br⁻) = 3.93 Å

2,4,5-trifluorophenylalanine---Br⁻

245FPheBr_C

0.00

245FPheBr_E

0.25

245FPheBr_D

3.97
d(ring center---Br⁻) = 4.03 Å
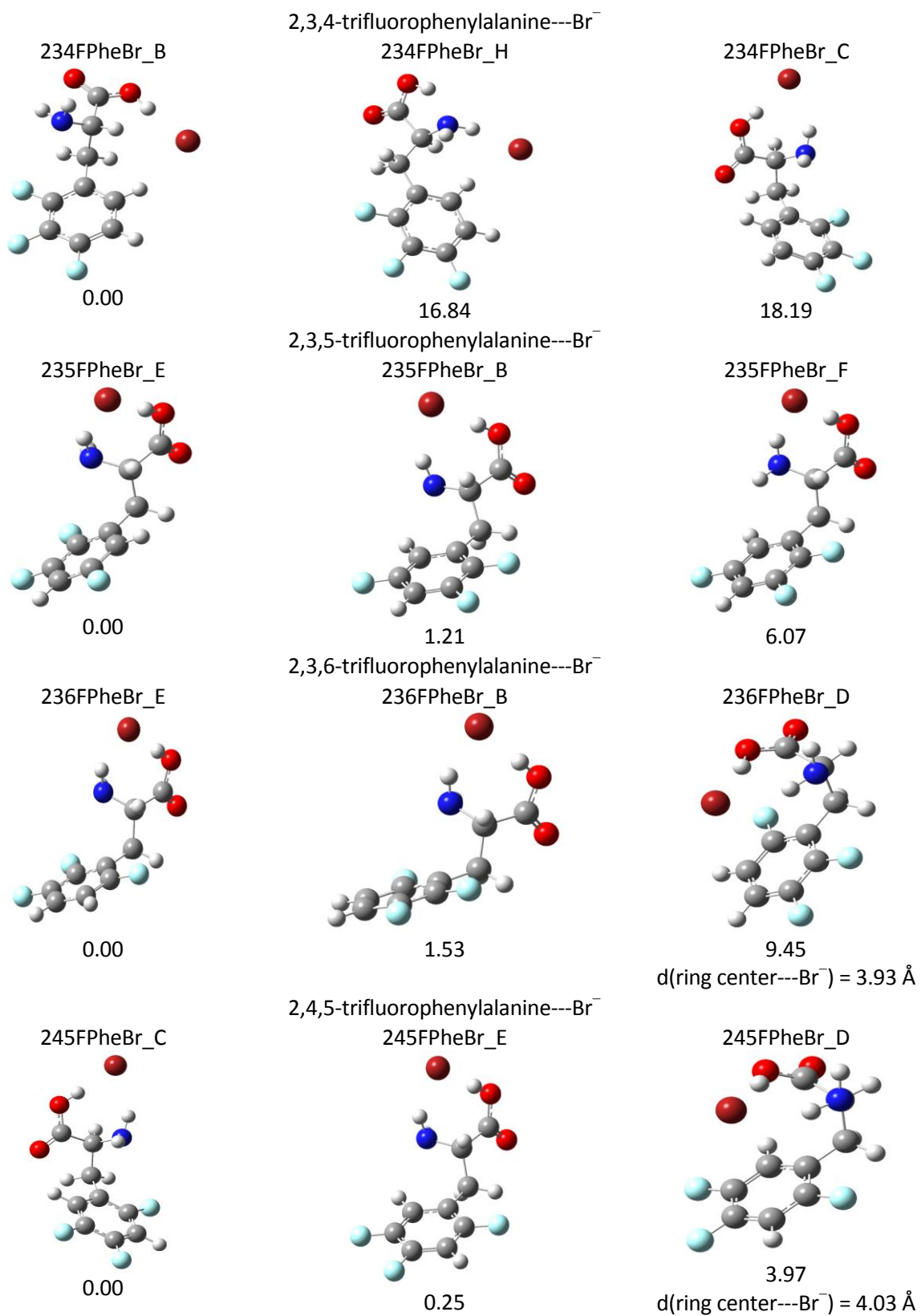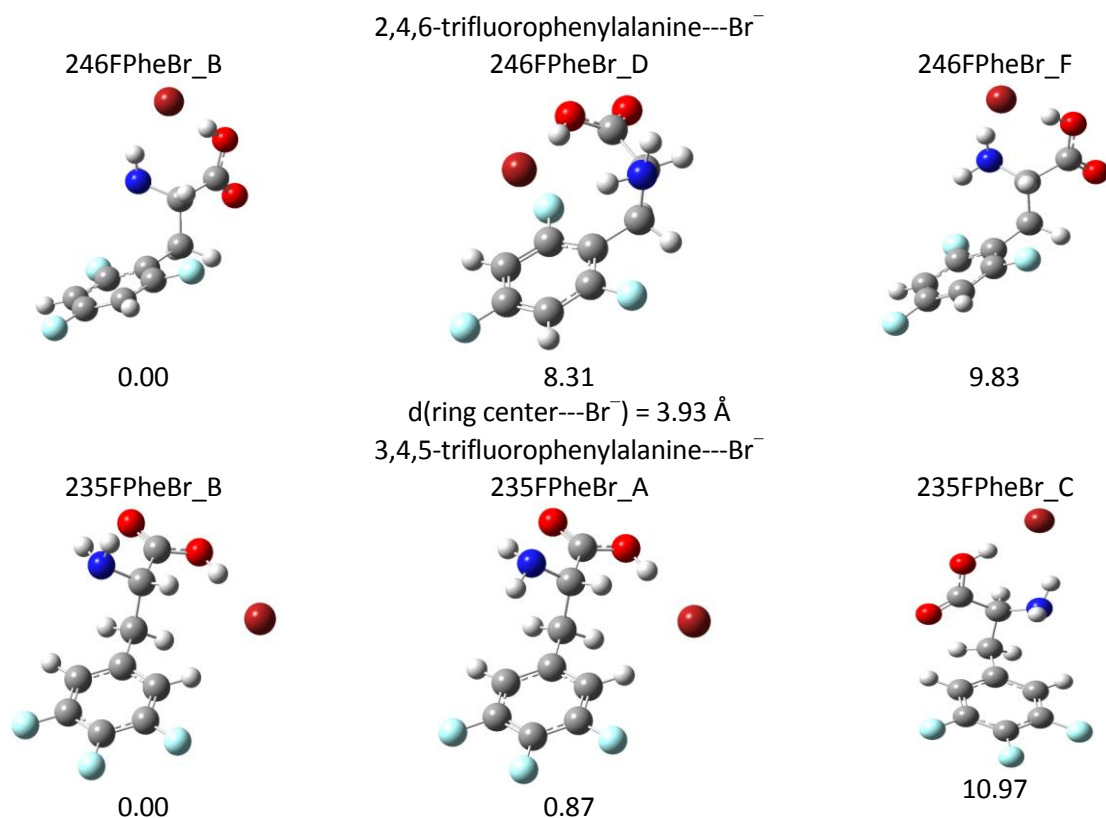
Figure 45: Trifluorinated phenylalanine clustered with bromide. Six permutations of fluorine location around the phenyl ring exist for trifluorinated phenylalanine clusters. Each permutation has isomers listed in increasing relative enthalpy in kJ/mol.

Addition of a third fluorine to the phenyl ring, as seen in **Figure 45,** is when the quadrupole interactions are beginning to dominate. The soft anionic nature of bromide allows the electron cloud to come into close proximity with the phenyl ring, thus promoting anion-quadrupole interactions.

Class 1 is where quadrupole-anion interactions are highest. These class 1 permutations (2,3,6- and 2,4,6-trifluorophenylalanine) give the first indication of ring interactions. Both permutations result in a mixture of claw and ring structures. The symmetry of fluorination around the ring (2,4,6-trifluorophenylalanine) shows ring interactions being the second lowest energy conformations with the remaining isomers adopting the claw formation. When the charge density lies predominately on one side of the ring, the ordering of the three isomers

changes making the ring conformation the highest in energy of the three isomers. Both class 1 conformations have the ring conformation being within 10 kJ/mol of the lowest energy conformation.

Class 2 permutations (3,4,5-trifluorophenylalanine) duplicate the structures and ordering of unfluorinated phenylalanine isomers as expected. It has already been seen that when the charge density is opposite the amino backbone, in the *para* position, the three lowest energy isomers will adopt both conformation and ordering of the unfluorinated situation.

Class 3A fluorination combinations (2,3,5- and 2,4,5-trifluorophenylalanine) show two different orders of lowest energy conformations. When the charge is dispersed so that it lies along one side of the ring, at positions closest to the backbone (2,3,5-trifluorophenylalanine), all three isomers are in the claw formation. When the charge is dispersed across the ring (2,4,5-triflurophenylalanine) three different conformations are lowest in energy, all within 3.40 kJ/mol of each other. The dispersion of the charge across the ring allows strengthening of the quadrupole moment as the quadrupole tensor lies more in the ring plane. This dispersion results in the following order of isomer: Y, claw and ring formations. The Y and claw formations are within 0.30 kJ/mol. This falls within the errors associated with the level of theory used and thus they are determined to be equivalent. As the ring formation is less than 4.00 kJ/mol higher in energy than the lowest energy conformation, it is likely that all three conformations are present.

The class 3B conformation (2,3,4-trifluorophenylalanine) shows the re-emergence of the unfluorinated structures with the exception of the second lowest energy isomer. The second lowest energy isomer is a distorted plane where the bromide and amino backbone carbons lie in

the ring plane. The size of the bromide electron cloud combined with the increasing inversion of

the quadrupole moment has allowed ring interactions to become favoured.

2,3,4,5-tetrafluorophenylalanine---Br⁻

2345FPheBr_C

2345FPheBr_E

2345FPheBr_B

0.00

0.05

1.23

2,3,4,6-tetrafluorophenylalanine---Br⁻

2346FPheBr_B

2346FPheBr_E

2346FPheBr_N

0.00

0.00

1.71

2,3,5,6-tetrafluorophenylalanine---Br⁻

2356FPheBr_B

2356FPheBr_E

2356FPheBr_D

0.00

0.00

5.78

d(ring center---Br⁻) =3.82 Å
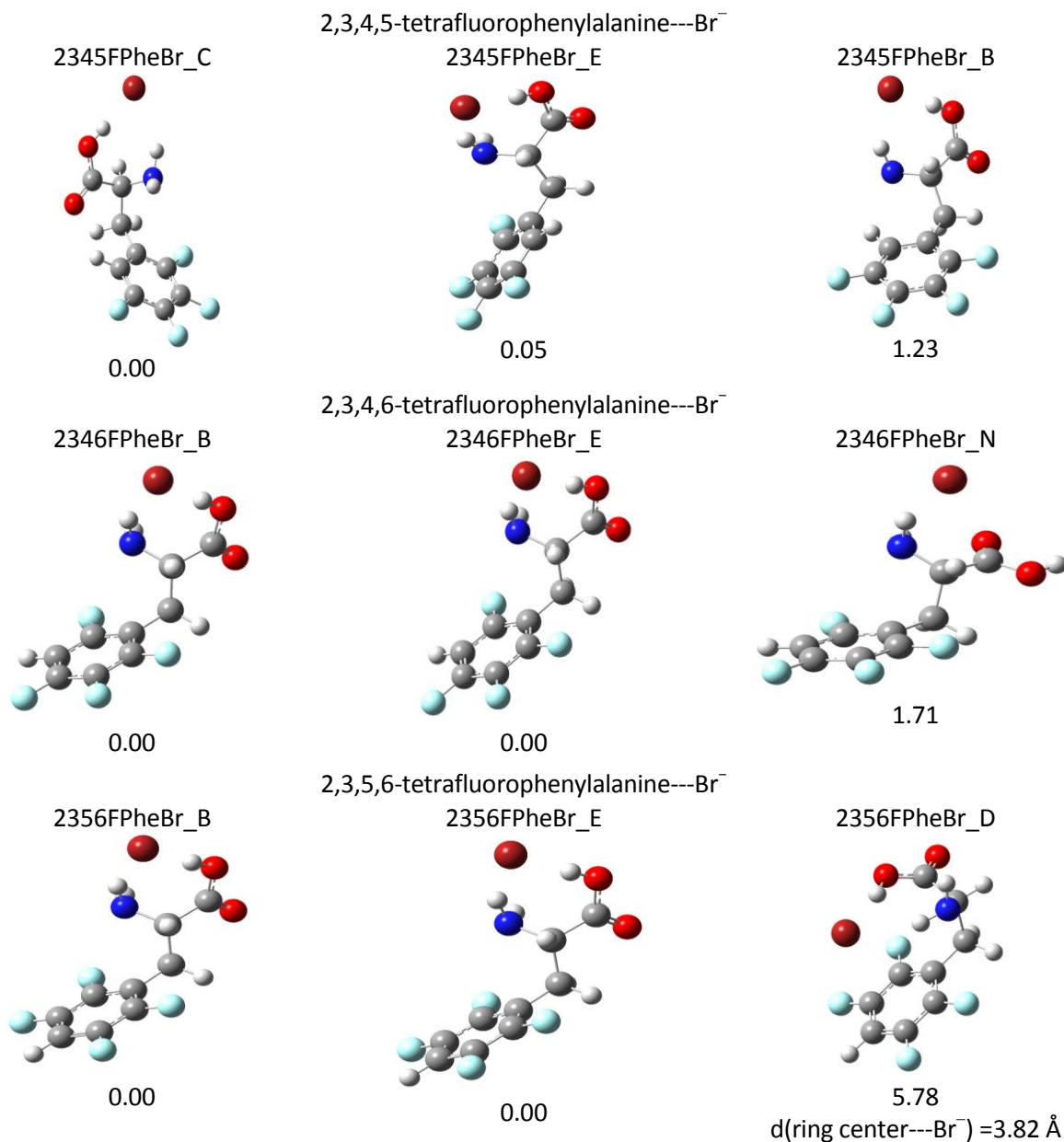
Figure 46: Tetrafluorinated phenylalanine clustered with bromide yields three permutations of fluorination locations. Each permutation has isomers ordered in increasing relative enthalpy in kJ/mol.

Additional fluorination as shown in **Figure 46** strengthens the quadrupole moment so that

inversion is almost complete.   With four fluorine substituents around the phenyl ring, anion

stabilization will be present. 2,3,4,5-tetrafluorophenylalanine results show that the Y formation is

dominant followed by the claw formation for this permutation around the ring. What isn't shown is that the fourth lowest energy isomer with enthalpy of 1.35 kJ/mol is in the ring formation with bromide located 3.91 Å from the center of the ring (See **Appendix A: Supplementary Information** for images and energetics). Moving the unfluorinated carbon to the *meta* position (2,3,4,6-tetrafluorophenylalanine) results in a similar scenario in which a ring structure is not present in the three lowest energy structures. The three lowest energy conformations consist of claw formations followed by a deviated Y formation with the carboxylic acid group being parallel to the ring plane. As before, the fourth lowest energy isomer (not shown) is in the ring formation with bromide located 3.84 Å from the center of the ring with relative enthalpy of 4.53 kJ/mol. As the energetics of these two permutations are both within 5 kJ/mol from their respective lowest energy conformations, it is believed that they will exist in the gas phase.

Symmetric fluorination around the ring with the unfluorinated carbon being *para* to the amino backbone (2,3,5,6-tetrafluorophenylalanine) produces a ring conformation within the top three energetically favoured isomers. This orientation of fluorines produces a ring structure with bromide located closest to the ring center. This ring proximity allows enhanced stabilization of the bromide. The ring conformation is not the lowest energy isomer. The lowest energy isomers are with the bromide in the claw formation. However, as all three isomers are within 6 kJ/mol it is likely that interconversions between the two conformations are likely to occur in the gas phase.
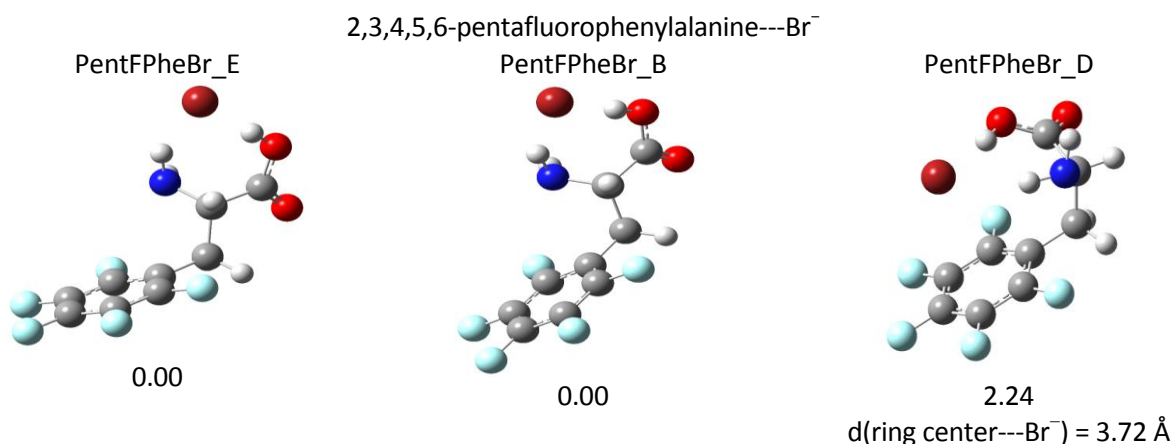
Figure 47: Isomers of pentafluorinated phenylalanine clustered with bromide. Isomers are listed in increasing enthalpy in kJ/mol.

Complete fluorination of the phenyl ring ensures full conversion of the quadrupole moment. This inversion means that anions can be stabilized directly over the center of the phenyl ring, provided appropriate anions are chosen. Electronic structure calculations for pentafluorophenylalanine produced the three isomers shown in **Figure 47**. The two lowest energy isomers have adopted the claw formation with bromide situated within the claw and the CH hydrogen directed towards ring fluorine. The third lowest energy isomer is in the ring formation with bromide located directly above the ring, 3.72 Å away from the center. The ring conformation is 2.24 kJ/mol higher in enthalpy than the lowest energy claw conformation. The comparable energies between the three isomers imply that all three are present in the gas phase.

Looking across the fluorination degrees, specifically at those that permit ring interactions, it is observed that as fluorination increases the distance between the bromide and the ring center decreases. Going from trifluorophenylalanine to pentafluorophenylalanine, ring structures had average ring to bromide distances of 3.96, 3.86 and 3.72 Å respectively. Thus the increasing fluorination is indeed affecting the anion-quadrupole interactions in a stabilizing manner.

5.4 Conclusions

It has been observed that both fluorination degree and location affect the observed lowest energy isomers. As fluorination increases so does the inversion degree of the quadrupole moment, and thus the ability for ring stabilization of the chosen anion also increases. Charge density around the ring, as dictated by fluorination location, alters the ordering and overall conformation of the three lowest energy isomers. When the charge is centralized opposite the phenylalanine backbone, in the *para* position, isomers will behave as if no ring fluorination exists. Fluorination close to the amino backbone has the opposite effect, where the quadrupole moment strength will be more strongly felt by the anion.

Fluorination of degrees 2 and 3 (di- and trifluorophenylalanine) result in three distinct class systems which can better predict which three lowest energy isomers will be present. These classes are based on the fluorination of the ring at positions 2 and 6. Class 1 consists of fluorination at both positions 2 and 6. This brings the charge density closer to the amino backbone which promotes anion-quadrupole interactions. Class 2 permutations are where neither position 2 nor position 6 are fluorinated. This class consists of conformations where the charge density is located furthest from the amino backbone. This class has been seen to replicate both the conformations and energy ordering of the unfluorinated phenylalanine clusters.

The third class, class 3, is where either position 2 or 6 is fluorinated. This class contains conformations that lie between classes 1 and 2, thus isomers within this class still have interactions with the quadrupole but on a lesser extent than class 2. Subclasses A and B exist within this class; they rely on secondary fluorination locations, positions 3 and 5 on the phenyl ring. Class 3A comprises of isomers where a secondary location across the ring is fluorinated. For

107

example if position 2 is fluorinated, then position 5 would also need to be fluorinated to be within class 3A. Fluorination at positions 3 and 6 is also included in class 3A. Class 3A anions typically feel the effects of the quadrupole more strongly than class 3B, and thus are governed slightly by the quadrupole. Class 3B is where the secondary fluorination location across the ring is unfluorinated. This unfluorination of the secondary location means that one side of the ring has at least two hydrogens in sequence on the ring. This opens up the ability for edgewise interactions between the amino backbone or anion and the ring hydrogens. This decreases any observed effects from the quadrupole. The three classes can aid in predicting which species will be present in the gas phase based on fluorination permutations.

Choice of anion also plays a key role in determining which conformations will be the most stable in the gas phase. Hard anions such as fluoride do not show anion-quadrupole interactions as they prefer to form structures where proton transfers are possible. The PT dominates which isomers will be formed as fluoride will prefer PT conformations over ring stabilization. Moving to softer anions increases the effect that the quadrupole moment has on anion stabilization. Experiments with chloride have shown that claw formations still dominate over ring interactions as the claw structures have additional hydrogen stabilization possibilities. Chloride is still a relatively small anion and thus it is difficult to interact with the quadrupole moment. The softest anion that was tested was bromide and this shows great promise for ring interactions. Higher fluorination degrees, of at least trifluorophenylalanine, begin to show the emergence of ring stabilization. As fluorination moves to higher degrees, the distance between the bromide and ring center reduces allowing stronger interactions.

In conclusion, three factors affect which conformations will be observed in the gas phase. Softer anions are more likely to have strong interactions with the quadrupole moment, while harder anions will prefer to create proton transfers in the gas phase. Increasing fluorination degree increases the inversion of the quadrupole moment allowing anion stabilization to occur. Location of fluorine substituents around the ring will dictate the overall structure. If the charge density of the fluorine atoms around the ring resides closer to the amino backbone, quadrupole interactions are more likely, while if the charge lies across the ring from the backbone, structures will mimic that of the unfluorinated phenylalanine scenario. It is the combination of these three factors that dictates the conformation of the lowest energy isomers.

Chapter 6
Conclusions and Future Work

The results of this thesis outline how factors such as fluorination degree and permutation influence the quadrupole moment and hence anion-quadrupole binding interactions. By increasing the degree of fluorination, the extent to which the phenylalanine quadrupole contains a positive ring face and thus the ability to stabilize an anion increases. Altering the permutation of fluorine substituents around the phenyl ring alters the direction of the quadrupole moment not the magnitude.

Spectral comparisons between experimental and computed spectra of phenylalanine and fluorinated phenylalanine derivatives (3-fluoro, 4-fluoro, and 2,5-difluorophenylalanine) clustered with chloride showed a better fit of higher energy isomers to the experimental IRMPD spectra. The higher energy isomers that increased the spectral match had the chloride ion located near the amino backbone in a claw-like formation. The lowest energy isomers for chloride, bromide and trifluoromethanolate ions clustered with phenylalanine and fluorinated phenylalanine derivatives showed a preference for edgewise interactions over quadrupole-anion interactions. Clusters involving a fluoride ion all contained proton transfers occurring between the fluoride and phenylalanine derivative, with the lowest energy structures having proton transfers with fluoride located in the ring plane outside of the ring.

Increasing fluorination of the phenyl ring showed that anion interactions with the ring face occurred for larger more diffuse anions (bromide). Harder anions, such as fluoride, showed proton transfers occurring for most of the isomers tested. Direct quadrupole-anion interactions with the ring face began to emerge after addition of three fluorine atoms to the ring

(trifluorophenylalanine). The charge density, or fluorine permutation, around the ring was seen to dictate the location of the anion and overall phenylalanine cluster formation. Permutation trends begin to emerge for difluorophenylalanine clusters and continued for clusters with higher fluorination degrees, up to and including tetrafluorophenylalanine clustered with a halide. These trends can be classified into three distinct classes.

Class 1 structures occur when positions 2 and 6 on the phenyl ring are fluorinated, creating a scenario where the charge density is located near the amino backbone. These isomers tend to adopt the conformations of pentafluorophenylalanine clusters. These clusters have the anion located in a claw-like formation with the amino backbone, or interacting with the ring face for softer anions.

Class 2 structures are when neither position 2 nor position 6 are fluorinated and therefore have the charge density located furthest from the amino backbone. This allows edgewise interactions between the ring edge and anion, thus mimicking unfluorinated phenylalanine anion cluster conformations.

Class 3 structures have fluorination of either position 2 or position 6. A secondary fluorination location across the phenyl ring will dictate which class, 3A or 3B, different isomers will fall into. Class 3A has fluorination across the ring (positions 2 and 5 are both fluorinated), these isomers tend to adopt conformations closer to the fully fluorinated pentafluorophenylalanine cluster conformations. Class 3B structures lack the fluorination at the secondary fluorination location. Due to this lack of fluorination at the secondary fluorination location, a region of unfluorination exists near the backbone, thus permitting edgewise

111

interactions. Therefore these isomers more closely resemble that of the Class 2 and hence the unfluorinated phenylalanine clusters.

Clusters involving fluoride showed proton transfers for all degrees of fluorination and permutation of fluorine atoms around the ring. Both bromide and chloride ions showed good correlation with the identified charge density classification system. The softer bromide showed the emergence of quadrupole-anion interactions with the ring face upon addition of three fluorine atoms to the phenyl ring. Results from the trifluorophenylalanine to pentafluorophenylalanine clusters with bromide illustrated that direct interactions between bromide and the ring face became more stable (energetically favoured) relative to the lowest energy isomer as fluorination increased. In addition, the distance between the anion and ring face also decreased as fluorination increased. Thus, softer anions are more likely to show anion-quadrupole interactions as fluorination of the phenyl ring increases, while the permutation of fluorine atoms around the ring will dictate which of the two extreme cluster conformations, phenylalanine or pentafluorophenylalanine, the isomers will adopt.

Future work will include investigating larger species, specifically a dipeptide of pentafluorophenylalanine. Anion-quadrupole interactions between the dipeptide and halides (X = Cl$^-$, Br$^-$, F$^-$) will be investigated using a molecular mechanical basin hopping algorithm with a CHELPG partition scheme to probe the potential energy surface to identify potential conformations. After acquiring the test set, the same computational and experimental methods used in this thesis with the exception of single point energy calculations will be used. Single point energy calculations will be run at a lower level of theory (MP2/aug-cc-pVDZ) due to continual convergence failures at MP2/aug-cc-pVTZ for the dipeptide systems. Completed computational

chemistry results indicate the preference of the two phenyl rings to interact in a T-shape. Lowest energy conformations suggest that for small anions such as fluoride, the anion will interact with one of the ring faces, allowing T-interactions between the rings to occur. Interactions with chloride also interact with a ring face but lose the strong ring T- interactions. Larger anions such as bromide are forced away from the ring face to the peptide bond for increased hydrogen bonding to allow the ring T-shape interactions to form. These preliminary results indicate a preference for T-interactions between the two rings, thus implying that T-interactions are more dominant than anion-quadrupole interactions in dictating where the anion will reside. Experimental IRMPD and anharmonic spectra generation is required to identify which structures are present in the gas phase.

Protonation of the dipeptide will also be investigated using the same methods as listed above for the anion-quadrupole investigations of the dipeptide to identify basic sites and preferred protonation locations. Preliminary investigations without the basin hopping algorithm have shown protonation is likely to occur along the peptide bond at the bridging carbonyl.

References

[1] Wade, Jr., L. G., Organic Chemistry Sixth Edition, New Jersy: Pearson Education Inc, 2006.

[2] D. Voet and J. G. Voet, *Biochemistry Third Edition,* New Yersy: John Wiley & Sons Ltd, 2004.

[3] P. R. Bovy, D. P. Getman, J. M. Matsoukas and G. J. Moore, *Biochemica et Biophysica ACTA,* vol. 1079, no. 1, pp. 23-28, 1991.

[4] P. P. Geurink, N. Liu, M. P. Spaans, S. L. Downey, A. M. van den Nieuwendijk, G. A. van der Marel, A. F. Kisselev, B. I. Florea and H. S. Overkleeft, *Journal of Medicinal Chemistry,* vol. 53, no. 5, pp. 2319-2323, 2010.

[5] S. Tetasang, S. Keawwangchai, S. Wanno and V. Ruangpornvisuti, *Structural Chemistry,* vol. 23, no. 1, pp. 7-15, 2012.

[6] J. Trudell, *Biophysical Chemistry,* vol. 73, pp. 7-11, 1998.

[7] S. Chakravarty, Z. Sheng, B. Iverson and B. Moore, *Federation of European Biochemical Societies,* vol. 586, pp. 4180-4185, 2012.

[8] J. Hernández-Trujillo, *Journal of Physical Chemistry,* vol. 100, no. 16, pp. 6524-6530, 1996.

[9] K. Cormier, M. Watt and M. Lewis, *Journal of Physical Chemistry A,* vol. 114, no. 43, pp. 11708-11713, 2010.

[10] A. Clements and M. Lewis, *Journal of Physical Chemistry,* vol. 110, no. 46, pp. 12705-12710, 2006.

[11] A. Rizzo, C. Cappelli, B. Jansik, D. Jonsson, P. Saek, S. Coriani, D. J. D. Wilson, T. Helgaker and H. Ågren, *Journal of Chemical Physics,* vol. 122, no. 23, p. 234314, 2005.

[12] J. Vrbancich and G. L. D. Ritchie, *Journal of the Chemical Society-Faraday Transactions II,* vol. 76, no. 6, pp. 648-659, 1980.

[13] T. D. Vaden, T. S. de Boer, J. P. Simons, L. C. Snoek, S. Suhai and B. Paizs, *Journal of Physical Chemistry A,* vol. 112, no. 20, pp. 4608-4616, 2008.

[14] M. R. Jackson, R. Beahm, S. Duvvuru, C. Narasimhan, J. Wu, H.-N. Wang, V. M. Philip, R. J. Hinde and E. E. Howell, *J. Phys. Chem B,* vol. 111, no. 28, pp. 8242 - 8249, 2007.

[15] J. O. Hirschfelder, C. F. Curtiss and R. B. Bird, Molecular Theory of Gases and Liquids, New York, USA: John Wiley & Sons, Inc., 1954.

[16] V. Philip, J. Harris, R. Adams, D. Nguyen, J. Spiers, J. Baudry, E. E. Howell and R. J. Hinde, *Biochemistry,* vol. 50, no. 14, pp. 2939-2950, 2011.

[17] M. Giese, M. Albrecht, T. Krappitz, M. Peters, V. Gossen, G. Raabe, A. Valkonen and K. Rissanen, *Chemical Communications,* vol. 48, no. 80, pp. 9983-9985, 2012.

[18] S. Pérez-Casas, J. Hernández-Trujilo and M. Costas, *Journal of Physical Chemistry B.,* vol. 107, no. 17, pp. 4167-4174, 2003.

[19] U. Purushotham, D. Vijay and G. N. Sastry, *Journal of computational chemistry,* vol. 33, no. 1, pp. 44-59, 2012.

[20] O. Perraud, V. Robert, H. Gornitzka, A. Martinez and J. Dutasta, *Angewandte Chemie-international edition,* vol. 51, no. 2, pp. 504-508, 2012.

[21] S. J. Xu, M. Nilles and J. K. H. Bowen, *Journal of Chemical Physics,* vol. 119, no. 20, pp. 10696-10701, 2003.

[22] K. T. Lee, J. Sung, K. J. Lee, S. K. Kim and Y. Park, *Chemical Physical Letters,* vol. 368, pp. 262-268, 2003.

[23] Gaussian 09 Revision A.1, M. J. Frisch, G. W. Trucks, H. B. Schlegel, G. E. Scuseria, M. A. Robb, J. R. Cheeseman, G. Scalmani, V. Barone, B. Mennucci, G. A. Petersson, H. Nakatsuji, M. Caricato, X. Li, H. P. Hratchian, A. F. Izmaylov, J. Bloino, G. Zheng, J. L. Sonnenberg, M. Hada, M. Ehara, K. Toyota, R. Fukuda, J. Hasegawa, M. Ishida, T. Nakajima, Y. Honda, O. Kitao, H. Nakai, T. Vreven, J. J. A. Montgomery, J. E. Peralta, F. Ogliaro, M. Bearpark, J. J. Heyd, E. Brothers, K. N. Kudin, V. N. Staroverov, R. Kobayashi, J. Normand, K. Raghavachari, A. Rendell, J. C. Burant, S. S. Iyengar, J. Tomasi, M. Cossi, N. Rega, J. M. Millam, M. Klene, J. E. Knox, J. B. Cross, V. Bakken, C. Adamo, J. Jaramillo, R. Comperts, R. E. Stratmann, O. Yazyev, A. J. Austin, R. Cammi, C. Pomelli, J. W. Ochterski, R. L. Martin, K. Morokuma, V. G. Zakrzewski, G. A. Voth, P. Salvador, J. J. Dannenberg, S. Dapprich, A. D. Daniels, O. Farkas, J. B. Foresman, J. V. Ortiz, J. Cioslowski and D. J. Fox, Gaussian, Inc.: Wallingford CT, 2009.

[24] GaussView, Version 5; Dennington, R.; Keith, T.; Millam, J., Semichem Inc.: Shawnee Mission KS, 2009.

[25] J. Cramer, Essentials of Computational Chemistry: Theories and Models Second Edition, West Sussex, England: John Wiley & Sons Ltd., 2010.

[26] R. Marta, Ph.D. Thesis, University of Waterloo, 2008.

[27] S. M. Martens, M. Sc.. Thesis, University of Waterloo, 2011.

[28] R. A. Marta, R. Wu, K. R. Eldridge, J. K. Martens and T. B. McMahon, *International Journal of Mass Spectrometry,* vol. 297, no. 1-3, pp. 76-84, 2010.

[29] R. A. Marta, R. Wu, K. R. Eldridge, J. K. Martens and T. B. McMahon, *Physical Chemistry Chemical Physics,* vol. 12, no. 14, pp. 3431-3442, 2010.

[30] S. M. Martens, R. A. Marta, J. K. Martens and T. B. McMahon, *Journal of the American Society for Mass Spectrometry,* vol. 23, no. 10, pp. 1697-1706, 2012.

[31] S. Martens, M.Sc. Thesis, University of Waterloo, 2011.

[32] A. Reddy and G. Sastry, *Journal of Physical Chemistry A,* vol. 109, no. 39, pp. 8893-8903, 2005.

[33] S. Rayne and K. Forest, *Journal of Molecular Structure-Theochem,* vol. 941, no. 1-3, pp. 107-118, 2010.

[34] J. VandeVondele and J. Hutter, *Journal of Chemical Physics,* vol. 127, no. 11, 2007.

[35] "Computational Chemistry Comparison and Benchmark Data Base," 2012. [Online]. Available: http://cccbdb.nist.gov/vsf.asp.

[36] K. Irikura, R. Johnson and R. Kacker, *J. Phys. Chem A.,* vol. 109, no. 37, pp. 8430-8437, 2005.

[37] S. F. Boys and F. Bernardi, *Molecular Physics,* vol. 19, no. 4, pp. 553-&, 1970.

[38] M. Gutowski, J. G. van Duijneveldt-van de Rijdt, J. H. van Lenthe and F. B. van Duijneveldt, *Journal of Chemical Physics,* vol. 98, no. 6, pp. 4728-4738, 1993.

[39] T. Engel and P. Reid, Thermodynamics, Statistical Thermodynamics, and Kinetics, Prentice Hall: New Jersey, 2006.

[40] K. Mizuse and A. Fujii, *Phys. Chem. Chem. Phys.,* vol. 13, no. 15, pp. 7129-7135, 2011.

[41] R. Wu, R. A. Marta, J. K. Martens, K. R. Eldridge and T. B. McMahon, *Journal of the Americal Society for Mass Spectrometry,* vol. 22, no. 9, pp. 1651-1659, 2011.

[42] J. M. Ortega, F. Glotin and R. Prazeres, in *International workshop on infrared microscopy and spectroscopy with acceleration based sources (WIRMS 2005)*, Rathen, Germany, 2006.

[43] L. Mac Alesse, A. Simon, T. B. McMahon, J. Ortega, D. Scuderi, J. Lemaire and P. Maitre, *Internationsl Journal of Mass Spectrometry,* vol. 249, pp. 14-20, 2006.

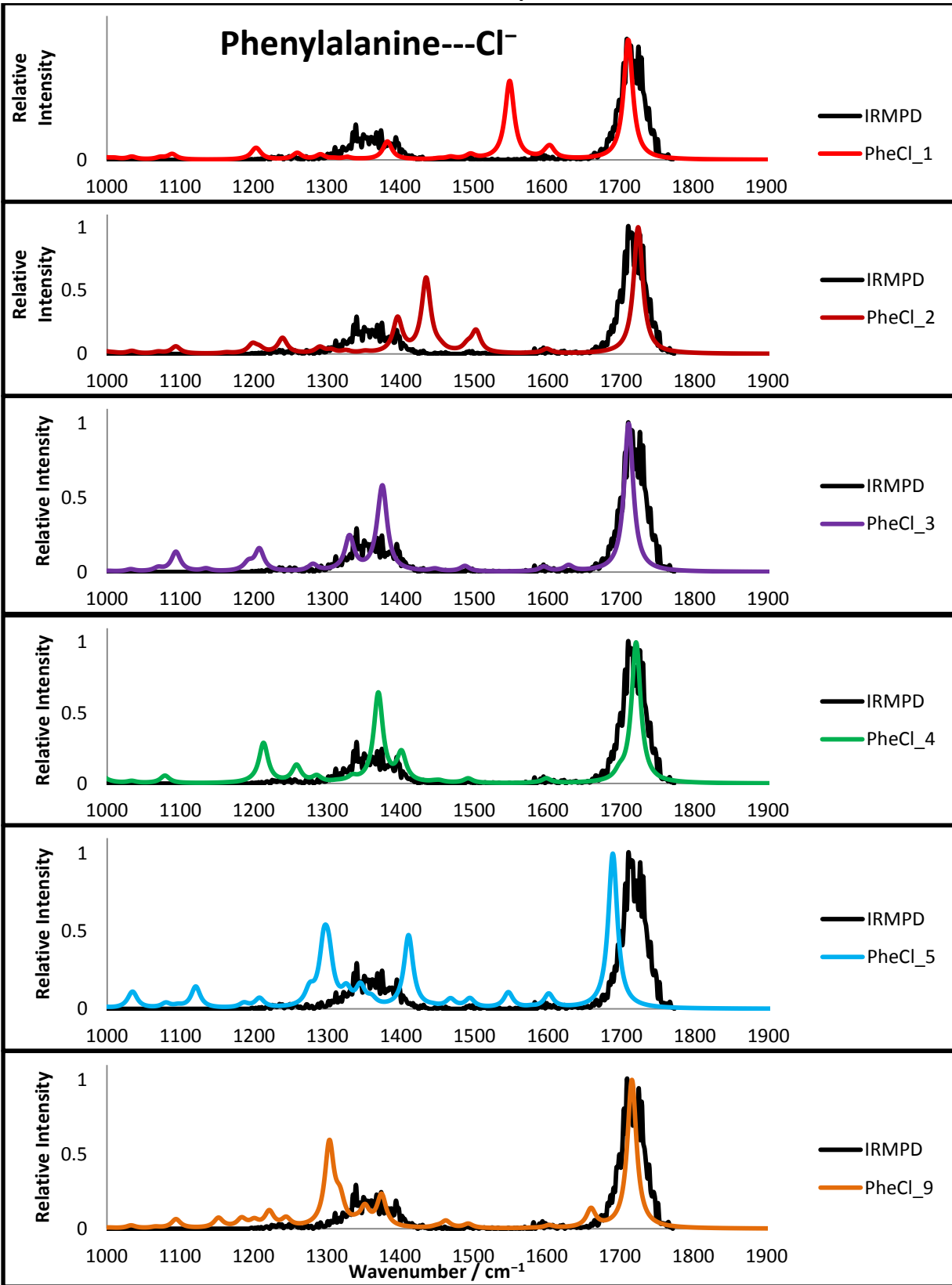[44] J. Lemaire, P. Boissel, M. Heniger, G. Mauclaire, G. Bellec, H. Mestdagh, A. Simon, S. Le Caer, J.

M. Ortega, F. Glotin and P. Maitre, *Physical Review Letters,* vol. 89, no. 27, 2002.

[45] P. Maitre, S. Le Caer, A. Simon, W. Jones, J. Lemaire, H. Mestdagh, M. Heninger, G. Mauclaire, P. Boissel, R. Prazeres, F. Glotin and J. Ortega, in *24th International Free Electron LaserConference/9th Free Electron Laser Users Workshop*, Argonne Natl Laab, Argonne, Illinois, 2002.

[46] R. L. Johnston, Atomic and Molecular Clusters, London: Taylor & Francis Group, 2002.

[47] W. S. Hopkins, R. A. Marta and T. B. McMahon, *Jornal of Phyeical Chemistry A,* vol. 117, pp. 10714-10718, 2013.

[48] D. Harris, Quantitative Chemical Analysis Seventh Edition, New York: W.H. Freeman and Company, 2007.

[49] R. C. Dunbar, J. D. Steill and J. Oomens, *Physical Chemistry Chemical Physics,* vol. 12, no. 41, pp. 13383-13393, 2010.

[50] R. A. O'hair, *Chemical communications,* no. 14, pp. 1469-1481, 2006.

[51] R. Prazeres, F. Glotin, J. M. Ortega, C. Rippon, R. Andouart, J. M. Berset, E. Arnaud and R. Chaput, *Nuclear Instruments and Methods in Physics Research A,* vol. 445, pp. 204-207, 2000.

[52] B. Chiavarino, M. E. Crestoni, S. Fornarini, J. Lemaire, P. Maitre and L. MacAleese, *Journal of the American Chemical Society,* vol. 128, no. 38, pp. 12553-12561, 2006.

[53] M. E. Courprie and J. M. Ortega, *Analusis,* vol. 28, no. 8, pp. 725-736, 2000.

[54] R. E. March, *Journal of Mass Sectrometry,* vol. 32, pp. 351-369, 1997.

[55] Centre Laser Infrarouge d'Orsay, "The accelerator," 2013. [Online]. Available: http://clio.lcp.u-psud.fr/clio_eng/accel.html.

[56] D. Oepts, A. F. G. van der Meer and v. A. P. W., *Infrared Physics and Technology,* vol. 36, no. 1, pp. 297-308, 1995.

[57] Centre Laser Infrarouge d'Orsay, "What is a Free Electron Laser," 2013. [Online]. Available: http://clio.lcp.u-psud.fr/clio_eng/FEL.html.

[58] S. Hopkins, *Chem 450/750: Atomic and Molecular Clusters Course Notes,* Waterloo Canada: University of Waterloo, 2013.

[59] D. Ortiz, P. Martin-Gago, A. Riera, K. Song, J. Salpin and R. Spezia, *International Journal of Mass Spectrometry,* vol. 335, pp. 33-44, 2013.

[60] L. Chirlian, M. Miller and M. Franel, *Journal of Computational Chemistry,* vol. 8, no. 6, pp. 894-905, 1987.

[61] C. Breneman and K. Wiberg, *Journal of Computational Chemistry,* vol. 11, no. 3, pp. 361-373, 1990.

[62] W. S. Hopkins, *NSERC Engage Grant Technical Report: Solvent Clustering in DMS,* Waterloo: University of Waterloo, 2014.

[63] E. B. Wilson, *Physical Review,* vol. 45, no. 10, pp. 706-714, 1934.

[64] A. M. Gardner and T. G. Wright, *Journal of Chemical Physics,* vol. 135, no. 11, p. 114305, 2011.

[65] D. J. Wales and J. P. Doya, *Journal of Physical Chemistry A.,* vol. 101, no. 28, pp. 5111-5116, 1997.

Appendix A: Supplementary Information

Ring Vibrations Using Wilson and Gardner Notation [63, 64]			
2	7b	8a	9a
9b	13	15	18a
$\mu_{23}(b2)$		$\mu_{24}(b2)$	$\mu_{25}(b2)$

118

Anharmonic Spectra

Phenylalanine---Cl⁻

3-Fluorophenylalanine---Cl⁻

4-fluorophenylalanine---Cl⁻

2,5-difluorophenylalanine---Cl⁻

Phenylalanine---F⁻

3-Fluorophenylalanine---F⁻

2,5-difluorophenylalanine---F⁻

3-Fluorophenylalanine---Br$^-$

4-Fluorophenylalanine---Br$^-$

2,5-difluorophenylalanine---Br⁻

Phenylalanine---CF$_3$O$^-$

3-fluorophenylalanine---CF$_3$O$^-$
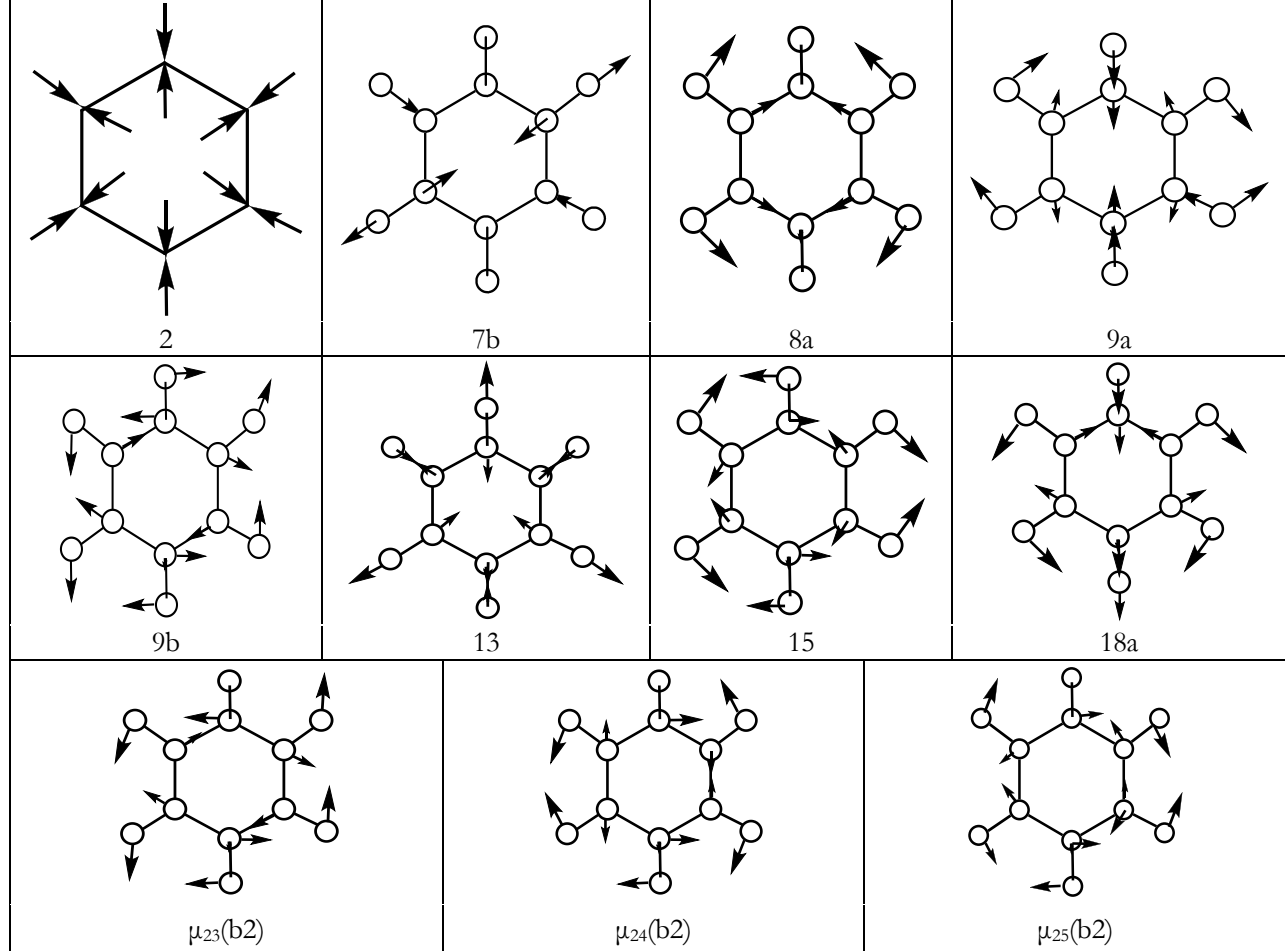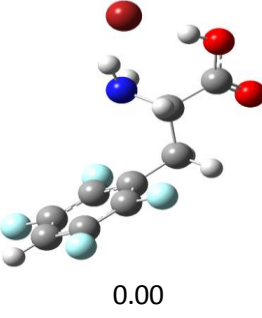
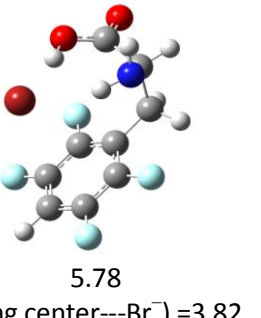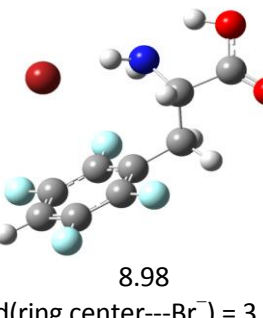# 4-fluorophenylalanine---CF$_3$O$^-$
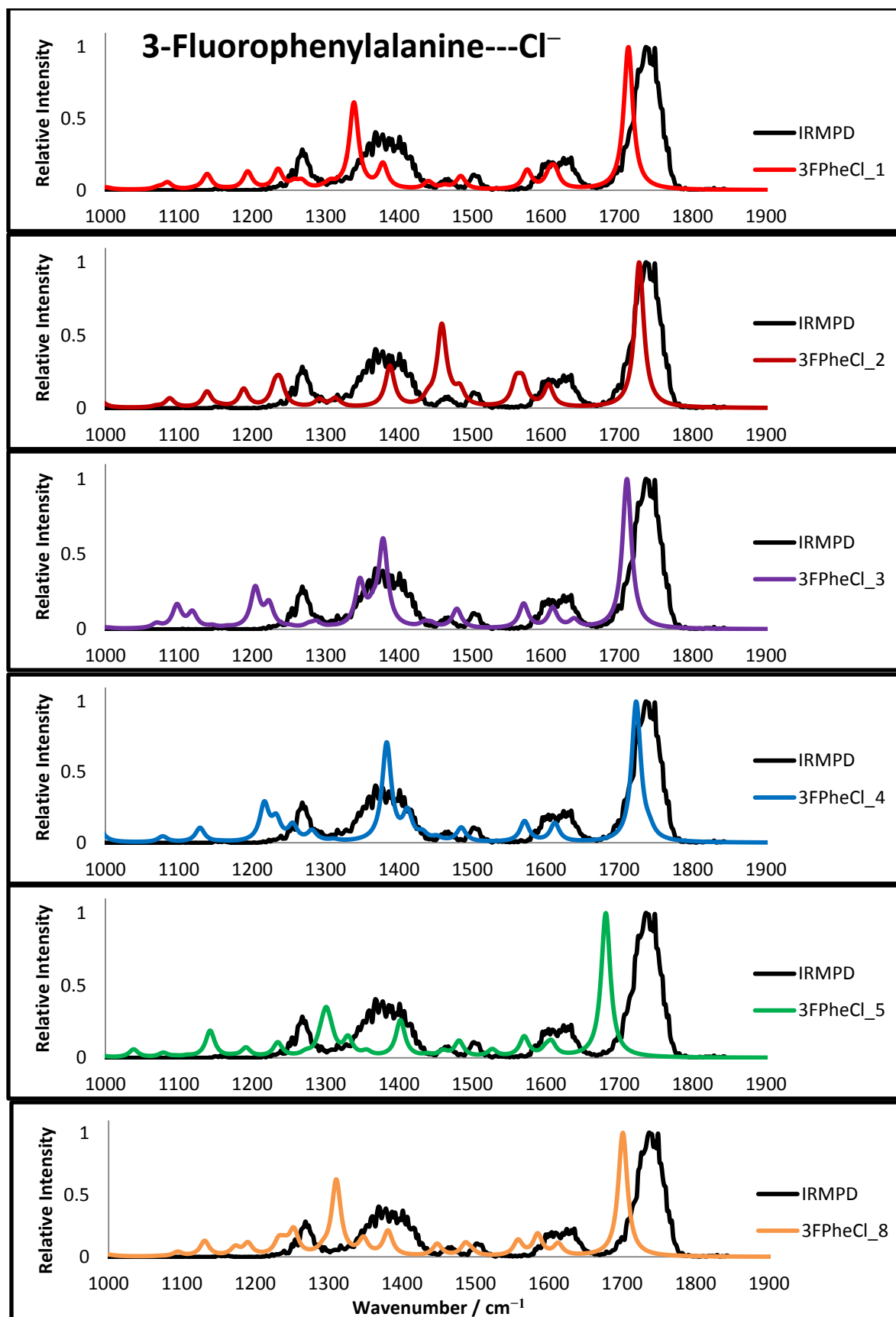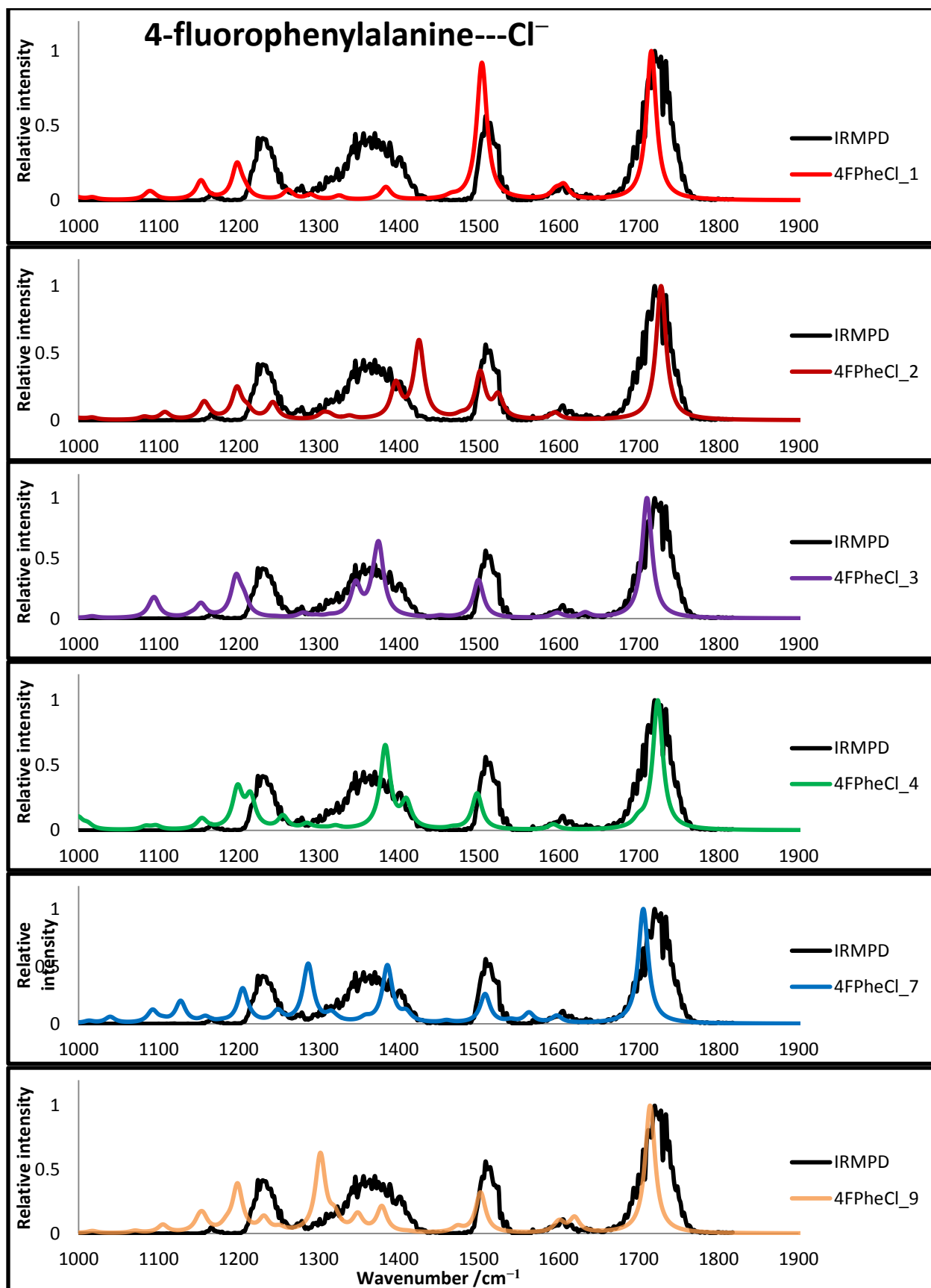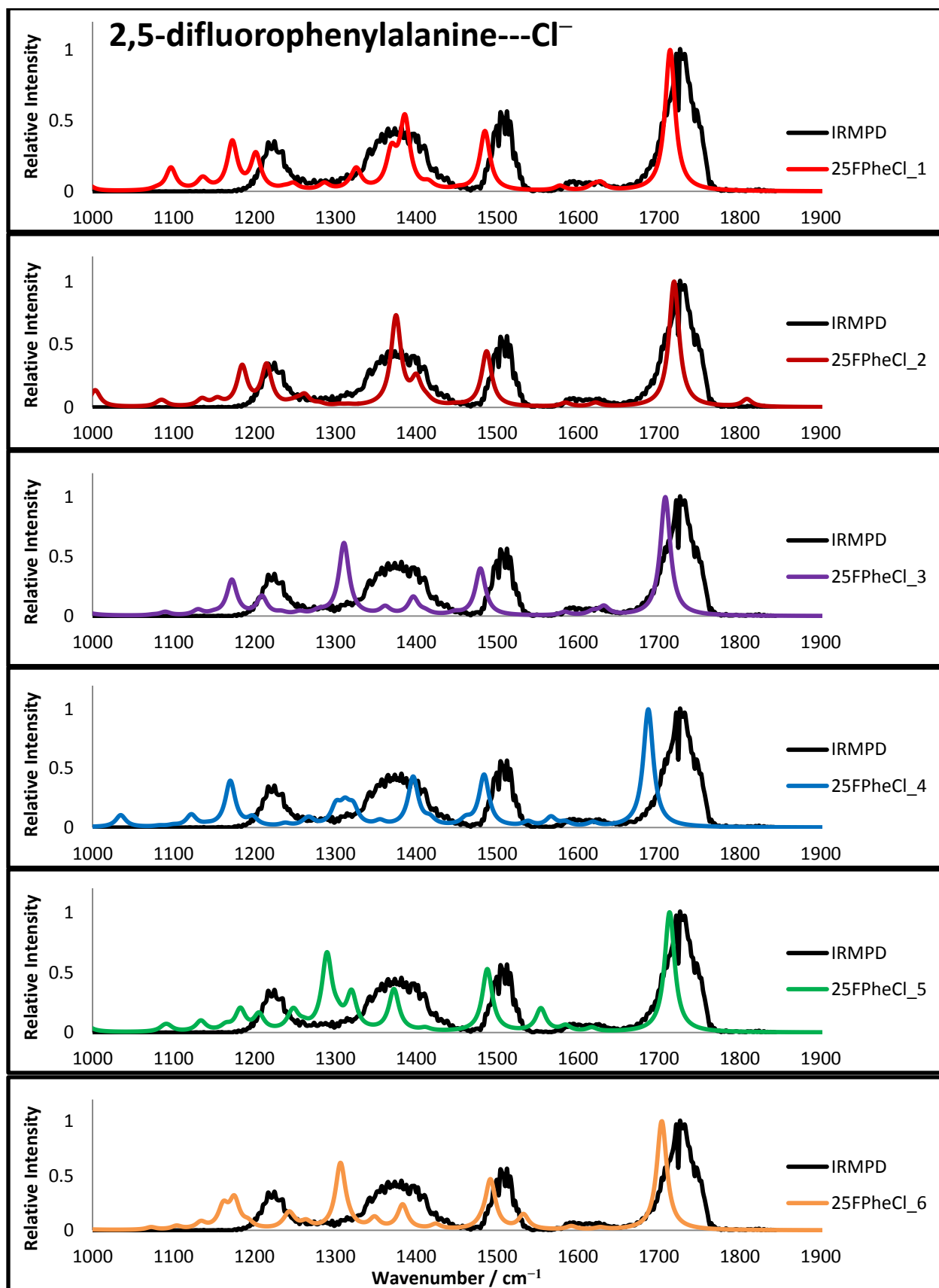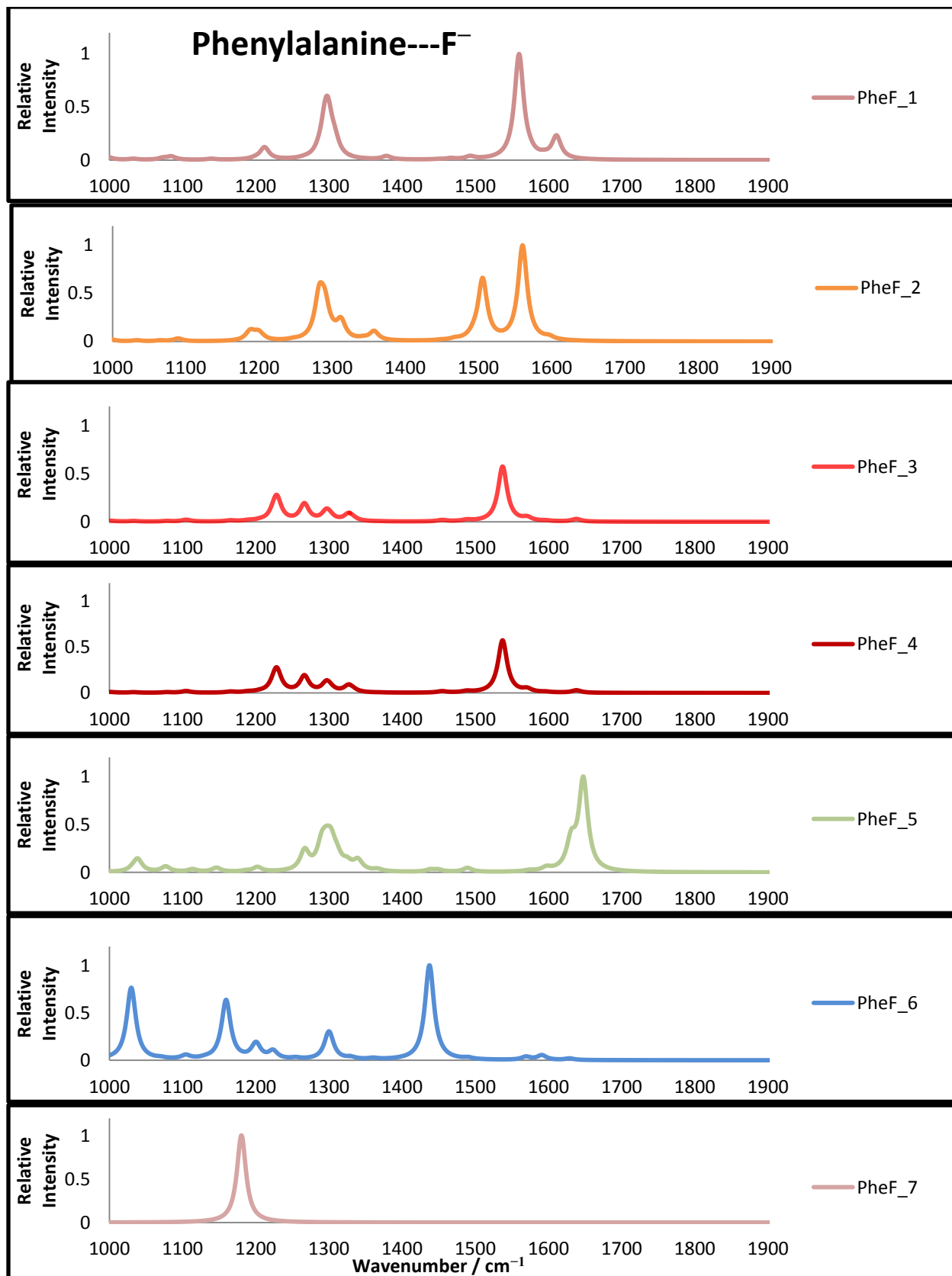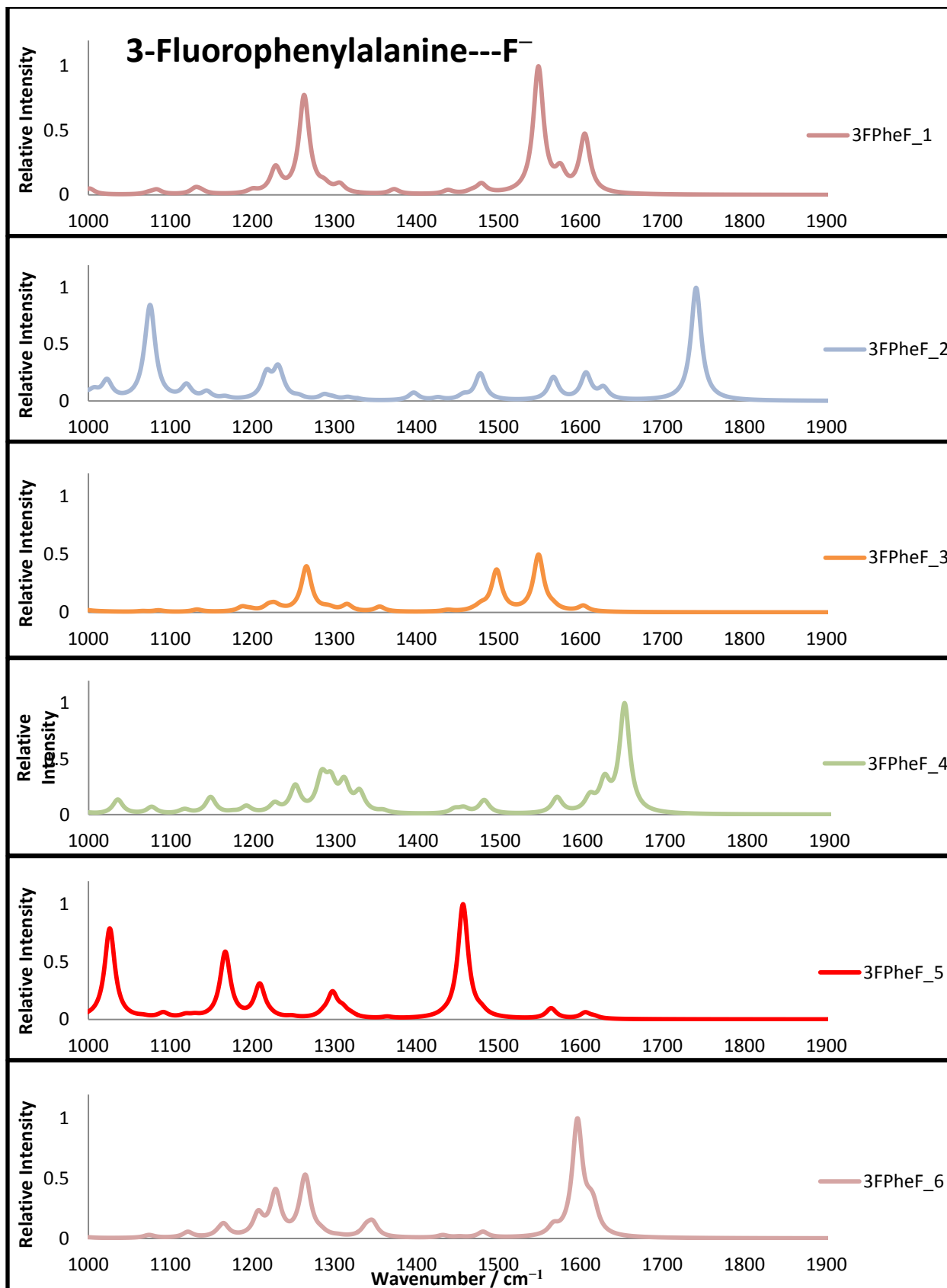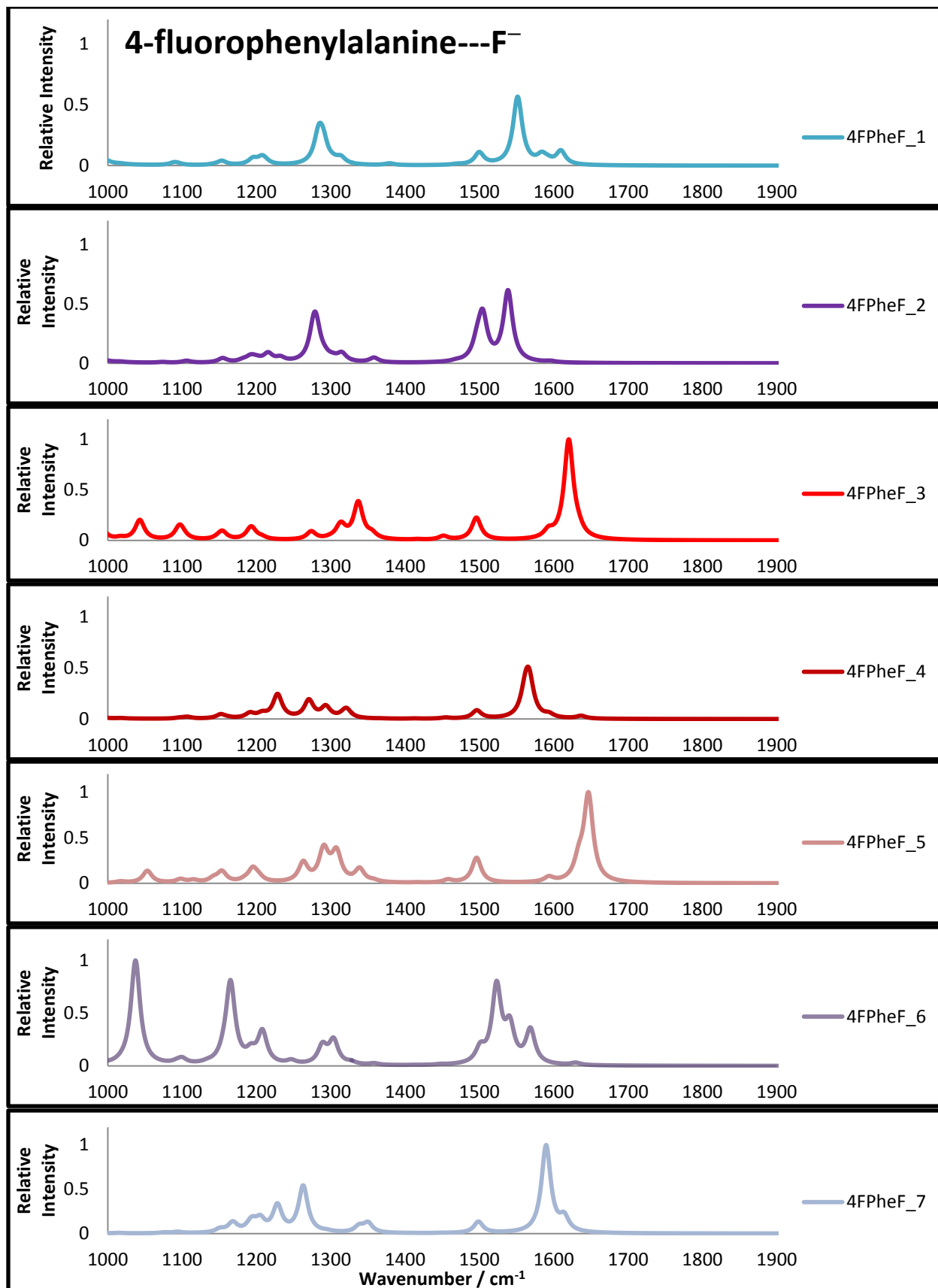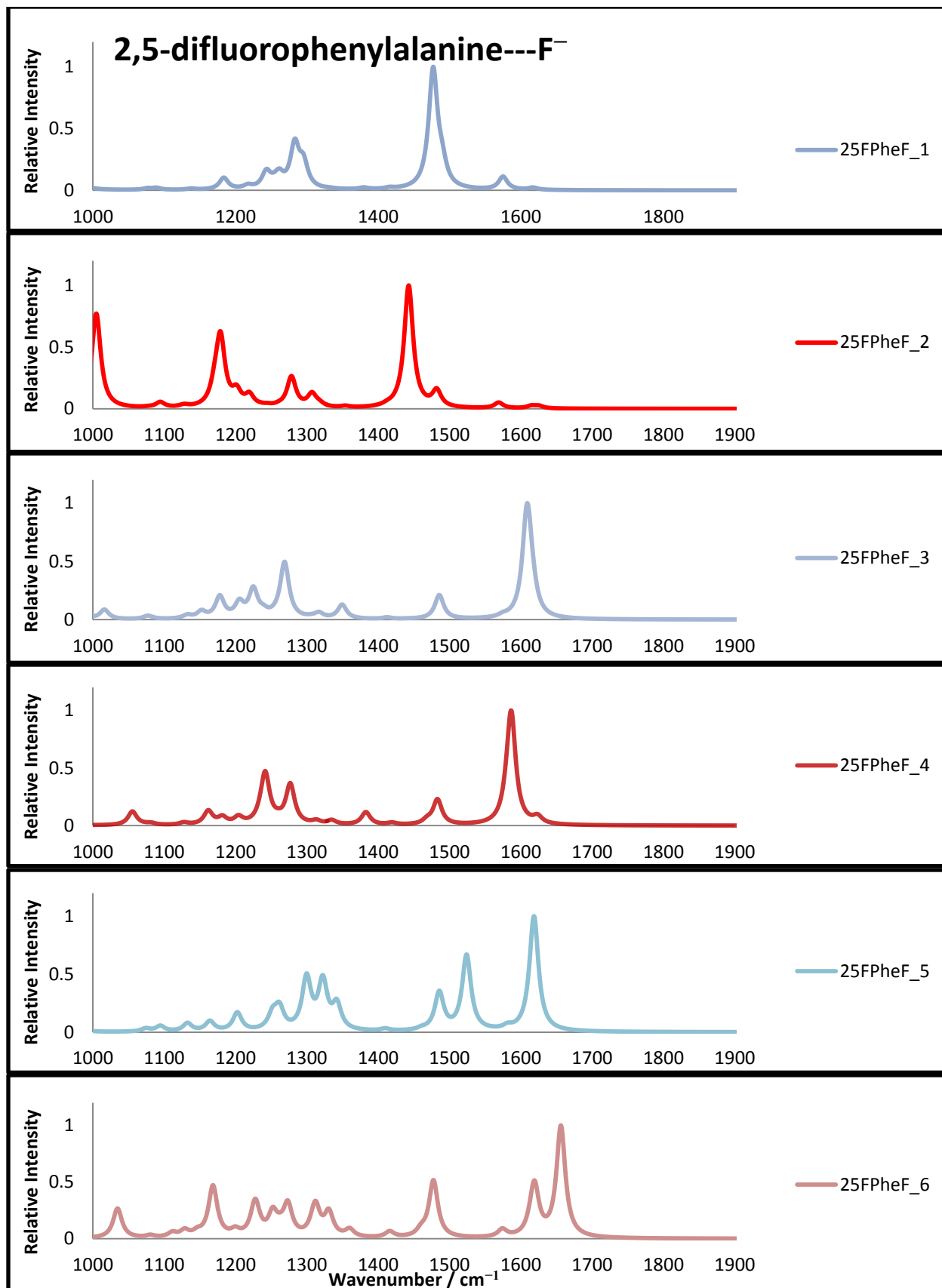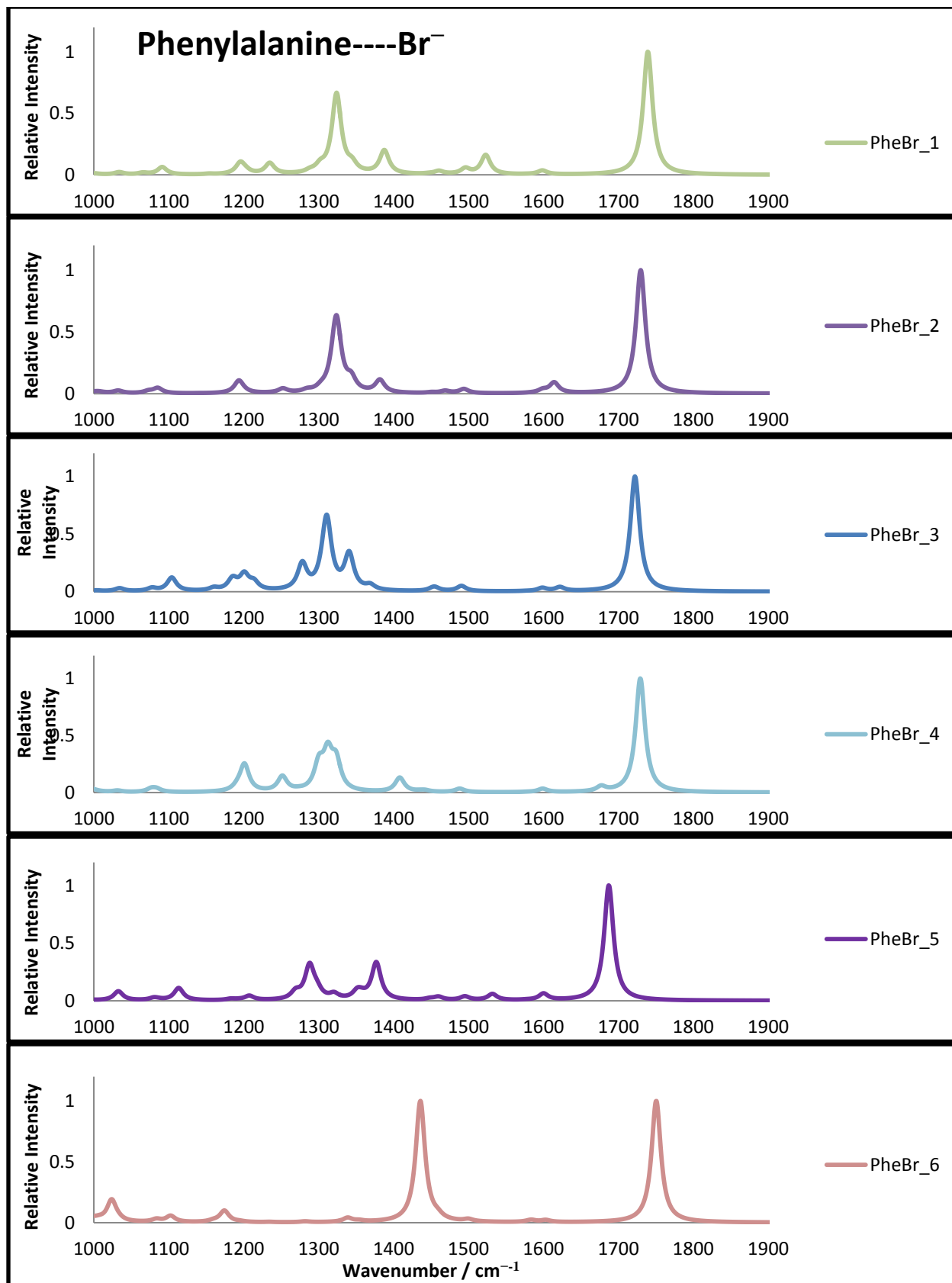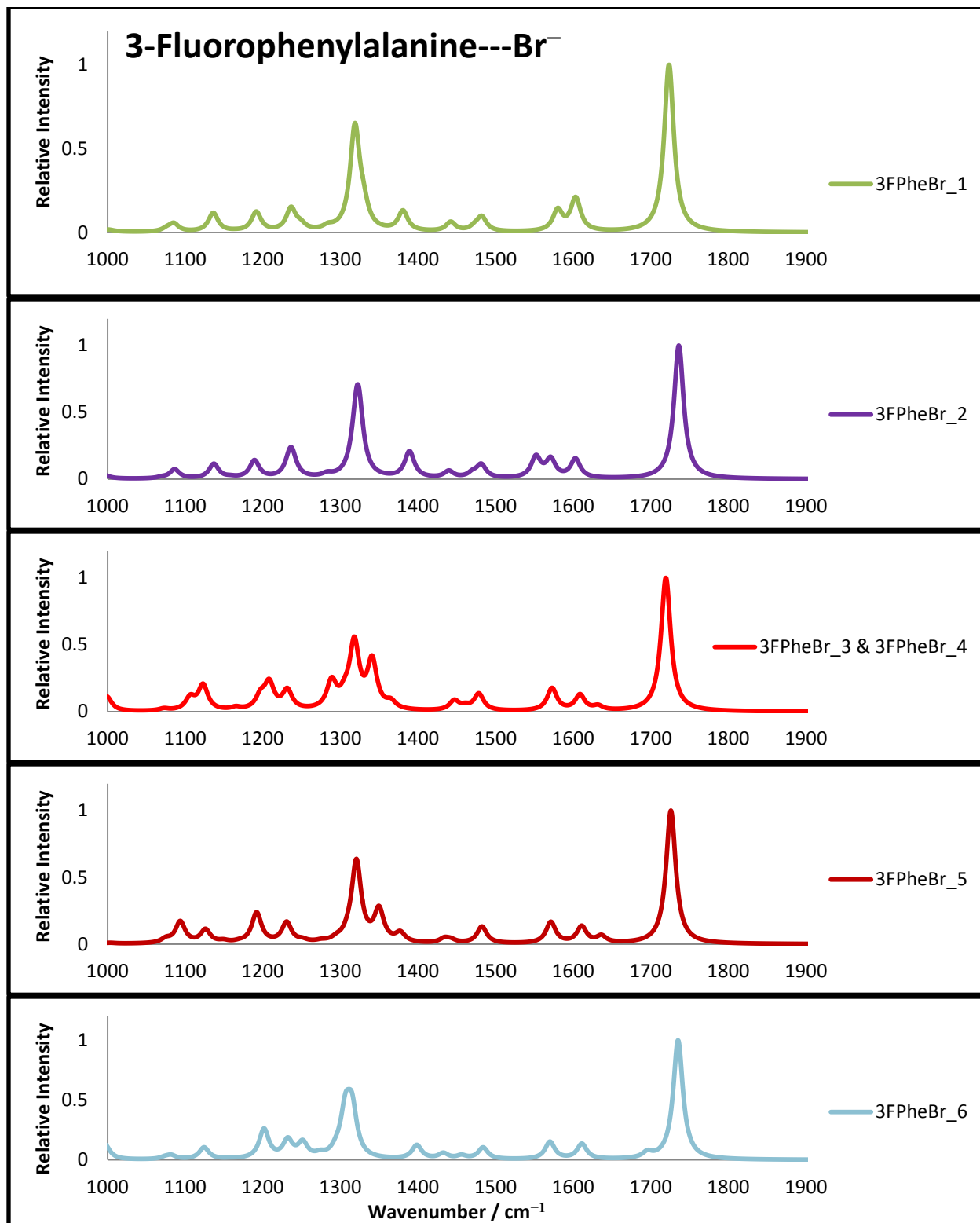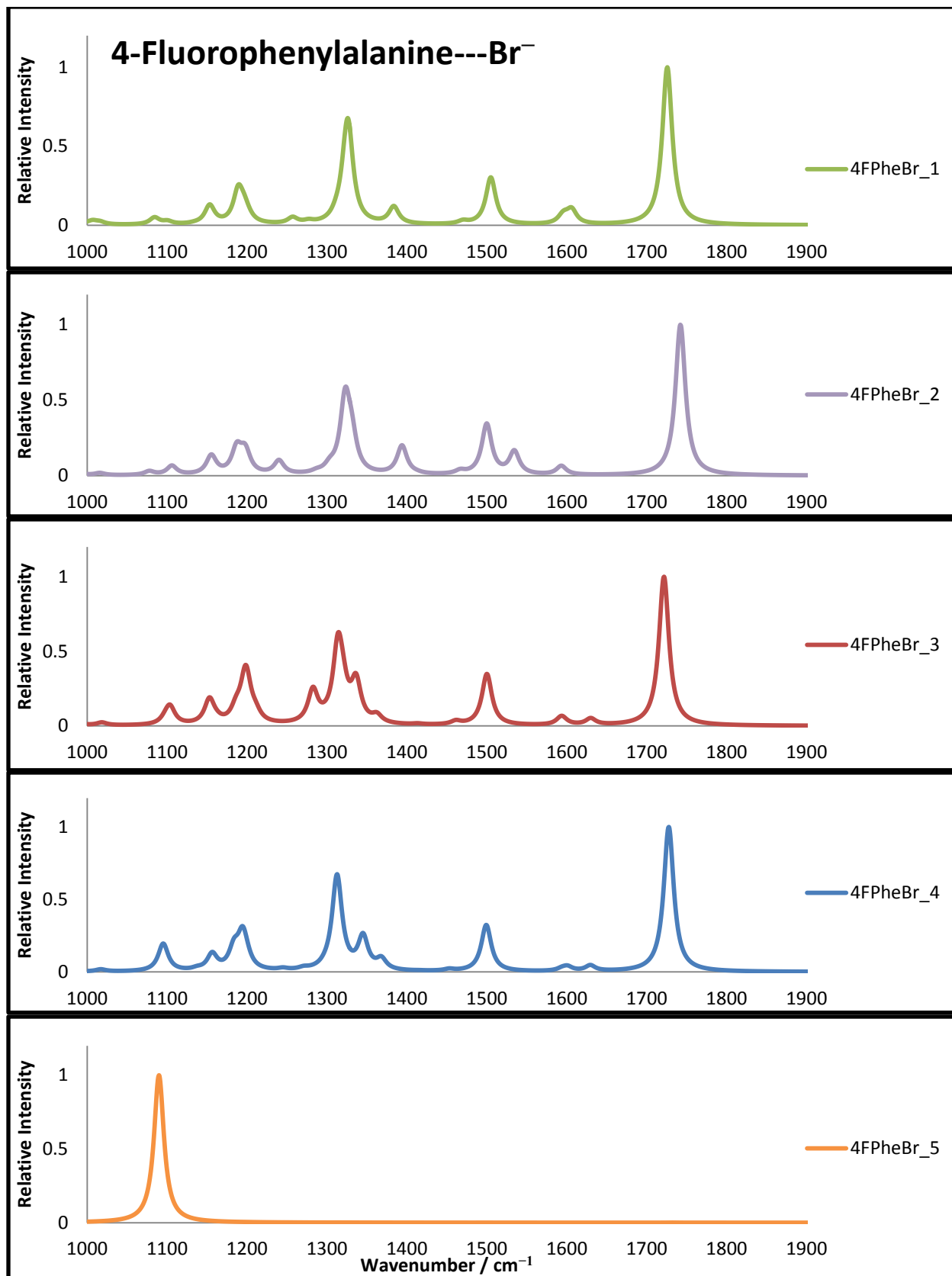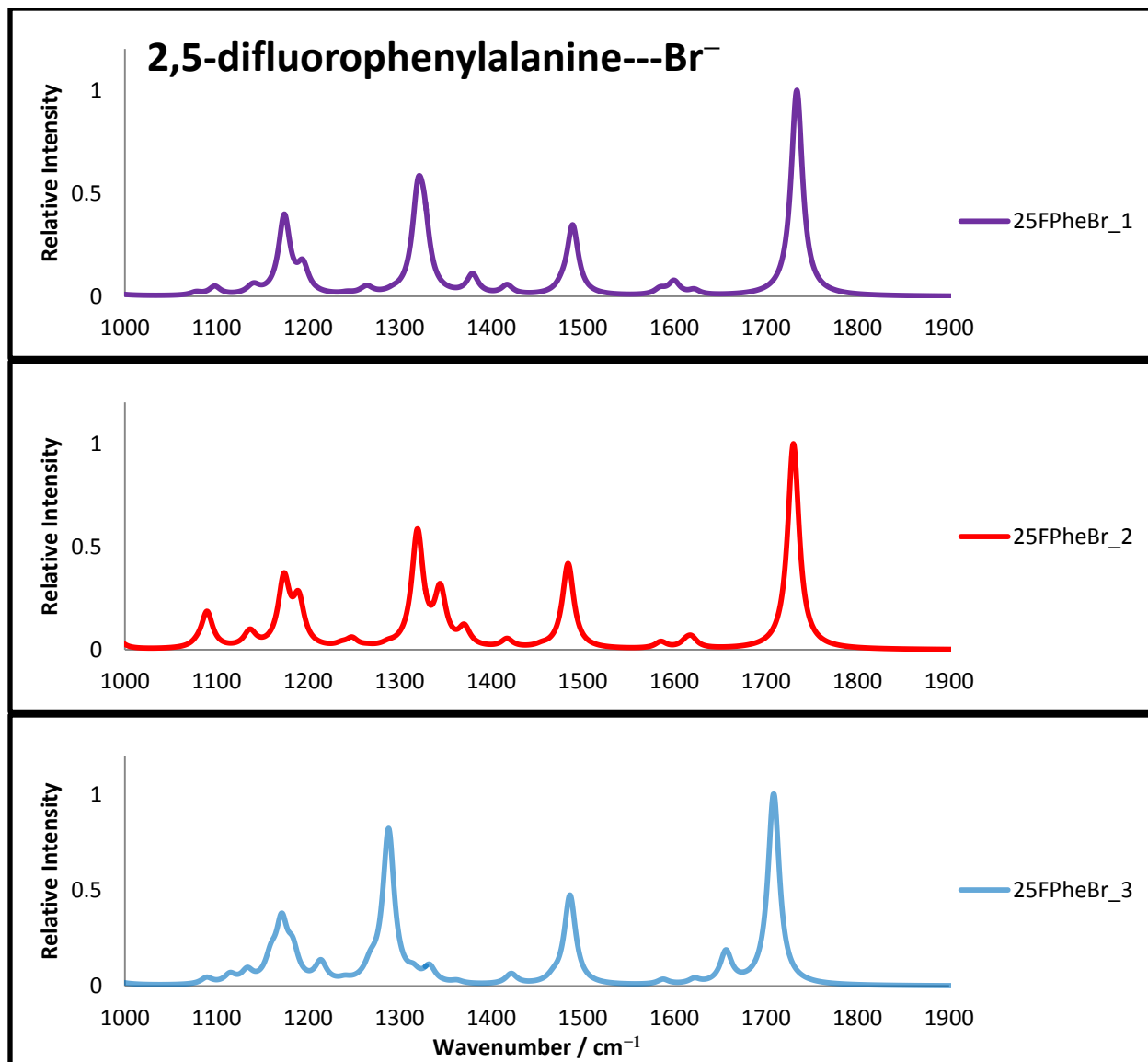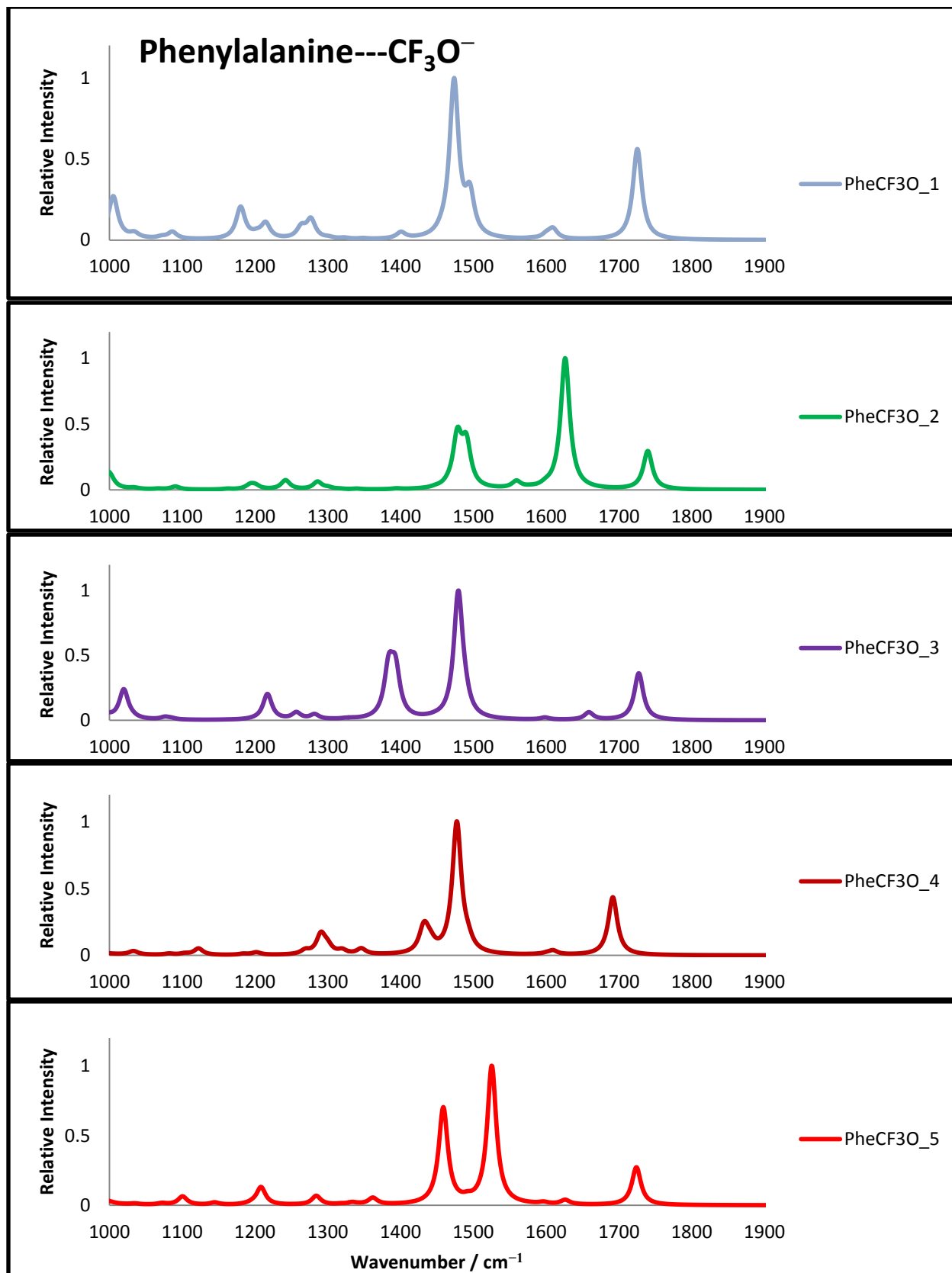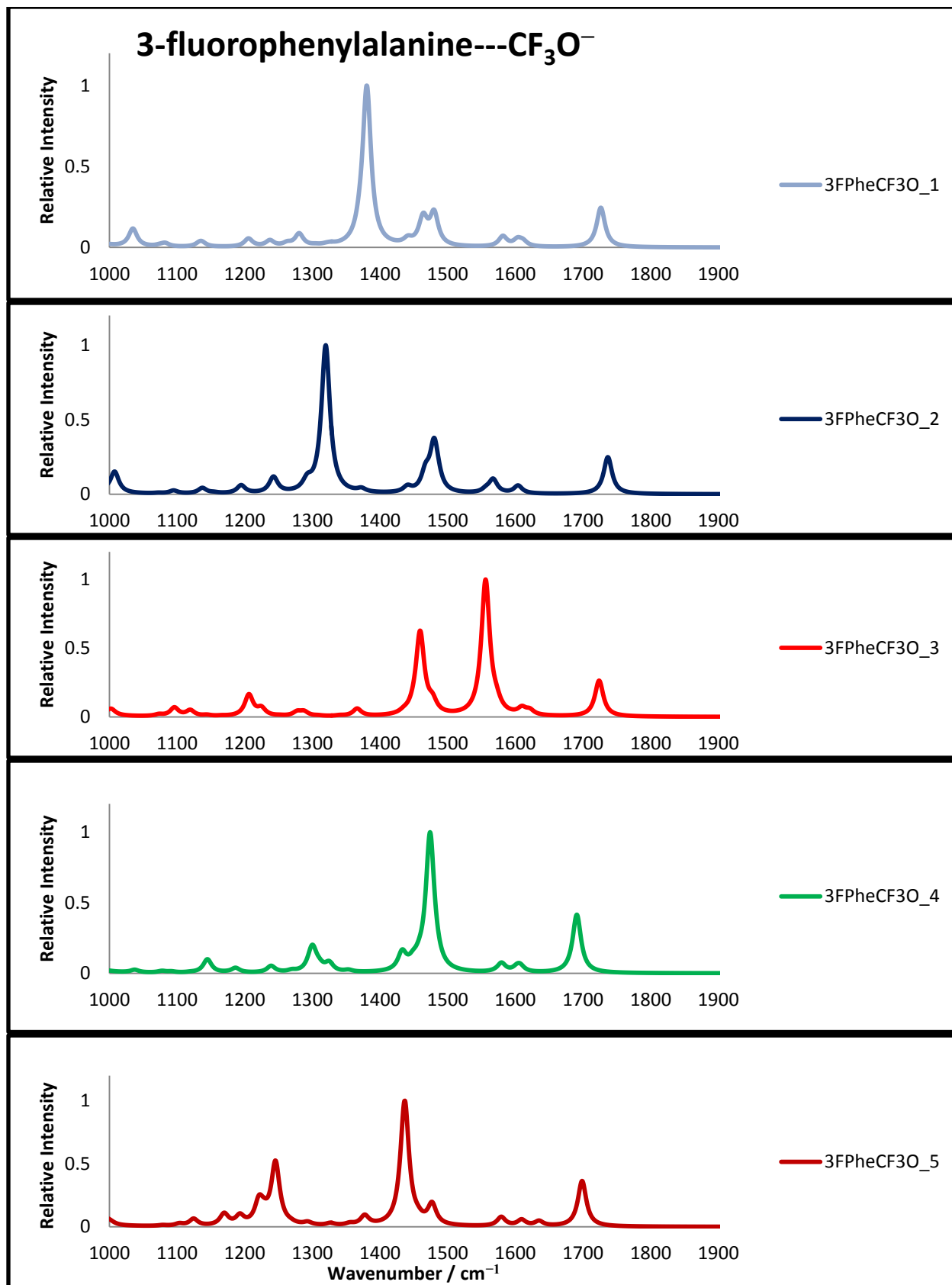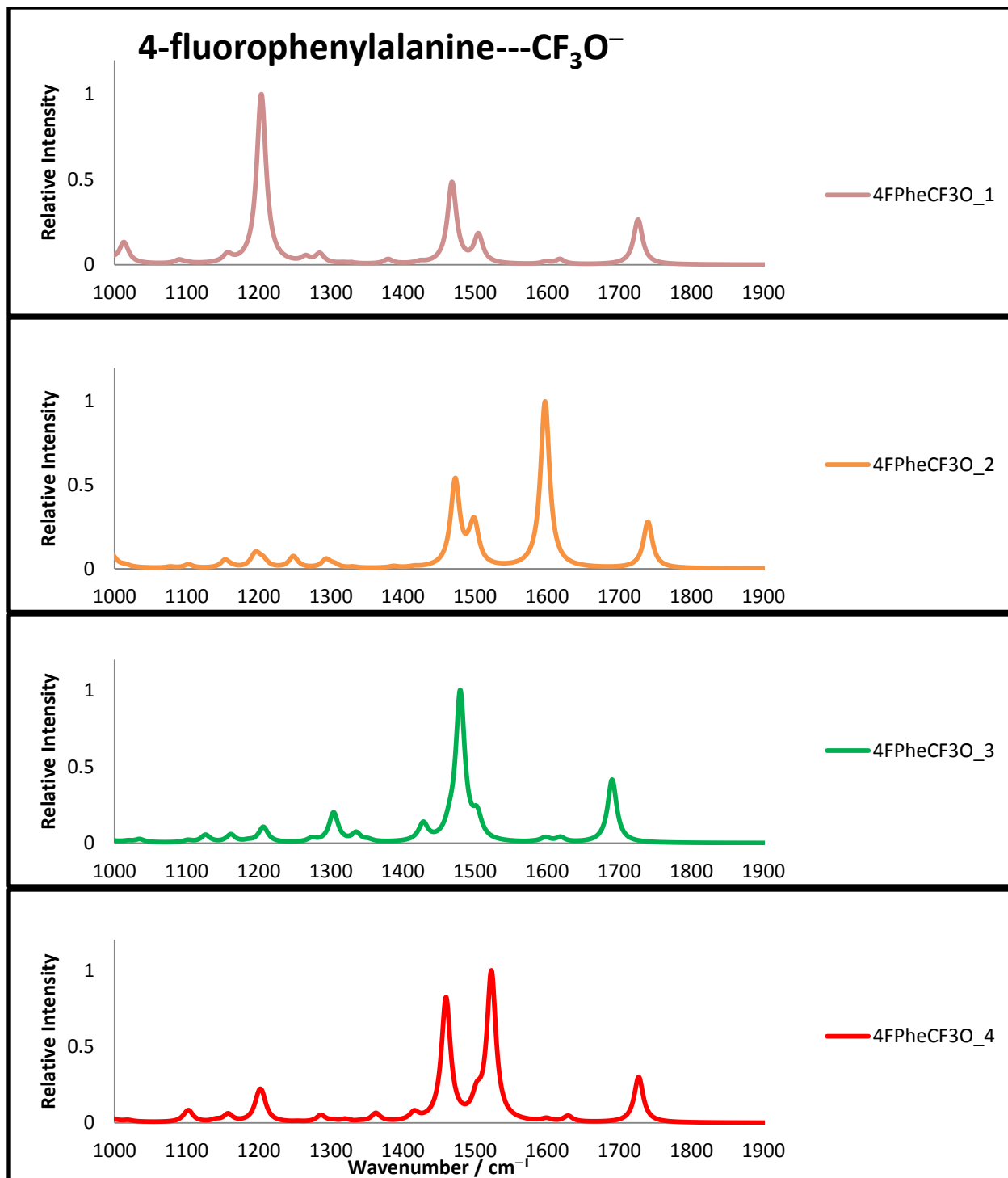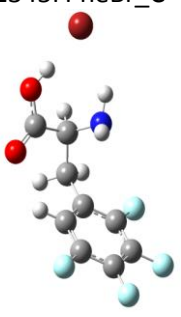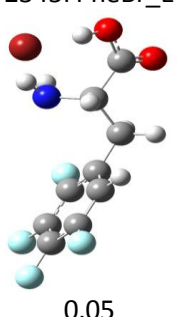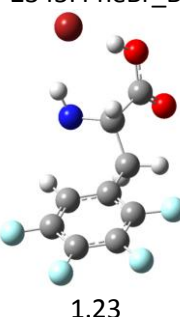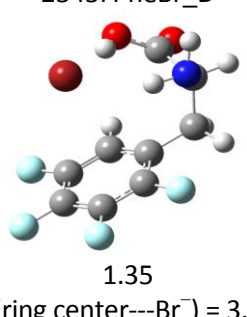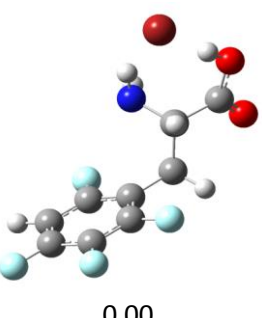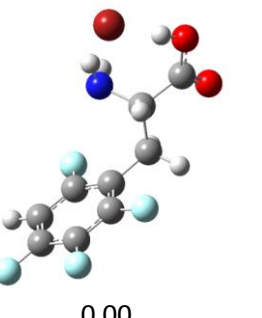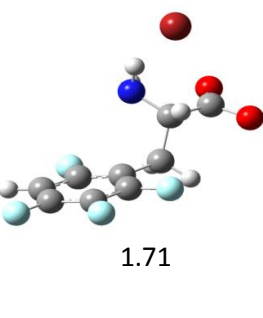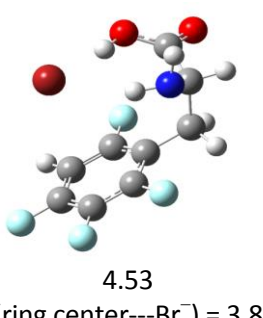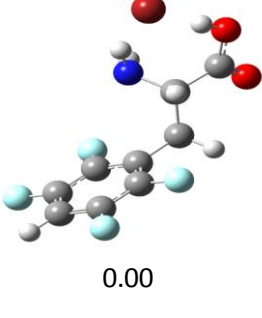
2,5-difluorophenylalanine---CF$_3$O$^-$
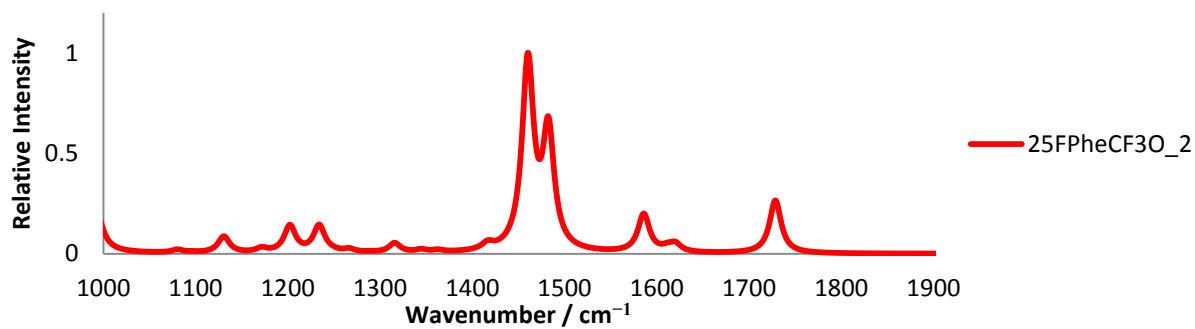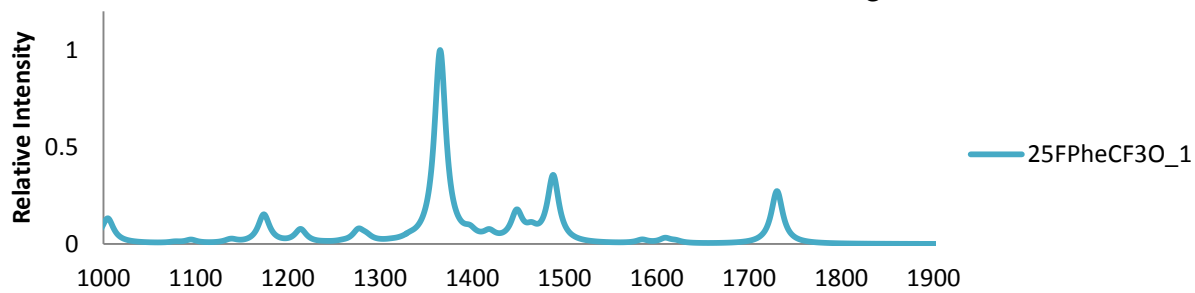
Lowest four isomers of tetrafluorophenylalanine clustered with Bromide

ΔH in kJ/mol
Distance in Å

2,3,4,5-tetrafluorophenylalanine---Br⁻

| 2345FPheBr_C | 2345FPheBr_E | 2345FPheBr_B | 2345FPheBr_D |

0.00   0.05   1.23   1.35
d(ring center---Br⁻) = 3.91

2,3,4,6-tetrafluorophenylalanine---Br⁻

| 2346FPheBr_B | 2346FPheBr_E | 2346FPheBr_N | 2346FPheBr_D |

0.00   0.00   1.71   4.53
d(ring center---Br⁻) = 3.84

2,3,5,6-tetrafluorophenylalanine---Br⁻

| 2356FPheBr_B | 2356FPheBr_E | 2356FPheBr_D | 2356FPheBr_H |

0.00   0.00   5.78   8.98
d(ring center---Br⁻) =3.82   d(ring center---Br⁻) = 3.86

135